OULU 2014
C 505

ACTA UNIVERSITATIS OULUENSIS

Tommi Tuovinen

OPERATION OF IR-UWB WBAN ANTENNAS CLOSE TO HUMAN TISSUES

*UNIVERSITY OF OULU GRADUATE SCHOOL;
UNIVERSITY OF OULU,
FACULTY OF INFORMATION TECHNOLOGY AND ELECTRICAL ENGINEERING,
DEPARTMENT OF COMMUNICATIONS ENGINEERING;
CENTRE FOR WIRELESS COMMUNICATIONS;
INFOTECH OULU*

ACTA UNIVERSITATIS OULUENSIS
C Technica 505

TOMMI TUOVINEN

OPERATION OF IR-UWB WBAN ANTENNAS CLOSE TO HUMAN TISSUES

Academic dissertation to be presented with the assent of the Doctoral Training Committee of Technology and Natural Sciences of the University of Oulu for public defence in Kuusamonsali (YB210), Linnanmaa, on 31 October 2014, at 9 a.m.

UNIVERSITY OF OULU, OULU 2014

Acta Univ. Oul. C 505, 2014

Supervised by
Professor Jari Iinatti
Doctor Markus Berg

Reviewed by
Professor Ben Allen
Professor Zhi Ning Chen

Opponent
Associate Professor Christophe Roblin

ISBN 978-952-62-0591-5 (Paperback)
ISBN 978-952-62-0592-2 (PDF)

ISSN 0355-3213 (Printed)
ISSN 1796-2226 (Online)

Cover Design
Raimo Ahonen

JUVENES PRINT
TAMPERE 2014

Tuovinen, Tommi, Operation of IR-UWB WBAN antennas close to human tissues.
University of Oulu Graduate School; University of Oulu, Faculty of Information Technology and Electrical Engineering, Department of Communications Engineering; Centre for Wireless Communications; Infotech Oulu
Acta Univ. Oul. C 505, 2014
University of Oulu, P.O. Box 8000, FI-90014 University of Oulu, Finland

Abstract

In this dissertation, the operation of planar impulse radio (IR) ultra wideband (UWB) antennas is examined for use in wireless body area networks (WBANs). The objective of the thesis is to consider electromagnetic phenomena due to coupling between an antenna and human body tissues and to analyse the challenges of wideband radiators. The aim is to understand the fundamental behaviour of an antenna in a WBAN, focusing on off-body and on-body communications. The thesis premises follow the international WBAN standard 802.15.6-2012 by the Institute of Electrical and Electronics Engineering (IEEE) and the Federal Communications Commission's (FCC) UWB regulations (3.1–10.6 GHz).

In the examinations, the frequency-dependent modelling of human tissues is considered. The impact of the variation of tissue layer thickness on the performance of an antenna is depicted. The demonstration of the impact of antenna input power is given in terms of generation of heat in tissues and specific absorption rate (SAR).

In order to theoretically contemplate the effect of reflections due to tissues on antenna patterns, the opportunities to influence polarization with an artificially anisotropic substrate are derived. With the proposed method, not earlier proposed for WBAN antennas, the smooth patterns without pattern minima can be achieved over the FCC UWB bandwidth. In addition, a theoretical two-path model is applied to the estimation of the antenna pattern shape close to tissues.

Various antenna parameters are explored as a function of the use distance to tissue surface to demonstrate the behaviour in the vicinity of a body. The size of the reactive near-field is an important factor for the evaluation of satisfactory on-body performance. The proportions of absorption, mismatch and body losses are analysed close to a body.

The connection between the complex input impedance and the dimensions of planar antennas is analysed by using lumped-element equivalent circuits. The impact of the actual width and length of the radiator on the impedance behaviour is presented for the first time. In addition, impedance is analysed in terms of capacitance, inductance and resistance within the reactive near-field for the first time. In order to understand the impact of tissues close to the antenna, the parasitic components for the stages in equivalents are proposed.

Keywords: anisotropic substrate, body loss, equivalent circuits, planar antenna, wideband antenna

Tuovinen, Tommi, Laajakaistaisten impulssiradioantennien toiminta langattomissa kehoverkoissa ihmiskudoksen läheisyydessä.
Oulun yliopiston tutkijakoulu; Oulun yliopisto, Tieto- ja sähkötekniikan tiedekunta, Tietoliikennetekniikan osasto; Centre for Wireless Communications; Infotech Oulu
Acta Univ. Oul. C 505, 2014
Oulun yliopisto, PL 8000, 90014 Oulun yliopisto

Tiivistelmä

Tässä väitöskirjassa tarkastellaan laajakaistaisten impulssiradioantennien (IR-UWB) toimintaa langattomissa kehoverkoissa (WBAN). Työn tavoitteena on tarkastella antennin ja ihmiskudoksen kytkeytymisestä johtuvia sähkömagneettisia ilmiöitä ja analysoida laajakaistaisen säteilijän haasteet. Päämääränä on ymmärtää antennin suorituskyky kontekstissa ja kohdeympäristöksi on fokusoitu toiminta kehon pinnalla (on-body) ja keholta poispäin seuraavaan liityntäpisteeseen (off-body). Tutkimustyö pohjautuu IEEE802.15.6-2012-standardiin sekä FCC:n UWB -säännöksiin.

Väitöstyössä tarkastellaan taajuusriippuvan ihmiskudoksen mallintamista. Ihmiskudoskerrosten paksuuden vaikutusta antennin suorituskykyyn tutkitaan simuloimalla. Lisäksi tarkastellaan antennin syöttötehon vaikutusta kudoksen lämpiämisen ja tehon absorboitumisen näkökulmasta.

Kehon aiheuttamien heijastusten vaikutusta säteilykuvioihin tarkastellaan teoreettisesti ja lisäksi esitetään menetelmä vaikuttaa antennin summapolarisaation kautta säteilykuvion muotoon keinotekoisella epäisotrooppisella substraatilla. Ehdotetulla menetelmällä, mitä ei ole aiemmin kirjallisuudessa esitetty kehoantenneille, voidaan minimoida nollakohtia ja saavuttaa tasainen säteilykuvio FCC UWB -taajuuskaistan yli. Kaksitie-mallia sovelletaan säteilykuvion muodon ennustamiseen kehon läheisyydessä.

Useita antenniparametreja havainnollistetaan antennin käyttöetäisyyden funktiona ihmiskudoksesta. Antennin reaktiivisen lähikentän koko on tärkeä tekijä kehoantennille riittävän suorituskyvyn saavuttamiseksi. Absorptio-, epäsovitus- ja kehohäviöiden osuudet edelleen eritellään ja analysoidaan työssä.

Työssä tutkitaan kompleksisen syöttöimpedanssin ja antennin fyysisten mittojen yhteyttä hyödyntämällä erilliskomponenteilla muodostettuja vastinpiirejä. Ensimmäistä kertaa antennin käytännön leveyden ja pituuden muutos esitetään suhteessa impedanssikäyttäytymiseen. Impedanssin muutos analysoidaan kapasitanssin, induktanssin ja resistanssin funktiona antennin reaktiivisen lähikentän alueella. Jotta kudoksen vaikutus antennin läheisyydessä voitaan ottaa suunnittelussa huomioon, työssä esitetään tarvittavat parasiittiset komponentit vastinkytkentöjen sarja- ja rinnanasteisiin.

Asiasanat: epäisotrooppinen substraatti, kehohäviöt, laajakaistainen antenni, planaarinen antenni, vastinpiirit

To my Family

Preface

My postgraduate studies at the Centre for Wireless Communications (CWC), University of Oulu, began in May 2011 under the supervision of Prof. Jari Iinatti and Dr Kamya Yekeh Yazdandoost. I had received my M.Sc. degree two months earlier by completing my Master's thesis for Nokia MeeGo products. The thesis topic was related to the long-term evolution (LTE) antenna design for a mobile handset.

When starting at CWC, my first project concerned the ultra wideband (UWB) antenna design in wireless body area networks (WBANs). The name of the project was "Wireless Body Area Network for Health and Medical-Care (WiBAN-HAM)" and it was funded by the Finnish Funding Agency for Technology and Innovation (Tekes). In addition to the direct antenna research, the project focused on the evaluation of a channel model and considerations of the health effects of antennas.

After the relatively brief period I worked on the WiBAN-HAM project, I joined another Tekes-funded project, "Enabling future Wireless Healthcare Systems (EWiHS)", in early 2012. The research tasks included examining the coupling between an antenna and a body, analysing the characteristics of UWB antennas, and other duties related to these. Since joining the EWiHS, in addition to Prof. Jari Iinatti, Dr Erkki Salonen and Dr Markus Berg also participated in the supervision of my studies.

In 2013, I received an Infotech Oulu Graduate School (IOGS) position. During the first year of the position, the research was co-planned with the EWiHS project. In addition to the research I carried out at the University, I was also given an opportunity to work for the antenna design company AntCore in March 2013. The nature of the work at AntCore was as a perquisite position (part-time), which continued until my dissertation.

The progress in doctoral studies during 2013 enabled the extension of the IOGS funding to cover the period of 2014–2015, i.e., until the dissertation. During 2014, the research was co-funded with the Academy of Finland project called "Reconfigurable Antennas and Over-The-Air Test for Cognitive Radios (RAOTA)" in addition to writing the thesis and finishing related studies.

I would like to thank my supervisor Prof. Jari Iinatti for giving me the opportunity to carry out my postgraduate studies at CWC. During the research work for this thesis, Jari was brimming with sympathy for his postgraduate students.

Dr Erkki Salonen surprised me in a positive way during the postgraduate studies with the profound ideas he had and which I was able to apply to my studies. Erkki was not a daily presence but provided me with food for thought every time we met. I am grateful to Erkki for sharing his scientific power of reasoning for my research.

From the very beginning, Dr Markus Berg shared daily working time with me. We had some fruitful discussions during the lunch and when exercising together. You gave me a needed boost to complete the postgraduate courses quickly and reminded me to concentrate on understanding phenomena in the research, not just looking at the performance graphs. In addition to research, it was a didactic to introduce in teaching as an assistant on some of his courses.

I would like to thank my present and former research colleagues, Dr Seppo Karhu, Dr Marko Sonkki, Lic. Tech. Timo Kumpuniemi, Lic. Tech. Mariella Särestöniemi and M.Sc. Ville Niemelä for sharing the time at CWC and discussions related to research problems. Furthermore, Jari Pakarinen, for manufacturing the antenna prototypes, and laboratory engineer Jari Sillanpää, for organising computing resources, deserve warm thanks.

During my postgraduate studies, the guys at AntCore shared their great knowledge and fruitful tips on how to design antennas for mobile devices and to force the simulator to work as desired. Thank you Sami Hienonen, Tatu Karvinen and Marko Kupari for giving me the opportunity to work with you while completing the post-graduate studies.

In addition, I would like to thank Dr Ilari Hänninen from Computer Simulation Technology (CST) for giving me personal support in problems related to the electromagnetic simulations, both remotely and hands-on.

Acknowledgement to the Finnish Foundation for Technology Promotion, Emil Aaltonen Foundation, Tauno Tönning Foundation, HPY Research Foundation, Walter Ahlström Foundation, and Nokia Foundation for the financial support of this thesis.

Finally, I want to thank my wife Annukka for supporting me during these days and our four children for reminding me what is really fundamental in life.

Oulu, 17 September 2014 Tommi Tuovinen

List of abbreviations and definitions

AWPL	Antennas & Wireless Propagation Letters
BAN	Body Area Network
BCC	Body-Centric Communications
CEPT	Conference Europèenne des Posteset Telecommunications – European Post and Telecommunications Conference
CSS-UWB	Chirp Spread Spectrum-UWB
CST	Computer Simulation Technology
CTIA	Cellular Telecommunications & Internet Association
CWC	Centre for Wireless Communications
DAA	Detect-and-Avoid
DS	Design Studio
ECC	Electronic Communications Committee
EHF	Extremely High Frequencies (30–300 GHz)
EIRP	Effective Isotropically Radiated Power
EM	Electromagnetic
EWiHS	Enabling future Wireless Healthcare Systems
EXT	External
FCC	Federal Communications Commission
FDTD	Finite-Difference Time-Domain
FIT	Finite Integration Technique
FM	Frequency Modulation
GPS	Global Positioning System
GSM	Global System for Mobile
HBC	Human Body Communication
ICNIRP	Institute Commission on Non-Ionizing Radiation Protection
IEEE	Institute of Electrical and Electronics Engineers
IEEE-T	IEEE Transactions
IET MAP	Institution of Engineering and Technology Proceedings – Microwaves, Antennas & Propagation
INT	Internal
IR	Impulse Radio
ISM	Industrial, Scientific and Medical
LDC	Low Duty Cycle
LTE	Long-Term Evolution
MWS	Microwave Studio

NFC	Near Field Communication
OFDM	Orthogonal Frequency Division Multiplexing
PCB	Printed Circuit Board
PHY	Physical layer technology
PIER	Progress in Electromagnetics Research
PSD	Power Spectral Density
RF	Radio Frequency
RX	Receiver
SAM	Standard Anthropomorphic Model
SAR	Specific Absorption Rate
SHF	Super High Frequencies (3–30 GHz)
Tekes	Finnish Funding Agency for Technology and Innovation
TM	Time Modulated
TPM	Two-Path Model
TRP	Transmitted Power
TX	Transmitter
UHF	Ultra High Frequencies, (300–3000 MHz)
UWB	Ultra Wideband (3.1–10.6 GHz)
VHF	Very High Frequencies, (30–300 MHz)
VNA	Vector Network Analyser
VSWR	Voltage Standing Wave Ratio
WBAN	Wireless Body Area Network
WiBAN-HAM	Wireless Body Area Network for Health and Medical-Care
WCDMA	Wideband Code Division Multiple Access
WLAN	Wireless Local Area Network
WPAN	Wireless Personal Area Network
Γ	Voltage reflection coefficient
δ_p	Penetration depth in tissue
ε	Permittivity, complex
ε'	Permittivity, real part
ε''	Permittivity, imaginary part
ε_r	Permittivity, relative value
ε_s	Permittivity, static value
ε_0	Permittivity of vacuum
ε_∞	Permittivity, infinity value
η	Refraction index
θ	Elevation plane

θ_i	Angle of incidence
θ_r	Angle of reflection
θ_t	Angle of transmission
λ	Wavelength
μ	Permeability, magnetic
μ_r	Permeability, relative value
μ_0	Permeability of vacuum
ρ_e	Volumetric density of electric charge
ρ_{par}	Reflection coefficient for parallel polarization
ρ_{per}	Reflection coefficient for perpendicular polarization
ρ_r	Reflection coefficient
ρ_t	Tissue density
σ	Conductivity
τ_{GD}	Group delay
$\overline{\tau_{\mathrm{GD}}}$	Mean value of group delay
τ_{par}	Transmission coefficient for parallel polarization
τ_{per}	Transmission coefficient perpendicular polarization
τ_t	Transmission coefficient
τ_r	Relaxation time
ω	Angular frequency
$tan\delta$	Loss tangent
φ	Azimuth Plane
ψ	Antenna phase
ψ_R	Phase term of the reflected wave
$\psi_{\Delta d}$	Phase term due to the path difference
$\vec{B}$	Magnetic flux density
C	Specific heat
c_0	Speed of light
$\vec{D}$	Electric flux density
D	Directivity of antenna
$\vec{E}$	Electric field intensity
$\lvert\vec{E}\rvert$	Electric field, rms value
E_i	Electric field, incident to the interface
E_r	Electric field, reflected from the interface
E_t	Electric field, transmitted through the interface
e_{c}	Efficiency, conduction

e_d	Efficiency, dielectric
e_r	Efficiency, reflection (mismatch)
e_0	Total antenna efficiency
f_BW	Fractional bandwidth
f	Frequency
f_C	Frequency, centre
f_H	Higher –10 dB bandwidth
f_L	Lower –10 dB bandwidth
f_r	Frequency, relaxation
G	Gain of antenna
G_TX	Peak gain of antenna in any orientation
$\vec{H}$	Magnetic field intensity
h_b	Rate of heat transfer from blood tissue
h_m	Rate of tissue heat production
$\vec{J}$	Surface density of electric current
K	Thermal conductivity
L_abs	Absorption Loss
L_body	Body Loss
L_mismatch	Mismatch Loss
k	Wave number
P_{RX}	Received power
P_TX	Transmitted power
S_{11}	Reflection coefficient, antenna 1
S_{21}	Scattering parameter, channel
S_{22}	Reflection coefficient, antenna 2
R_A	Resistance, input
R_L	Resistance, loss
R_R	Resistance, radiation
T	Temperature, tissue
ΔT	Temperature, difference
Δt	Duration of time period
v	Propagation velocity of wave
X_A	Reactance, input
Z_A	Impedance, input
Z_0	Impedance of transmission line, characteristic

List of original publications

The thesis is based on the following nine peer-reviewed articles. The papers included in this thesis are referred throughout the text by their Roman numerals (I–IX):

I Tuovinen T, Berg M, Yekeh Yazdandoost K & Iinatti J (2013) Ultra Wideband Loop Antenna on Contact with Human Body Tissues. In: IET Microwaves, Antennas & Propagation 7(7): 588–596.

II Tuovinen T, Berg M, Yekeh Yazdandoost K, Hämäläinen M & Iinatti J (2013) On the Evaluation of Biological Effects of Wearable Antennas on Contact with Dispersive Medium in Terms of SAR and Bio-Heat by Using FIT Technique. In: IEEE 7th International Symposium on Medical Information and Communication Technology (ISMICT), Special Organized Session: Antennas and Propagation for Body Area Network. Tokyo, Japan: 149–153.

III Tuovinen T, Berg M, Yekeh Yazdandoost K, Salonen E & Iinatti J (2012) Radiation Properties of the Planar UWB Dipole in the Proximity of Dispersive Body Models. In: EAI 7th International Conference on Body Area Networks (BodyNets). Oslo, Norway: 1–7.

IV Tuovinen T, Berg M & Salonen E (2014) Antenna Close to Tissue: Avoiding Radiation Pattern Minima with Anisotropic Substrate. In: IEEE Antennas and Wireless Propagation Letters. (In press)

V Tuovinen T, Kumpuniemi T, Yekeh Yazdandoost K, Hämäläinen M & Iinatti J (2013) Effect of the Antenna-Human Body Distance on the Antenna Matching in UWB WBAN Applications. In: IEEE 7th International Symposium on Medical Information and Communication Technology (ISMICT). Tokyo, Japan: 193–197.

VI Tuovinen T, Berg M & Salonen E (2013) The Comparative Analysis of UWB Antennas with Complementary Characteristics: A Functionality in FS and Applicability for the Usage Close to Tissues. In: 34th Progress in Electromagnetics Research Symposium (PIERS). Stockholm, Sweden: 134–138.

VII Tuovinen T, Berg M, Salonen E, Hämäläinen M & Iinatti J (2014) Conductive Layer under a Wearable UWB Antenna: Trade-off between Absorption and Mismatch Losses. In: IEEE 8th International Symposium on Medical Information and Communication Technology (ISMICT). Florence, Italy: 1–5.

VIII Tuovinen T & Berg M (2014) Impedance Dependency on Planar Broadband Dipole Dimensions: An Examination with Antenna Equivalent Circuits. In: Progress in Electromagnetics Research (PIER) 144: 249–260.

IX Tuovinen T, Berg M & Iinatti J (2014) Analysis of the Impedance Behaviour for Broadband Dipoles in Proximity of a Body Tissue: Approach by Using Antenna Equivalent Circuits. In: Progress in Electromagnetics Research (PIER) B 59: 135–150.

Prof. Iinatti supervised Papers [I]–[III], [V], [VII] and [IX], and Dr Salonen Papers [III]–[IV] and [VI]. Dr Berg participated in supervising each of the papers ([I]–[IX]) in the thesis. Dr Yekeh Yazdandoost was the instructor and supervisor of Papers [I]–[II] and [V].

In addition to having a leading role in the preparation of Papers [I]–[IX], the author has conducted all the simulations required for each paper, including, for instance:

- the optimization of the UWB antenna structures in terms of impedance bandwidth, group delay, radiation pattern and other parameters,
- the evaluations of free space and on-body performance in the proximity of various tissue models, and
- the generation and analysis of lumped-element equivalent circuits for antennas.

In Paper [I], introduction to the properties of human body tissues and the overview of dispersive modelling were prepared and the examination of different tissue combinations for the outermost body tissues by simulations was carried out by the author. The idea to design a planar UWB loop antenna was instructed by Dr Yekeh Yazdandoost and the radiator structure was co-designed by the author. The verification of the obtained results by measurements and writing of the paper was carried out together by the author and Dr Berg.

In Paper [II], Dr Berg planned the content for the paper with the author. Dr Yekeh Yazdandoost instructed with the theoretical part related to thermal effects and Dr Ilari Hänninen from CST guided on how to perform the temperature simulations.

The idea and theoretical calculations for Papers [III] and [IV] were invented and derived by Dr Salonen, whereas the ideas for Papers [VI] and [VII] were planned together by the author, Dr Berg and Dr Salonen. In Paper [IV], the theoretical approach was derived solely by Dr Salonen. Papers [III]–[IV] and [VI]–[VII] were written and prepared together by all the three authors.

The conclusions of the analysis for Paper [V] were stated together by the author, Dr Berg and Dr Salonen. The experimental user study was realized with Lic. Tech. Timo Kumpuniemi. The antennas were designed by the author following the instructions by Dr Yekeh Yazdandoost. Other authors helped with the scientific presentation of the work.

The approach to utilize antenna equivalent circuits for the BAN context in the last two papers ([VIII] and [IX]) was planned by the author and Dr Berg. The author prepared the content of the studies, realized all the simulations and finalized the analysis and writing of the paper with the supervisors.

The work for Papers [I]–[IX] in this thesis was done during the two Tekes–funded projects, “Wireless Body Area Network for Health and Medical-Care (WiBAN-HAM)” and “Enabling future Wireless Healthcare Systems (EWiHS)”. In the research projects, several commercial companies were involved in order to share technology transfers and research objectives in addition to comment the research results.

During the postgraduate studies in 2011–2014, the author has also contributed to several publications related to antenna and propagation research or directly to UWB WBAN applications. The articles can be found in the list of references in [1–19] and are not directly included in the thesis.

Table of contents

1 Introduction

This chapter introduces the motivation for the thesis and the research background. The scope of the dissertation is indicated and the research questions are presented. In addition, the materials and methods of the research work are presented.

1.1 Research background

Radio communication systems, where data is transmitted using electromagnetic waves, cannot be realized without antennas. The importance of antennas to wireless connections cannot be dismissed. This is the reality for every mobile device without a wire connection.

Considering the evolution of wireless systems and the special need for antennas, the most recent decades have shown a rapid development in cellular mobile communications with several new applications. At the beginning of the 1990s, the first Global System for Mobile (GSM) calls, known as the 2nd generation, were operated in Finland. The 3rd generation Wideband Code Division Multiple Access (WCDMA) services became available in 2004. Only six years later, the author was completing his Master's thesis at Nokia. The topic was related to the diversity antenna design for the 4th generation Long-Term Evolution (LTE) mobile phone concept. In addition to the generations of mobile communications, which have rapidly developed, other technologies, such as Global Positioning System (GPS), Wireless Local Area Network (WLAN) and Near-Field Communication (NFC), have been introduced into mobile devices. Nowadays, the number of required antenna radiator structures for a mobile device concept can vary roughly between four and eight, depending on the device concept requirements. The number of antennas in mobiles is likely to increase in future.

At the same time as mobile devices have become smaller and more complicated, the recent advances of the last decade in the fields of biomedical engineering and wearable hardware have generated possibilities for the creation of body-centric communications (BCC) [20]. It is evident that the current BCC development trends can be compared with the past evaluation work of mobile communications. The BCC systems enable several applications that can be used, for instance, for the collection of health and sports data from a human body. In the envisioned scenarios, the aim is to collect measurement data from a patient/user wearing multiple sensors aligned on the body. The sensors are used to record various health parameters such as blood pressure, sugar level, heart signals or temperature [21].

P. S. Hall & Y. Hao have categorized the BCCs into three classes: off-body, on-body and in-body communications [20]. The most often used term to describe the BCC system is 'wireless body area network' (WBAN). Related to the WBAN context, the Institute of Electrical and Electronics Engineers (IEEE) published the international standard 802.15.6 [22] in early 2012, which is targeted for short-range, low-power and highly reliable wireless communications.

In the standard, three possible physical layer solutions are introduced. In this thesis, the focus is on the wideband technology, namely the ultra wideband (UWB), allocated from 3.1 GHz up to 10.6 GHz in the United States. Regulations [23] concerning the unlicensed use of UWB were issued by the Federal Communications Commission (FCC) in 2002. The research in thesis concerns the impulse radio (IR) based waveform [24], and the focus is on WBAN off-body and on-body communications.

In a WBAN, the operation of an antenna in the proximity of a human body means several challenges to achieve the desired performance. The well-known body effect was found to harm the performance of a mobile antenna a long time ago [25]. The demands for the operation of an antenna arise due to the presence of highly lossy tissues and the tissues' impact on impedance characteristics, pattern shape and current distribution.

Even though the effect of body tissues due to hand or head effect is also existent in mobile communications, the effect is not exactly same with the envisioned WBAN technologies. WBAN devices are not particularly designed to be held in hand but are mainly aligned on a body and assumed to be removed when changing clothes or a battery, for instance. These devices are most probably exposed to moisture and relatively cold or warm circumstances for long periods of time.

In the focus application, an antenna might be integrated into an electronic measurement device, aligned individually on-body as a repeater, aligned to a sensor node in order to improve the connection between channel paths, or integrated into clothing. Several design challenges increase the complexity to design an antenna for a WBAN device. These include:

- requirements for a sensor due to a specific use position on a body,
- restrictions of a device due to mechanical limitations,
- additional loss factors due to materials used, and
- tight areas/spaces available.

These are some reasons why fundamental understanding of the operation and characteristic of antennas is essential for WBAN applications. The author wishes to emphasize the word ‘understanding’ particularly in the context of underlying purpose of academic research work: to research phenomena and to offer the results for use by commercial companies. In addition to an antenna, which is the key enabler of wireless operation, there are several other important aspects of WBAN to study, such as durability of a power source, low-energy technology, bit error performance, and complexity and performance of transceiver structures.

Understanding the operation of an antenna is of utmost importance for the UWB, where a wide impedance bandwidth is created with the shape and form of an antenna. This is the substantial difference compared to mobile antennas which are usually matched with circuit components. A physical size of a small antenna (but not electrically small) covering the UWB bandwidth causes a headache for designers since the higher frequencies of a wide bandwidth might introduce higher-order resonance modes. The modes result in undesired changes with a pattern shape with the frequency, for instance. A design of an efficient IR-UWB WBAN is not possible without a profound understanding of the fashion to excite the extremely wide bandwidth, constant operation over the FCC regulations, and problems due to the existence of a human body. These issues create a demand for studies that increase the understanding of the behaviour of WBAN antennas.

Even though the open literature reports solutions of UWB WBAN antennas, the author considers that there is a lack of available material in terms of the WBAN context and of straightforward research related to the analysis of the antenna operation in the operating environment. It is the focus this dissertation tackles. The research problems are presented in detail in the following section.

1.2 Aims and scope of the research

The plan for the thesis objectives is fundamentally based on the CWC research projects “Wireless Body Area Network for Health and Medical Care (WiBAN-HAM)” and “Enabling future Wireless Healthcare Systems (EWiHS)”. The research work for the thesis was carried out solely in these projects. The objectives include several sub-objectives such as:

- to become acquainted with the properties of human body tissues,
- to investigate how to model frequency-dependent tissues by simulations,
- to design planar antennas for studies based on the FCC UWB regulations,
- to examine the impact of the use distance to body on performance,
- to analyse the antenna behaviour in the proximity of a body in detail,
- to find out methods to compensate body effects for an UWB radiator, and
- to understand the challenges of a body to a broadband antenna.

At the beginning of the postgraduate studies, the research problem in the WiBAN-HAM project was divided into two larger research entities in order to consider different types of antennas for WBAN on-body communications, and to realize radio channel measurements and the channel model investigation for WBAN.

The objectives and action points in the project plan were focused and the starting point for the thesis was formulated at the beginning as:

1. How do the tissue characteristics vary when following the FCC UWB bandwidth and how is the variation taken into account for the modelling by a phantom?

The first problem involved a literature review and getting acquainted with electromagnetic wave propagation at the interface of two absolutely different media: free space and tissues. Several studies reported a decrease in antenna efficiency and detuning for a wearable antenna in contact usage or at some distance to tissues. Tissues were often modelled by using an object with a fixed-size phantom or with fixed tissue-layer thicknesses.

Information about the effects of variation in the thickness of tissue layers on antenna performance was not available, which is the reason why the next question of interest was defined:

2. How is variation in the thickness of the outermost body tissues observed to change antenna performance?

Variation in tissues' dielectric properties and a modelling are concluded and discussed in Subsections 4.3.1 and 4.3.2.

The next topic of interest was to examine the thermal effects and specific absorption rate (SAR) for a WBAN antenna against the restrictions set out by the IEEE in [26] and the International Commission on Non-Ionizing Radiation

Protection (ICNIRP) in [27]. Based on the restrictions in the FCC regulations [23, 24], the maximum effective isotropic radiated power (EIRP) cannot be higher than approximately 0.5 mW over the entire UWB bandwidth. In order to gain understanding about the thermal effects and SAR, the following statement was considered:

3. What is the amount of power that can be fed to the antenna until tissues are harmed?

The aim of the next phase of the research was to get information about the impact of a use distance to body surface on the antenna performance. In this experimental part, the objective was to investigate the effect of the distance between an antenna and a body on individual antenna parameters. The following research questions were presented:

4. What is the distance to body required to achieve the level of operation close to that of free space in terms of matching, efficiency or patterns?
5. Can one estimate the required distance to achieve the performance level of the previous question?

Based on the findings related to Questions 4–5 about the behaviour of antenna parameters as a function of use distance, it was interesting to investigate in detail the pattern properties in order to find out:

6. How can one estimate the shape of pattern with distance to tissues?
7. How can one achieve patterns with a smooth shape (without notable minima) over the UWB bandwidth and higher gain to the normal direction relatively to a body surface?

One of the reasons to study Question 6 is that antenna simulations over the UWB bandwidth, including tissue phantom, are time-consuming. In addition to the previous questions, WBAN antennas with complementary characteristics and their effect on the body were studied in this phase.

Next, due to the importance of UWB antennas, the objective was to investigate the impedance behaviour of the radiator in detail in free space and in the proximity of body tissues. The approach was realized by using lumped-element antenna equivalent circuits to answer the research questions:

8. What is the connection between impedance variation and physical antenna dimensions?

9. How can one estimate the physical antenna impedance variation in the vicinity of a body in order to understand the connection between antenna dimensions and effects on a body?

Behind all the presented objectives and interests is the ideology that we need to first understand the operation of a broadband antenna in the proximity of tissue before we can design it properly. Table 1 shows the relationship between the research questions and the original papers investigating them.

Table 1. Relationship between the research questions and the results of this thesis.

Results of the thesis	Research question number								
	1.	2.	3.	4.	5.	6.	7.	8.	9.
[I]	x	x							
[II]		x	x						
[III]	x			x	x	x			
[IV]					x		x		
[V]				x	x				
[VI]				x	x				
[VII]				x	x				
[VIII]								x	
[IX]				x	x				x
in thesis manuscript						x			

1.3 Research methods and materials

The problem-solving method used in the research work was analytic. The research was started by carrying out a literature review based on the stated project objectives and following the focus of the presented research questions.

After defining the hypotheses, the research work started to progress systematically towards the problem solutions. The information related to the system description was based on the available information by the IEEE802.15 WPAN Task Group 6 [28], in which an antenna expert from the WiBAN-HAM project had participated. In addition, books by acknowledged researchers in the field, such as P. S. Hall & Y. Hao [20] and Z. N. Chen [21], were reviewed. The immersion related to the subject of tissues and electromagnetic propagation inside it was mainly based on the books by F. S. Barnes & B. Greenebaum [29], D. A. Sànchez-Hernàndez [30] and D. M. Pozar [31]. The fundamental antenna theory, required throughout the work was taken from the books covering the topic of antennas by C. A. Balanis [32], S. R. Saunders [33], W. L. Stutzmann & G. A. Thiele [34], and B. Allen *et al.* [35].

Since the design of an UWB antenna requires work with changes at the level of millimetres or even micrometres, finding the required variations of the radiator figure shape for the proper wideband impedance matching is impossible to achieve by prototyping with a copper tape. The copper tape-based mock-ups are often used by antenna designers, however, they are not suitable for UWB radiators. Another aspect to consider is the tissues with different thicknesses close to an antenna. Due to these reasons, the simulation-oriented approach was essential.

All the electromagnetic antenna simulations were carried out by using an electromagnetic software by Computer Simulation Technology (CST) [36], which is widely used in the academic world and in industry. The simulation tool uses the finite integration technique (FIT). Simulation packages such as microwave studio (MWS) and design studio (DS) were used in this thesis. The use of a simulator was the enabler and the basis for the work with UWB antenna designs, evaluation of antenna equivalent circuits and consideration of antenna–tissue interactions.

The IR-UWB antennas on a printed circuit board (PCB) were designed and optimized to cover the FCC UWB band [23] based on the bandwidth where the reflection coefficient $S_{11} < -10$ dB. The operation of the antenna simulation models was verified by manufacturing prototypes in the workshop laboratory of the University of Oulu. For the antennas, a widely available substrate material FR4 was used due to its convenient prize and availability, ensuring that the threshold to repeat the investigations is not too high. Real human tissues were used for the comparison of matching performance with simulations, since a valid tissue block/phantom from 3.1 GHz to 10.6 GHz was not available at the University of Oulu. According to the best knowledge of the author, based on the queries to the phantom manufacturers, the current situation in 2014 is that a phantom material valid for the FCC UWB frequency bandwidth does not exist. In the prototype verifications, the vector network analyser (VNA) and Satimo Starlab measurement system [37] were used to verify antenna operation in terms of efficiency and impedance bandwidth.

Several skills and understanding were required through the research of the simulations and practical prototyping. In addition to the measurement skills, understanding about the electromagnetic propagation in free space, in tissues and at their interface, theoretical (mathematical) applicability to solve equations and ability to apply matters and issues from a number of different fields were required.

1.4 Dissertation outline

In Chapter 2, the thesis subject use and application environment is determined. The focus is to study the operation of the IR-UWB antenna in the proximity of tissue. The important characteristics of the antenna are presented in Chapter 3 and the impact of the electromagnetic field on tissues in Chapter 4. Chapter 5 compiles the studied phenomena and interaction mechanism between the body and antenna performance. A summary of the original papers is presented in Chapter 6, followed by the discussions in Chapter 7. The thesis is concluded in Chapter 8.

2 Ultra wideband wireless body area network

In this part, an overview of wearable body-centric communications (BCCs) is provided in Section 2.1. The object of interest is a wireless body area network (WBAN) with ultra wideband (UWB) technology [23]. Section 2.2 generally concentrates on the studied wideband physical layer technology, which is introduced in the international WBAN standard IEEE802.15.6-2012 [22].

2.1 Wearable communications around a human body

Wearable communications around a human body has received lots of attention in the recent years. Research of on-body technologies has become possible because of the continuous miniaturization of devices over the long term as well as the development of computer and sensor technologies.

In [20], P. S. Hall & Y. Hao parallel the latest advances in wearable technologies with the past trends of mobile phones. The dimensions of mobile devices have become smaller and user experience more convenient. From the users' perspective, the corresponding development paths of mobile and wearable communications can be seen as follows [20]:

a) In the beginning of the mobile phone history, "the first equipment was large and heavy, and was used only by those people whose job required it."
b) Then, when the possibility to profit was seen, "the business community saw it as a way improving business operations."
c) "Finally, mobile phone became popular with general population, who used it for social and entertainment purposes, and, more recently, as a fashion accessory."

Currently, the direction of communication systems is towards the future where the range of devices that people carry with them is expanding and devices will probably be designed to handle more user-specific information.

2.1.1 Wireless body area network

As a natural progression from the concept of wireless personal area network (WPAN), WBAN is a possible application in the field of BCCs. The advances in BAN research have been obvious in the recent years: a significant example is the publication of the international standard IEEE802.15.6 [22]. Published in early

2012, the standard is targeted for short-range, low-power and highly reliable wireless communications.

In the WBAN concept, the network nodes are aligned on a body or, alternatively, in close proximity to a body. Some envisioned positions for the nodes, including the sensor(s) and antenna, are shown in Fig. 1.

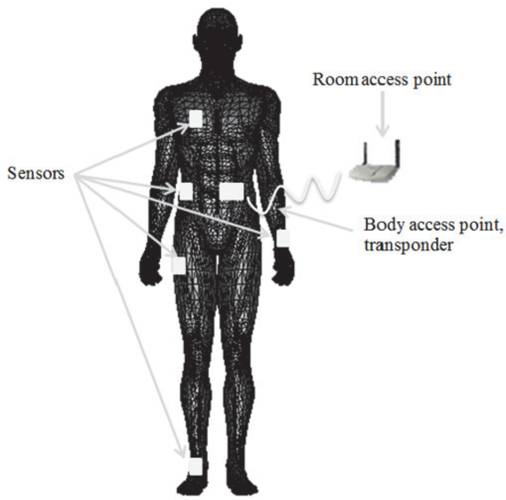

Fig. 1. Illustration of a possible wireless body area network concept.

The original idea for WBANs was based on the interests of the medical and healthcare industry to continuously record patients' blood pressure, heart signals or temperature [21]. An alternative application is to use the sensors to measure some specific sports parameters for athletes, such as acceleration of legs or arms, or strain on foot. In addition, a wide range of potential emergency technology applications are under planning to assist, for example, in emergency and rescue services, military operations, sports, or navigation [21], or in smart home, surveillance and monitoring [20]. One of the visions concerns data transmission primarily from various sensors to a main device or a wearable computer on a body. Then the data is transmitted to a room access point. Finally, the acquired data is transmitted to a hospital, where a nurse or a doctor can study the data on a monitor.

Another regularly discussed application has been monitoring of health parameters by a user with his/her own mobile phone. In the ideal case, WBAN "allows users to enjoy any application with minimum interference and inconvenience and low complexity [21]". Since WBANs are intended to be used around/on a body, the propagation environment comprises free space and lossy medium.

The author wishes to highlight the following characteristic of WBANs: the 'body' of a WBAN can also be an animal or a car. This thesis only covers the human body and the term 'lossy medium' is used to refer to the human body tissues.

2.1.2 WBAN communications

For a WBAN, the communication range is introduced in Fig. 2. In the research field, a typical classification has three categories [20]:

- *off-body*, in the case that only one antenna of the link is on the body and the channel is mainly off the body,
- *on-body*, in the case that both antennas of the link are on the body, and
- *in-body*, in the case that either both antennas are inside the body or one antenna is located in connection with an on-body node and the channel is mainly in the body.

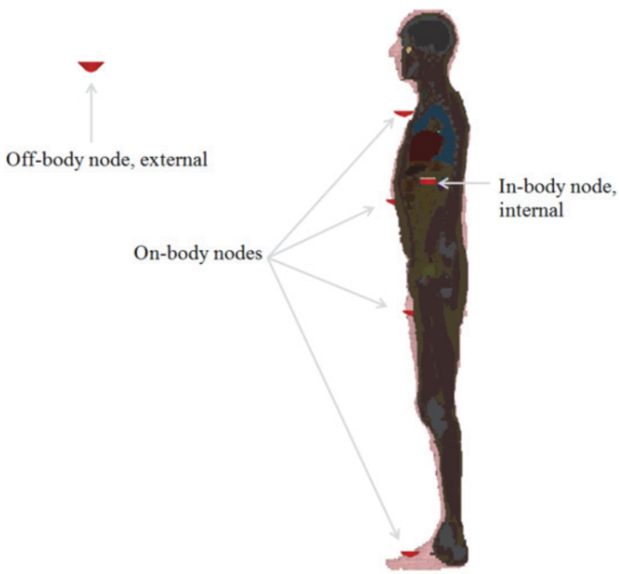

Fig. 2. Demonstration of different methods WBAN communications.

In IEEE802.15.6 [22], the possible physical layer solutions are specified as human body communication (HBC), narrowband technologies and a wideband technology.

For on-body and off-body communications, IEEE802.15.6 specifies both narrowband and wideband frequency areas, such as industrial, scientific and medical (ISM) at 868 MHz (in the EU), 915 MHz (in the US), 2.4 GHz (in the EU & the US) or UWB at 3.1–10.6 GHz. Implantable communications are determined to be handled at the ISM band of 400 MHz due to a better penetration in-body than at higher frequencies. The allocations based on IEEE802.15.6 are presented in Fig. 3.

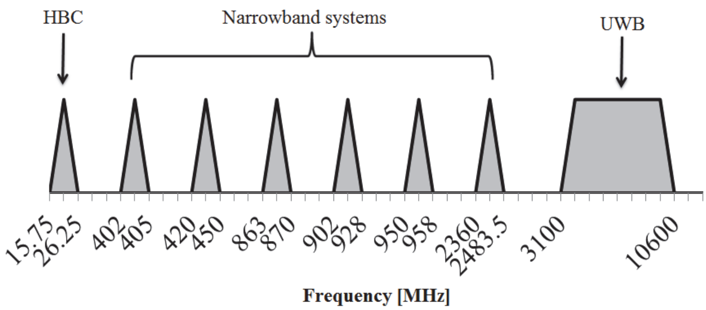

Fig. 3. IEEE802.15.6 PHY-layer technology frequency allocations.

The operation in the vicinity of a body sets conditions for electromagnetic radiation in WBANs, which is one of the reasons for the need of low transmission power. The preferably small size of a BAN device limits the possible sources of energy. Thus, regular battery recharging is not possible for the implanted device. Moreover, large attenuation of electromagnetic waves is faced because of the absorption in body. These are some reasons why UWB is highly suitable for WBAN usage.

2.2 Ultra wideband technology

In the impulse radio technology, very short pulses are sent over a huge bandwidth. The technology has been around for decades, having applications originally in military systems.

The roots of the UWB are in the so-called spark gap transmitters at the initial stages of radio engineering [38]. The FCC issued regulations for the unlicensed use of UWB in 2002 [24]. It gave a significant boost for the research and development in the academic world and in industry [21]. The entire FCC UWB frequency band is occupied from 3.1 GHz to 10.6 GHz and is defined in IEEE802.15.6, as was shown in Fig. 3.

The impulse-based technology is one of the most promising solutions for the future high-data-rate short-range wireless communication. Even though there are challenges with the realization of UWB systems in terms of signalling schemes, complicated algorithms and overall complexity, several advantages make the UWB as an attractive physical layer solution, for instance [24, 35]:

- low complexity and low cost arising from a baseband nature of signal transmission,
- no need for an additional RF mixing stake (due to the baseband nature as an UWB transmitter produces a short pulse in the time domain),
- low energy density and signal characteristic to be noise-like (making the unintentional detection difficult),
- good time domain resolution (providing accurate location and tracking),
- low battery consumption (due to low transmit power and a relatively simple way to generate the transmitter side).

The aim is to achieve efficient use of the limited frequency spectrum. The technology is particularly targeted for low-power radio communication systems.

2.2.1 Signal definition

Based on the FCC regulations, the signal is classified as ultra wideband if the fractional bandwidth f_{BW} by [23]

$$f_{BW} = 2\frac{f_H - f_L}{f_H + f_L}, \tag{1}$$

is greater than 0.20. In (1), f_L and f_H are the lower and higher $S_{11} \leq -10$ dB bandwidths. An alternative way for the classification is that the signal is ultra wideband when exceeding the bandwidth of 500 MHz. The bandwidth for the FCC band is 7.5 GHz and centre frequency f_C is 6.8 GHz.

2.2.2 Waveforms

The FCC regulations [23] made it possible to count the various waveforms with the UWB. The two most common ones, according to [21, 39, 40], are:

i. impulse radio UWB (IR-UWB), i.e., time-modulated UWB (TM-UWB) and
ii. multi-band orthogonal frequency division multiplexing UWB (MB-OFDM-UWB).

In i), the waveform is characterized by the periodic emission of a very short pulse with the typical duration of 2 ns [40]. Thus, it is inversely proportional to the used bandwidth. In this thesis, the IR waveform is only considered.

In ii), the basic idea is to divide the spectrum into several sub-bands, each covering 528 MHz [40]. Thus, 13 sub-bands are required to cover the FCC band. It is emphasized that the waveform in ii) was created in order to separate the FCC UWB spectrum in the US from these sub-bands to fulfil the regulations defined in Europe and Japan (frequency allocations in detail in Subsection 2.2.3).

In [22] and [40], also a frequency modulation UWB (FM-UWB) is introduced, which is sometimes referred to as 'chirp spread spectrum' (CSS-UWB). Even though the waveform is different, in practice both the FM-UWB and the CSS-UWB are close to the MB-OFDM-UWB as both are carrier modulated systems. The exception is in the several sub-bands that are realized in the MB-OFDM to cover the bandwidth according to the FCC regulations. The FM-UWB is also standardized in IEEE802.15.4a [41].

2.2.3 Radiation limits

The FCC has specified the radiation limits for the indoor and outdoor communication applications.

The effective isotropically radiated power (EIRP) can be defined as [42]

$$\mathrm{EIRP} = P_{\mathrm{TX}} G_{\mathrm{TX}}, \tag{2}$$

where P_{TX} is the transmitted power and G_{TX} is the peak gain of an antenna. The FCC regulations determine the total effective transmitted power of the radio to be –41.3 dBm/MHz for indoor scenarios [23, 24]. This means that the maximum power available to a transmitter is only approximately 0.5 mW.

The spectral masks depend on the applications and regions, which are presented in Fig. 4. A recent overview [43] presents the bands intended for UWB communications in different regions. The US FCC regulations cover the unrestricted frequency band of 3.1–10.6 GHz, which is also covered in this thesis.

In early 2006, the European Post and Telecommunications Conference (CEPT) defined the first European authorization [40]. This definition allowed the usage of the unrestricted band from 6.0 GHz to 8.5 GHz only for devices without any mitigation techniques and with the same maximum EIRP as in the US. The definition was given by the Electronic Communications Committee (ECC) Task

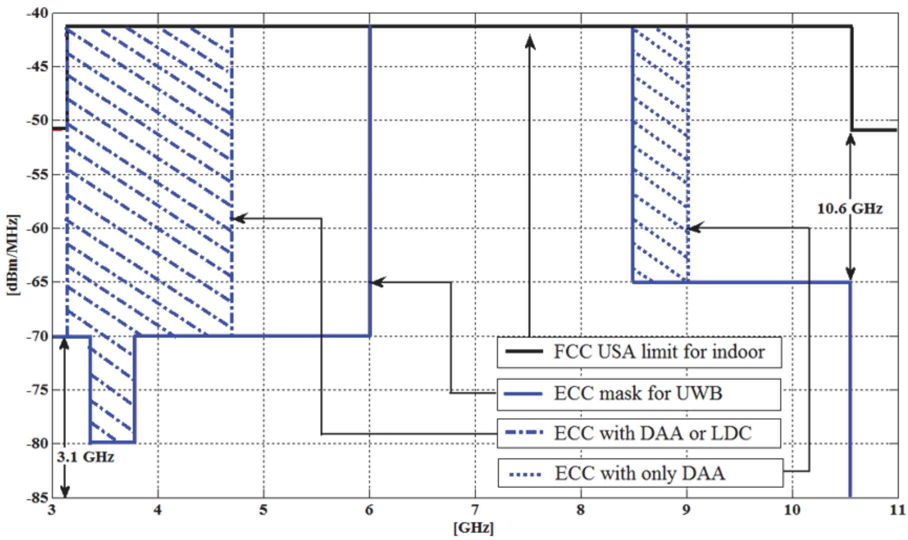

Fig. 4. UWB emission masks for USA and Europe.

Group 3. At the end of the same year, the ECC accepted the use of the detect-and-avoid (DAA) or low-duty cycle (LDC) band from 4.2 GHz to 4.8 GHz [43]. In addition, the ECC have approved the use of the DAA band from 8.0 GHz to 9.0 GHz. In addition to the US and Europe, allocations have been provided in countries such as Canada, China, Japan, Singapore and South Korea. For instance, in Japan, the frequencies 3.4–4.8 GHz are aligned for the DAA and 7.25–10.25 GHz for the unrestricted use. The allocations can be found in [39, 40, 43].

3 UWB antennas: theory, design principles and overview

Throughout the thesis, the aim is to understand the operation of an UWB antenna and to examine its operation in the proximity of human body tissues. The extremely wide bandwidth causes additional challenges for the design of an UWB antenna in comparison with the conventional mobile antennas. The total UWB impedance bandwidth is roughly 80 times larger than in the mobile systems where the antennas are to produce a single, dual or triple resonance. The difference in bandwidth is demonstrated in Fig. 5.

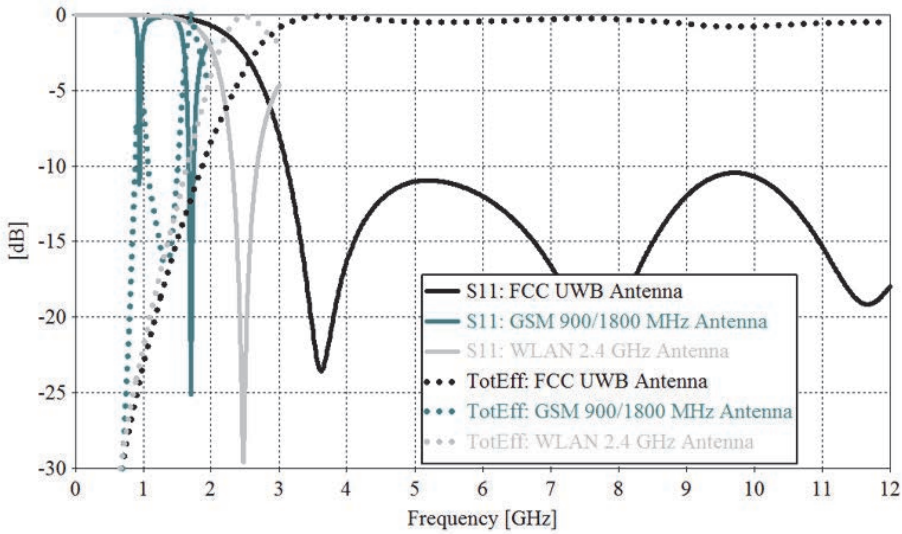

Fig. 5. An example: comparison of impedance bandwidth and total antenna efficiency for GSM900/1800, WLAN/2.4G and UWB/FCC antennas.

The present Chapter 3 discusses several subjects related to UWB antennas and reflects the wide spectrum of the topics to understand in the context. The information is mainly based on books [20–21, 24, 35, 40, 44] and top-class journals [45–46] in addition to the reviewed articles in Sections 3.4–3.5. The following paragraphs describe the content of each section of this chapter.

In [24], an UWB antenna is presented to act as a pulse-shaping filter for the generated signal allowing only the radiated signal components to be passed. In particular, the antenna produces a derivative of the transmitted or received pulse waveform. The impact of the waveform on the characteristics of an antenna is discussed in Section 3.1.

Producing the derivative has a drawback in terms of the impact on extending the duration of the pulse, which decreases the time resolution of the system further. The phenomenon can be mitigated by designing the antenna to own the non-resonating operation. At the end, the distortion of a signal is avoided. The undesired characteristics of the UWB antennas are discussed in Section 3.2.

As antennas in narrowband systems are usually resonant elements, they are simply tuned to the right resonant frequency and can be characterized by using a reflection coefficient, gain and efficiency, for instance. However, the same parameters are not directly useful for the characterization in the case of UWB [20]. In Section 3.3, the additional parameters are determined, which are needed for the analysis [21] in order to take into account the large frequency bandwidth and the type of the waveform.

Due to the above-mentioned reasons, the design of a suitable antenna is one of the challenges in the implementation of an entire UWB system. An apt remark was stated by X. Begaud, who has said that the design of the UWB antenna is "more delicate because it is subjected to more constraints and because their behaviour is more difficult to understand and to qualify" [40]. Actually, this is one of the objectives of the thesis: to concentrate on the analysis of the operation of the IR-UWB (WBAN) antenna. An example of useful and accepted tools for gaining understanding about the antenna operation are the antenna equivalent circuits, which are investigated in the thesis. The IR-UWB antenna designer is more interested in the physics of an antenna, and particularly in the time-related operation. A brief overview of the suitable IR-UWB antenna types is given in Section 3.4, followed by an overview of the UWB WBAN antennas in Section 3.5.

Section 3.6 concludes Chapter 3 by discussions. Since the objective of the research is to understand the UWB antenna operation in the vicinity of tissues, the simple radiator structures are preferred to consider. H. Schantz has proposed a planar elliptical dipole antenna in [47, 48] to be an example of a non-dispersive antenna and demonstrated transmitted (TX) and received (RX) impulses without distortion for the antenna [48]. In this thesis, the elliptical dipole is considered as a reference antenna several times, particularly in the studies that require understanding about the behaviour in the proximity of a body. The operation of a dipole is easy to understand and it is widely known in addition to the polarization purity it has. In the case that one understands the operation of a simple dipole antenna comprehensively for the surroundings of a WBAN, the favourable prerequisites can be assumed to be able to apply the information for the analysis of more exciting antenna solutions.

3.1 Impact of waveform on antenna characteristics

The UWB system waveform is reported to have an impact on the antenna design objectives. Even though the differences in design targets have not been widely reported, the information is available in the open literature. The distinct specifications of antennas in this section are based on the references [21, 24, 35, 42, 49–50]. Despite this, a comprehensive understanding about the different antenna requirements between the waveforms is not clearly visible in the references. This insight is based on the facts that there is only limited amount of information available on the issue and the available knowhow about the antenna requirements between the references is slightly conflicting. The discrepancies may arise from the fact that the research is ongoing and these issues will hopefully be clarified in the future.

3.1.1 IR-UWB

Due to the impulse-type operation, the IR waveform is discussed in the open literature as being the more challenging approach than the MB-OFDM from the antenna point of view [21, 42, 49].

The IR-UWB antenna works as a band-pass filter, reshaping the spectra of the radiated and received pulses [21]. Ideally, the antenna should produce the radiation fields of constant magnitudes and a phase shift varying linearly with the frequency. One of the most used antenna parameters to analyse the phase linearity is group delay (defined in Subsection 3.3.3). In addition to group delay, constant gain and unchangeable polarization with high radiation efficiency and a wide impedance bandwidth are the most critical requirements [21, 42, 49].

In general, the UWB antenna parameters should be optimized for avoiding the distortion of radiated and received pulses. A resistive loading is reported causing the unwanted signal component to die away quickly [24]. However, the information is slightly discordant with some other references [21, 49, 42] because the resistive loading is realized by introducing more losses in practice, thus resulting in the trade-off with antenna efficiency.

In addition to H. Schantz [44], Z. N. Chen [21] mentions that a small element antenna as a planar elliptical dipole will be a good choice for the IR-UWB since it tends to radiate a more compact, non-dispersive waveform, similar to the Gaussian pulse. Based on the recommendations in the open literature, the planar elliptical dipole is used for the examinations several times in this thesis.

3.1.2 MB-OFDM-UWB and FM-UWB

The titled waveforms are reported to be more tolerant for the dispersive antennas, such as a log-periodic antenna, compared to the IR-UWB. The FM-UWB endures the dispersive characteristics because of the fashion to cover multiple sub-bands [21]. Each sub-band is to cover the bandwidth of some 500 MHz, which is the reason why the effect of phase linearity within the sub-bands is not as significant as for the IR-UWB. Thus, the design is more intent to achieve constant frequency response in terms of only efficiency, gain and reflection coefficient. Based on the references [21, 42, 49], the design of the MB-OFDM-UWB and FM-UWB antennas seems to be closer with the design of a mobile antenna, with the exception of a notably wider bandwidth.

3.2 Undesired characteristics

Dispersion is probably one of the most often discussed design challenge, problem or unwanted feature of an UWB antenna according to conference and journal articles. However, dispersion is not the only undesirable UWB antenna characteristic [21, 40, 44]. Thus, this section determines the terms ‘dispersion’ and ‘distortion’ in more detail.

3.2.1 Distortion

In [40], X. Begaud defines that any deformation of a signal waveform is related to the phenomenon called distortion. Z. N. Chen supports the insight by stating that the UWB antenna should produce the radiation fields of constant magnitude and a phase shift varying linearly with the frequency to prevent the distortion of received pulses, which is the reason why distortion is a parameter that is related to signals [21]. The term is not used incorrectly when referring to distortion of a system or device, but typically distortion is used for signal waveform deformation [40]. Against this context, due to the nature of the UWB antenna to be a passive linear component, we are only interested in the sources of linear distortion [40]. Unsuitable antenna design is the reason for signal distortion at the end. However, distortion is not a parameter to be examined, but the antenna might have dispersive features defined in the following section, which is the reason why the signal distorts.

3.2.2 Dispersion

Generally, dispersion is related "to the frequency variation of the propagation velocity of waves". H. Schantz states that "dispersion is the stretching out of a UWB signal waveform into a longer, more distorted waveform." [44]

Dispersion might be the reason to constitute some forms of distortion such as the phase distortion. The parameter has the dependency on a look angle [44]. In addition, dispersion is connected with the antenna phase centre (defined in Subsection 3.3.3): "If the phase centre moves as a function of frequency, the resulting radiated waveform will be dispersive." [51] However, dispersion can be compensated as it happens in a predictable fashion [44]. A possible method to mitigate the phenomenon is with the help of a filter that may undo the dispersive effect of an antenna [52]. An alternative approach is to compensate the dispersion by using the resistive loading for the antennas with low Q-values [24]. This is explained to enable the unwanted signal components to die away quickly; however, introducing resistive loading is achieved in practice by decreasing antenna efficiency.

A dispersive nature of an UWB antenna resulting in distortion can be avoided with the proper antenna design. One of the most important parameters to optimize to avoid dispersion is antenna impedance in a way that it appears smooth. This can be achieved by optimizing antenna impedance with the radiator shape, which is one of the issues highlighted in this thesis. Another related issue is the way to excite an antenna, which has an impact on the dispersive characteristics. In the case that an antenna is linear in phase with a fixed phase centre, the circumstances are favourable to avoid ringing. Nevertheless, the mitigation of the dispersive characteristics of the antenna structure is not achieved easily. This requires understanding about the broadband features of an antenna. There are parameters that can be used to reveal the non-dispersive behaviour of an antenna, which are discussed in the next section.

3.3 Parameters to analyse the IR-UWB antenna

Most of antennas are traditionally designed in the frequency domain. Even though the UWB antenna can also be analysed in the frequency domain, time domain responses are useful at the time of evaluating the entire system performance to consider channel impulse responses. In the time domain, the characterization of an antenna is realized to examine the ability of an antenna to preserve the waveform of the ultra-narrow pulse, and the impulse response is of the highest importance [21]. A presentation of the useful parameters for the IR-UWB antenna is given in this part.

3.3.1 Impedance matching

An UWB antenna designer is firstly interested in achieving wide impedance matching. The impedance of an antenna and the shape of a radiator have a significant impact on the operation because an antenna shape is usually modified to acquire the optimal input impedance in order to widen the bandwidth. It should not be diminished by the fact that matching components, which are often used with the narrowband antennas, are not allowed in the IR-UWB systems due to causing additional time-delays [53].

Matching the UWB antenna concept is something that is required in the design process from the very beginning due to the above-mentioned connection with the radiator shape and the feeding area. The inherent impedance match is the keyword for an UWB antenna. An apt remark is given in [42], according to which "to match an ultra-wideband antenna one must first start with a well-matched antenna."

Compared to the evaluation of traditional antenna matching, where the Smith chart is an invaluable tool, UWB antennas are considered by using the real and imaginary parts of input impedance Z_A together with the reflection coefficient Γ that is expressed by using $|S_{11}|$. An alternative way is to use voltage standing wave ratio (VSWR). The definition of Z_A includes the antenna resistance R_A and the antenna reactance X_A at terminals as [32, 33]

$$Z_A = R_A + jX_A = (R_R + R_L) + jX_A. \quad (3)$$

The antenna resistance can be announced with the sum of the radiation resistance R_R and loss resistance R_L. Usually, the specifications of –10 dB bandwidth for S_{11} and VSWR < 2:1 are used for UWB antennas [21, 24].

As an UWB antenna operates over the large FCC bandwidth, multiple resonances are fundamentally introduced for the frequency coverage. The issue that is particularly important to understand concerns the reflection coefficient: even though the antenna impedance bandwidth is created by introducing multiple resonances, the reflection coefficient must be optimized in a way that it appears smooth. In other words, $|S_{11}|$ should look like a non-resonant operation despite the fact that there are multiple resonances behind the picture. In the case that the non-resonant $|S_{11}|$ cannot be achieved, the antenna operates most likely in a different way with the frequency, resulting in the non-linear phase, and thus the signal will most probably face dispersion. The resonant-type antennas should be shirked or their impedance characteristics should be modified such that the reflection coefficient appears as smooth as possible. This causes additional design challenges for the antenna, for instance, in a real UWB device where the antenna should be operated with the sufficient distance to near-by mechanics to force the desired impedance behaviour.

3.3.2 Radiation characteristics

Radiation performance is characterized in terms of the traditional antenna parameters such as efficiency, gain, patterns, and polarization.

Total efficiency e_0 is the parameter taking into account losses at the input terminals and within the structure of an antenna by [32]

$$e_0 = e_c e_d e_r = e_{cd}\left(1 - |\Gamma|^2\right), \tag{4}$$

where $e_r = 1 - |\Gamma|^2$ is the reflection (mismatch) efficiency, e_c conduction and e_d dielectric efficiencies forming the radiation efficiency $e_c e_d = e_{cd}$. Thus, e_0 includes all the losses of the antenna structure in addition to the losses caused because of the environment, e.g., of body tissues. The parameter e_{cd} only describes the ratio of the total power radiated by an antenna to the power accepted by an antenna from the connected transmitted [54].

Gain is discussed to be the parameter with the connection to possible signal distortion in the IR-UWB systems. In the case that gain is constant, the antenna tends to avoid the dispersion of the transmitted pulse [55].

The pattern dependence on the frequency for a planar elliptical dipole with the doughnut-shape in the lower frequencies in Fig. 6 is an important criterion for the UWB antenna. The pattern shape should be maintained over the bandwidth [42]. The appearance of the higher-order modes is visible in the upper end of the frequency range. The change of the pattern shape with the frequency is rapid. This challenge is linked to the appearing reflections in the proximity of a body (discussed in Subsection 4.2.2). However, the pattern shape does not disintegrate close to body as strongly. Fig. 7 depicts the following higher-order modes at 11 GHz and 15 GHz after 3 GHz, which appear in the case that the bandwidth is further extended.

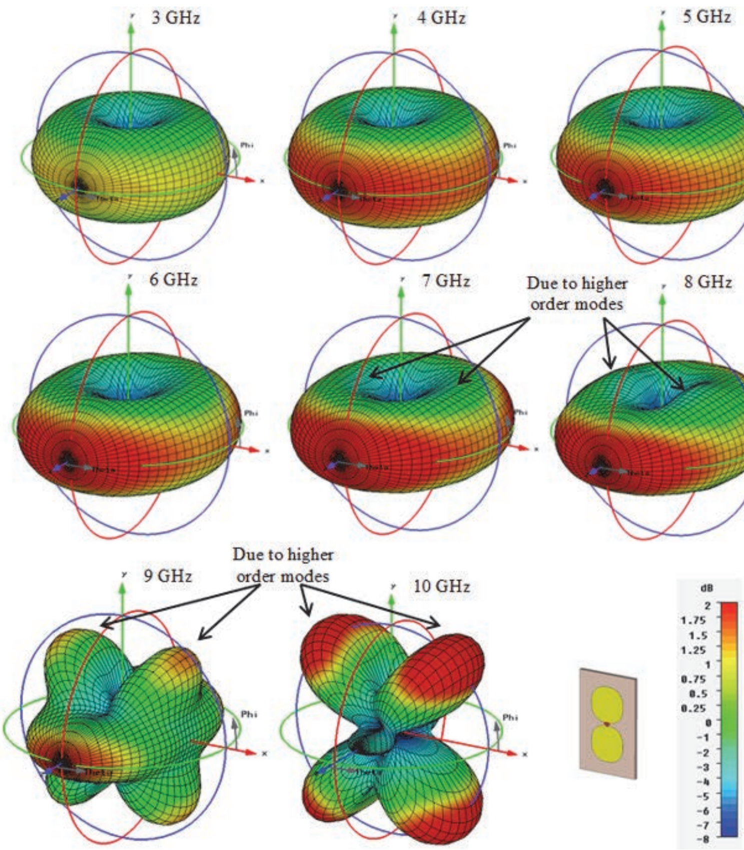

Fig. 6. An example: patterns of a planar elliptical UWB dipole.

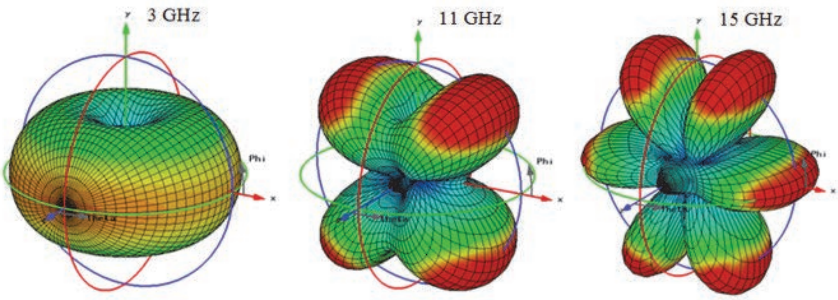

Fig. 7. An example: generation of some higher-order modes for UWB dipole.

3.3.3 Group delay and phase centre

The non-dispersive antenna behaviour can be evaluated based on group delay. The parameter is used to verify the constant phase characteristics of an antenna. In the case that the radiator structure owns a constant group delay, the phase of the antenna is linear for the frequencies of interest. At the end, there are no significant nonlinearities implicating that the radiator structure stores the energy. The energy preserve results in the dispersive fashion and signal distortion.

The group delay τ_{GD} is calculated with the rate of change of the total phase shift $\Delta\psi$ with respect to the angular frequency $\omega = 2\pi f$ as [21, 56]

$$\tau_{GD} = \frac{d\psi}{d\omega}. \quad (5)$$

In some contexts, also mean group delay is used, which describes the mean value of τ_{GD} as a number over the band.

The way to use group delay is not always specified in the literature. Some papers present the group delay to verify the constant phase characteristic of an antenna. However, the confusion is that the parameter is calculated from the phase of S_{21}, which concerns the phase of the channel. In the case of an individual antenna, the phase should be calculated by using S_{11}. If the phase is calculated based on the channel, S_{21} is different for each studied distance between the antennas, thus causing variation. In addition, the channel is dependent on several variables such as the environment and angles. Due to these reasons and the discussions with colleagues in the field, an UWB antenna designer should be interested in optimizing the phase of an individual antenna by S_{11}. At the time of the system verification, it is also reasonable to consider τ_{GD} based on S_{21}.

The effect of the rounding of a planar elliptical dipole on the group delay performance and reflection coefficient is depicted in Fig. 8. The figure shows a basic feature, which should be optimized for the IR-UWB antenna in order to create a smooth S_{11}. In other words, the deep resonances should be avoided: for the studied dipole, the smooth impedance is achieved by making the radiator shape elliptical. The desired operation is acquired since the lowest resonance at 3.6 GHz, created with the length of the dipole, diminishes because of the shape of the rounding. In practice, the imaginary part of Z_A in (3) increases and becomes more inductive. At the end, the result is a constant τ_{GD} because of the linear phase. In WBAN scenarios, group delay is automatically more flat in comparison with free space because tissues smoothen the deep resonances of the reflection coefficient.

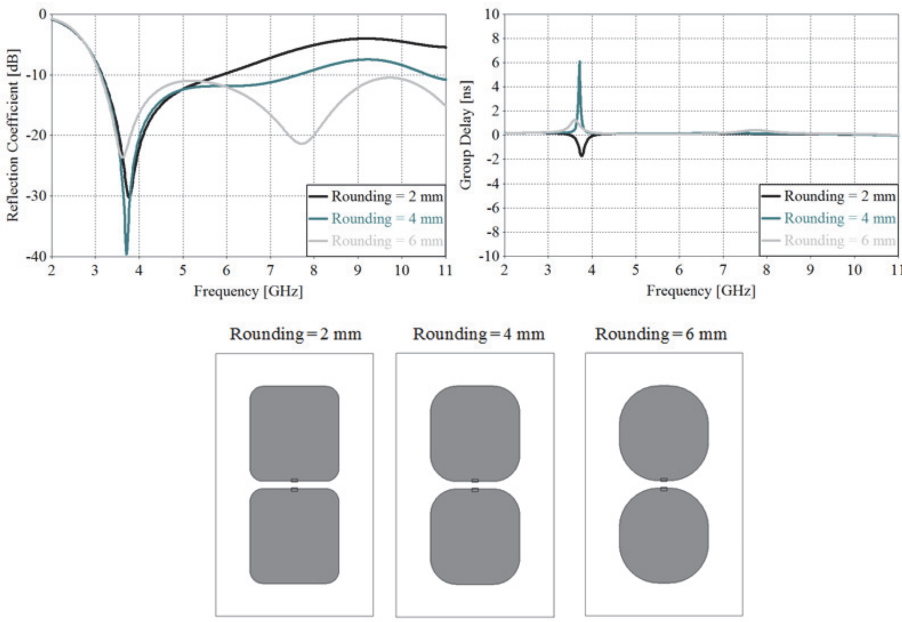

Fig. 8. An example: impact of dipole plate rounding on group delay and reflection coefficient performance.

In the context of the linear phase of an antenna or a possible inconvenience of nonlinearity such as phase distortion, the term phase centre is often used in the field. As the linear $\psi(\omega)$ results in the constant τ_{GD}, the phase centre is not then dependent on frequency [46]. C. A. Balanis explains that the phase centre is assigned as the reference point for the antenna in the situation that the phase is independent of azimuthal and elevation angles for a given frequency [32]. This can be expressed with the help of each far-field component, which are radiated by an antenna as presented by [32]

$$E_{\mathrm{u}} = \hat{\mathrm{u}} E\left(\theta,\varphi\right) e^{-j\psi(\theta,\varphi)} \frac{e^{-jkr}}{r}, \tag{6}$$

where the terms $E(\theta, \varphi)$ and $\psi(\theta, \varphi)$ represent the variations of θ and φ of amplitude and phase, and $\hat{\mathrm{u}}$ is unit vector. In (6), a fixed phase centre means the independency of phase ψ of angles azimuth φ and elevation θ angles for a given frequency which is the reference point. C. A. Balanis explains about the nature of the considered parameter that "the fields radiated by the antenna are spherical waves with ideal spherical wave fronts [32]", if referred to the phase centre. The phase centre is the point from which radiation is said to flow (i.e., emanate) and these radiated fields have the same phase when measured on the surface of a sphere whose centre coincides with the phase centre [32]. The phase centre of the planar elliptical dipole is considered in Fig. 9.

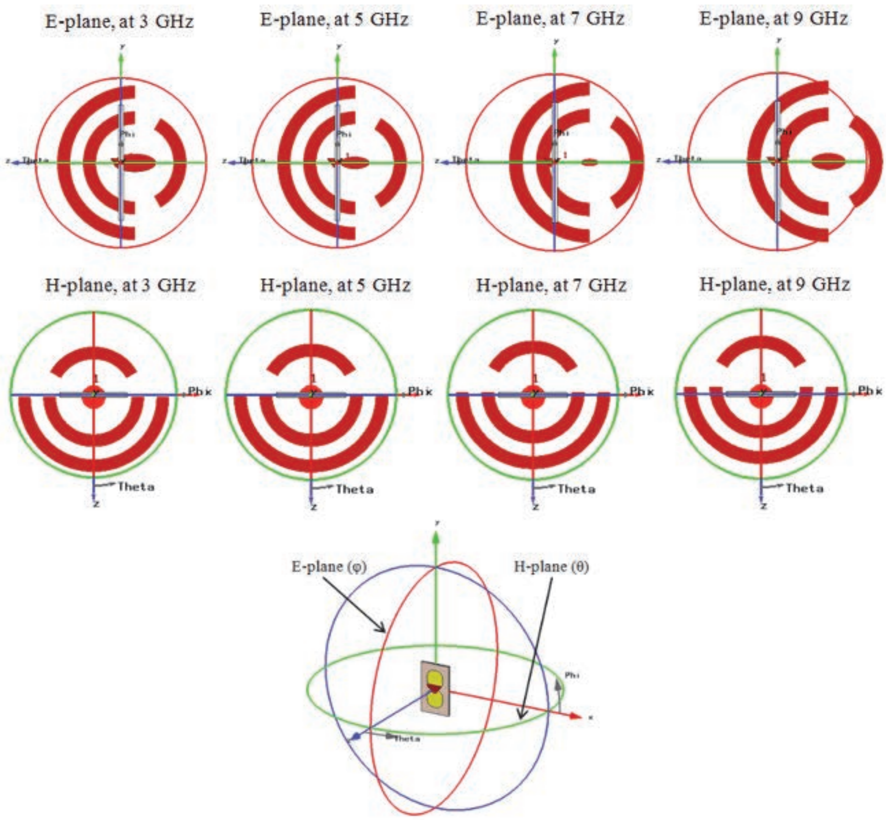

Fig. 9. An example: phase centre for the planar elliptical dipole.

3.4 Overview of the IR-UWB antennas

The opening of the spectrum for the unlicensed radio applications by FCC in 2002 gave a great boost for the research of UWB antennas. A huge number of articles were published between 2002 and 2014.

As concluded in [45], the goal in the numerous UWB antenna publications in the literature is often to present some kind of antenna that covers the desired S_{11} bandwidth and the moderate radiation patterns with the frequency. As introduced ahead, there are several additional characteristics need to be considered in the design. The antenna type has a significant impact on the suitability of the antenna for the UWB system. Based on the review of the open literature, the antenna types of dipoles and monopoles are widely used for UWB systems. The small-sized UWB antennas with omnidirectional characteristics are of interest. The following paragraphs provide an overview of the antenna types suitable for the IR-UWB.

Several types of IR-UWB dipoles have been examined. H. Schantz & L. Fullerton reported a diamond-shaped dipole to have the good characteristics of the IR-UWB systems such as non-time dispersive response with the matched input impedance [57]. A planar elliptical element and bottom-fed elliptical dipoles are also verified as well-matched high-efficiency radiators for the IR-UWB usage [47, 48]. Even though a planar dipole structure might suffer from cable leakage currents, the study in [58] presents that a co-planar waveguide-fed dipole design can mitigate the undesirable cable current effects. It should be noted that the leakage current cannot be stopped altogether, but a strong component can be decreased in a way that antenna patterns with the proposed slots are closer to the patterns of an ideal dipole than the antenna without such slots. X. N. Low *et al.* have reported that the length of an UWB dipole can be reduced by using a shorting bridge [59], while the radiation performance in terms of the maximum gain and the gain stability were observed to improve. Hence, flat gain (in the frequency domain) or less distortion (in the time domain) can be achieved with the proposed antenna structure. By modifying the shape of a dipole or slotting it, antenna gain can be increased while low ringing and pulse distortion are achieved [60, 61]. Also, band rejection characteristics, which might be required for some applications, have been examined earlier for UWB dipoles in [62]. X. H. Wu *et al.* have further presented the comparison of four different planar dipoles for UWB applications in [63]. A traditional dipole has been widely accepted for the usage in the IR-UWB.

In addition to dipoles, monopole-type antennas are widely studied for the IR-UWB operation. The performance of wideband planar monopoles, such as circular and elliptical disc, and rectangular and hexagonal antennas has been compared in [64]. In addition, J. A. Evans *et al.* have examined the operation of an UWB trapezoidal and pentagonal monopoles for low frequencies to show desirable characteristics for the wideband operation [65]. The matching properties of the monopoles were investigated and the studied structure was found to have nearly omnidirectional radiation over the entire UWB band in [66]. In addition, a slotted ground plane solution has been studied in order to examine ways to reduce the ground effects on monopoles [67]. The size of the antenna can be reduced from the general size of such antenna, i.e., 40 × 40 mm, down to 30 × 30 mm or 25 × 25 mm. However, as a drawback, the impedance characteristics of the printed designs might suffer. The authors in [67] found that by slotting the ground plane, i.e., making a notch, the structure concentrates on the majority of the electric current on the radiator, particular at lower frequencies.

Some co-planar waveguide-fed quasi-magnetic antennas have been optimized for UWB applications in [68, 69]. In addition, the printed rectangular slot antenna with a co-planar waveguide feeding can yield a wide bandwidth operation [69]. The advantages of these, e.g., the injurious effect of employed feeding techniques, which is the origin of limiting bandwidth, can be counteracted with the proposed structures while maintaining a wide bandwidth and stable patterns. H. Schantz has introduced complimentary tapered bow-tie magnetic slot antennas to achieve beneficial advantages such as reduced cable currents and to allow polarization diverse for the UWB systems if used in conjunction with a UWB dipole [70, 71]. In addition, studies of low-profile wideband loop antennas have been presented [72–74]. These papers reported that in particular the shape and form of the feeding has a strong impact on the achieved impedance bandwidth of an UWB antenna.

The used antenna substrate materials in the articles were also considered to get an idea if there are some widely used materials in the field. Most of the substrate materials in the reviewed papers were in the range of $2 < \varepsilon_r < 5$ similar as to the widely available FR4 or some substrate products by Rogers [75]. The substrate thickness varied between 0.8 mm and 1.6 mm.

3.5 Overview of the UWB WBAN antennas

At the end of the last decade, interest in BCC research started to spread. Even though there are thousands of UWB antenna designs for free space operation in the literature, the number of wearable UWB WBAN/on-body antennas is significantly smaller.

A summary of the literature review of the published journals presenting UWB antennas for WBAN applications is provided in this section. The journals considered are published by the IEEE (e.g., Transactions series or Antennas & Wireless Propagations Letters), IET (e.g., Microwave, Antennas & Propagation proceedings) and Progress in Electromagnetics Research.

The first journal article of the reviewed papers discusses the effect of the human body on UWB antenna operation. It was published at the same time with the FCC regulations in 2002 [76]. This preliminary study was experimental and the main output was that the human body creates a deeper null in a light than in a dense multipath environment.

In 2005, A. Alomainy *et al.* [77] presented the statistical path loss parameters and channel characteristics based on the measurement campaign with two types of antennas. They also indicated that the hybrid use of different antenna types can improve the on-body channel performance. During the same year, the study in [78] was carried out to design a directional wearable UWB antenna. As in the normal WBAN operating scenario, also the performance of the proposed antenna was examined in free space and close to a body. It was concluded that in free space situations, a directional antenna performs better than a monopole because of the more stable pattern over the frequencies of interest. The impedance matching of the proposed antenna was observed to be stable on a body and the SAR performance was concluded to improve compared to omnidirectional antennas.

In 2006, Z. N. Chen *et al.* presented two articles regarding wearable UWB antennas in [79] and [80]. The former article [79] is more like an overview and a summary of the evolution of planar antenna structures. In the article, the authors concluded that planar antennas and their variations have shown, in general, attractive features such as broadband impedance and radiation bandwidth, small size and easy to fabricate. The latter article [80] reports the study of the effect of the human head on the operation of two planar UWB antennas. The results showed that when the antenna is aligned close to a head, although matching is not strongly affected, the radiation patterns become very directive on the horizontal planes. Interpolation techniques based on the sub-band finite-difference time-domain (FDTD) method and the combination of theory of diffraction and ray tracing were examined in [81] in order to model the dispersive fashion of tissues for UWB on-body channel modelling. The advantage of sub-band FDTD was concluded to have the ability to model materials with any type of frequency dependency. In addition, the modelling results of this study highlighted the strong impact of the antenna pattern on the on-body channel performance. In the article in [82], the effect of an antenna on electromagnetic energy absorption in terms of SAR for UWB antennas was studied, which was aligned on a three-layer tissue model including skin, fat and muscles. Different distances to the tissue model were considered, and the general conclusion was that very high SAR levels were found close to the body.

The perpendicular and parallel wave polarizations with respect to a body surface were considered for UWB antennas in 2008 in [83]. The authors stated that perpendicular polarization outperforms the parallel one. In 2009, T. S. P. See

& Z. N. Chen [84] published a comparison of three different UWB antennas (omnidirectional, directive and diversity) where the experimental characterization of pattern properties was examined on a chest of a body. They concluded that the omnidirectional antenna is the most sensitive to effects caused by a body in terms of polarization and pattern. The transient characterization of wearable UWB antennas is presented in [85] and a significant size reduction with the proposed antenna structures were shown.

In 2011, the electromagnetic coupling between an antenna and a body in BAN communications was considered for UWB application in [86]. Two different antennas were examined and a mounting method was proposed to provide a more stable response for the UWB WBAN antenna. The proposed mounting was observed to decrease the amount of coupling as well as the radiation passing into the user. Another UWB WBAN antenna for on-body communication was presented during the same year by N. Chahat *et al.* [87]. The proposed structure was characterized in free space and at different distances to tissues for various body models, and satisfactory performance in terms of matching, patterns, e-field distributions and pulse distortion was acquired.

T. S. P. See *et al.* presented an experiment of UWB WBAN applications for on-body communication in 2012 [88]. They found that radiation properties (omnidirectional, directive, diversity) and polarization (vertical and horizontal) have a strong impact on the link reliability. If the body is on the channel as a blockage, normal polarization is more stable from the path gain perspective compared to the tangential one with respect to a body surface. The article in [89] also presented results for a wearable UWB antenna in free space and an evaluation of on-body performance. As in [88], the authors in [89] found a significant effect on antenna polarization on link performance. The very recent studies in [90–91] presented two different wearable UWB antenna structures. The former discussed dielectric loading resulting in enhanced impedance bandwidth. The latter proposed a band-notched UWB antenna which is able to reject the WLAN band at 5 GHz.

Review notes

During the review, the exhaustive repetition of the studies was found challenging. Obviously, on the academic side, the repetition should be an appreciated, self-evident feature of articles. The shortcoming in many papers concerned the indication of all the required

– dimensions to model the antenna,
– properties (ε_r, thickness, name, supplier) to model the antenna substrate,
– information about the tissue model and tissue properties, or
– measures in the measurement setup.

In addition, the missing information made it more difficult to fully understand the overall performance of the wearable antennas in question and to assess the method to verify the on-body performance.

A usual approach to start the design process of a wearable UWB antenna was first to evaluate the operation and behaviour in free space. The natural next step was to acquire information about the on-body performance, and finally, to implement the possible required changes to achieve the desired operation on or close to a body. The approach sounds effective and reasonable due to the fact that simulations including phantom models following the FCC regulations are time-consuming. Another point of view supporting the approach is that the same wearable antenna might be used either in free space or close to a body, depending on the WBAN scenario. Thus, it is straightforward to study the free space antenna design and to implement the needed turns to achieve the desired operation and performance. Naturally, due to the presence of lossy tissues, the antenna size was notably reduced on a body in comparison with free space. Several papers reported stable matching characteristics for the UWB antennas, which is understandable, since they are known to be robust against detuning on a body due to their broadband fashion to operate [45]. The behaviour on a body differs with the narrowband radiator that faces clear resonant detuning. Even though the UWB antenna bandwidth is seen to broaden close to the body for the lower and higher frequency bands, it is not seen as the clear shift of a resonant frequency.

During the review of literature on UWB WBAN antennas, the content of the journal articles was summarized in terms of the used 1) antenna type, 2) substrate permittivity, 3) substrate thickness, and 4) ways to define tissues if realized by electromagnetic simulations. From the aggregate results in Table 2, it can be seen that monopole antennas were used in 52% of the studies, dipoles in 35% and slot antennas in 11%, respectively. In each study, due to the deliberate non-disclosure or the poor way to present the information, it was not understandable which antenna substrate was used for the examination. The decipherable values of substrate relative permittivities vary in the range of 2–5, see Table 3. As visible in Table 4, the thickness of the antenna substrate was mostly larger than 1.0 mm.

Seven studies reported the evaluations of the results with a phantom by using a simulator. In Table 5, only in three of these papers, the dispersive tissue model definitions in terms of Debye or Gabriel were used. In addition, one study reported using the interpolation method for tissue determinations. In the last three articles, a single-point method of modelling tissues over the UWB frequencies was reported.

Table 2. Summary of the antenna types used in the reviewed papers.

Type (amount)	References: [number]-year of publication
Dipole (6)	[76]-2002, [77]-2005, [81]-2006, [83]-2008, [85]-2011, [89]-2013
Monopole (9)	[77]-2005, [78]-2005, [80]-2006, [81]-2006, [82]-2006, [84]-2009, [87]-2011, [88]-2012, [90]-2013
Slot (2)	[82]-2006, [85]-2009

Table 3. Summary of the antenna substrate permittivity used in the reviewed papers.

Permittivity ε_r (amount)	References: [number]-used ε_r
ε_r< 4.0(10)	[77]-3.0, [78]-2.2, [80]-3.38, [81]-3.0, [82]-2.2, [85]-3.0, [84]-3.38, [87]-3.5, [88]-3.38, [77]-3.0
4.0 <ε_r (3)	[82]-4.3, [84]-4.3, [85]-4.3

Table 4. Summary of the antenna substrate thicknesses used in the reviewed papers.

Thickness t_s [mm] (amount)	References: [number]-used t_s
textile (1)	[86]
t_s < 1.2 (4)	[80]-1.0, [84]-0.8, [85]-0.6, [88]-0.8
1.2 < t_s (8)	[77]-1.5, [78]-1.6, [80]-1.5, [81]-1.5, [82]-1.5&1.6, [85]-1.5, [84]-1.6, [87]-1.6

Table 5. Summary of the ways to define tissues in the reviewed papers.

Tissue Definition	References: [number]-used model
Dispersive	[80]-Debye; three-pole, [83]-Gabriel/Cole-Cole; four-pole, [85]-Debye; one-pole
Single-point	[78], [82], [87]
Interpolation	[81]-12 point

3.6 Discussion

As mentioned ahead, thousands of UWB antenna structures have been reported in the open literature. When searching the IEEE Xplore library [92] with the term ‘UWB antenna’, some 5,500 results were returned in March 2014. Approximately 79% of the results of the search were published in conferences, while some 20%

in journals and magazines. By limiting the search by adding the term ‘on-body’ to the earlier search, only around 100 results were achieved (23% of which were published in journals and magazines and 77% in conferences). The content of the last search ‘UWB antenna on-body’ does not directly provide the publications giving answers to the designer who is interested in analysing the operation of the UWB WBAN antenna. For example, for the last search, the most relevant result suggested a conference article discussing on-body UWB MIMO antennas with only some results of matching and patterns, practically without any explanations and reasons for the operation and behaviour on a body. As can be seen from the search, on-body UWB antennas have obviously been the topics with minor interest in research in relation to free space radiators. Based on the literature review, the analysis of the research results seems to been rather superficial. The go-ahead idea in the literature often seems to be to find out some solution to cover S_{11} bandwidth close to a body with some specific antenna structure. It was challenging to get an idea of how to design a WBAN on-body antenna or which additional tools were required for the design. It seems rational to study the interaction mechanisms and desirable antenna properties first before presenting novel solutions.

It was observed that there are several differences in the design principles between the UWB and narrowband antennas. In addition to the discussed issues, a significant discrepancy comes from the device concept’s perspective, which is related to the ideology of how to design an UWB antenna for a device in the future. In mobile phones and laptops, the concept evaluation approaches seem to be primarily based on the industrial design and a mechanical concept followed by the addition of antennas to a device. As the antennas are designed independent of the other mechanical elements, the design has a significant impact on the operation of the antennas. For narrowband radiators, the approach could be possible since the requirements are often rather simple: to meet S_{11} of –4 dB or –6 dB over the band or efficiency against some operator requirements. In addition, another important thing is that narrowband antennas can be forced for the proper frequency band by matching components. However, in the case of an UWB device, the uncoupling of an antenna afterwards is complicated, or probably impossible, due to the nature of the UWB antenna to establish the impedance bandwidth based on the shape of the radiator and feeding areas.

In [40], X. Begaud presents that ‘temporal behaviour’ of the operation of an UWB antenna is more complex than with narrowband antennas. The UWB antenna is more difficult to understand. Therefore, it is highlighted that “the design of UWB antennas is thus not only subjected to the ‘ordinary’ constraints of antenna design (cost, size, integration, efficiency, etc.), but is subjected to ‘particular constraints’” [40]. For example, the author mentions three issues of these constraints. The first is the matching bandwidth (which is very wide in UWB), the second is control of dispersion (e.g., phase centre), and the third is distortion (the deformation of the waveform).

4 Electromagnetic field in the proximity of body tissues

In Chapter 4, electromagnetic fields in propagation media are first considered in Section 4.1, followed by examinations of field reflections on the boundary between a body surface and free space in Section 4.2. Since the computer-based modelling is necessary for the topic of the thesis, the modelling of body tissues in Section 4.3 is an essential part of the research. Finally, Section 4.4 discusses the exposure of a body to electromagnetic fields.

4.1 Electromagnetic fields

All classic phenomena related to electromagnetic fields can be derived from Maxwell's equations [93], which form the basis of RF engineering and of the whole of electrical engineering. A dielectric matter as human body tissues is known to impact electromagnetic fields in terms of penetration and absorption. In the case that one is interested in analysing or characterizing any antenna, the starting point is in the following 'general form' of Maxwell's equations by [30, 31, 94]

$$\nabla \cdot \vec{D} = \rho_e, \tag{7}$$

$$\nabla \cdot \vec{B} = 0, \tag{8}$$

$$\nabla \times \vec{E} = -\frac{\partial \vec{B}}{\partial t}, \tag{9}$$

$$\nabla \times \vec{H} = \vec{J} + \frac{\partial \vec{D}}{\partial t}, \tag{10}$$

where $\vec{D}$ is the electric flux density, ρ_e the volumetric density of electric charge, $\vec{B}$ the magnetic flux density and $\vec{J}$ the surface density of electric current. Practically, equations (7), (9) and (10) are known as Gauss', Faraday's and Ampere's laws, and (8) tells that $\vec{B}$ is sourceless. The following Section 4.1.1 shows the connection between a dielectric medium and (7)–(10).

4.1.1 Electromagnetic fields in propagation media

The strength and flux density of electromagnetic field are bound with the electric and magnetic properties of media. Electric flux density is related to $\vec{E}$ through the permittivity ε of the medium by [30, 31, 94]

$$\vec{D} = \varepsilon \vec{E}. \tag{11}$$

Magnetic flux density has relation with $\vec{H}$ with the magnetic permeability μ as

$$\vec{B} = \mu \vec{H}. \tag{12}$$

In (11) and (12), ε and μ are the properties of the medium. In a vacuum, the values of $\varepsilon = \varepsilon_0 = 8.854 \times 10^{-12}$ F/m and $\mu = \mu_0 = 4\pi \times 10^{-7}$ H/m are used. In other homogeneous media, the values are presented as $\varepsilon = \varepsilon_r\varepsilon_0$ and $\mu = \mu_r\mu_0$, where the relative permittivity ε_r and relative permeability μ_r are factors depending on the construction of the material [94]. In the context of a WBAN, the level of magnetic absorption is low, because a human body does not have magnetic properties [30]. Thus, the interest is mainly in the electric properties of a human body.

4.1.2 Complex permittivity, loss tangent and penetration depth

Complex permittivity in (11) can be generally defined as [94, 29]

$$\varepsilon = \varepsilon' - j\varepsilon'' = \varepsilon' - \frac{j\sigma}{\omega\varepsilon_0}, \tag{13}$$

where ε' and ε'' are the real and imaginary part of permittivity, σ is conductivity, $\omega = 2\pi f$, and f is frequency. The dielectric constant ε' describes the stored energy in the medium. The imaginary part is the factor accounting for loss in the medium arising from the attenuation of vibrating dipole moments [31]. The losses of medium can also be caused by the conductivity σ of the material in the case that the material has free charges resulting in the moves of *E*-field [94]. If the material has conductivity unequal to zero, the losses are electrical, which are generated based on the conduction current density $\vec{J} = \sigma\vec{E}$ (i.e., Ohm's law). *E*-field generates current density and the electric power is worn as a heating [31].

The real part of permittivity is usually expressed as the relative permittivity ε_r by scaling with ε_0. The loss tangent $tan\delta$ (< 1 for tissues) is the parameter used to characterize losses by [31, 94]

$$tan\delta = \frac{\omega\varepsilon'' + \sigma}{\omega\varepsilon'}, \tag{14}$$

The field penetration inside body tissues can be calculated by using [30]

$$\delta_{\mathrm{p}} = \frac{1}{\omega \cdot \sqrt{\frac{\mu_0 \varepsilon_0 \varepsilon'}{2}\left[\sqrt{1+\left(\frac{\varepsilon''}{\varepsilon'}\right)^2} - 1\right]}}, \tag{15}$$

where the penetration depth is seen to be dominated by the dielectric constant.

4.2 Reflections and penetration from medium interface

In the WBAN scenarios, propagating electromagnetic fields face interfaces and edges where the reflection, penetration and scattering occur. In the case one considers a perpendicular plane wave that propagates to the interface of two materials, some proportion of the wave magnitude reflects while penetrates through the interface. Reflection ρ_r and transmission τ_t coefficients are dependent on the polarization of the incident wave. The parallel and perpendicular polarizations are the special cases. The situation is visualized for these polarizations in Fig. 10.

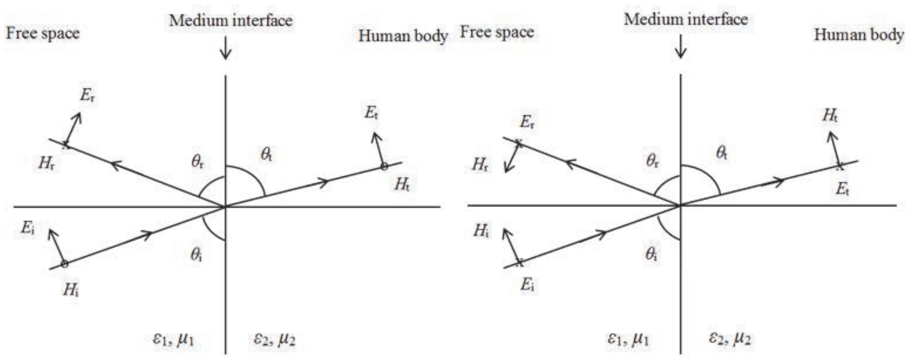

Fig. 10. Reflection and transmission of a plane wave for parallel (left) and perpendicular (right) wave polarizations.

Boundary conditions state that tangential components for *E*- and *H*-fields are equal on both sides of the interface on each point of the interface plane [94]. For the parallel polarization, E-field is on the same plane with the normal of the interface, while in the perpendicular case, E-field is perpendicular to the plane. The phenomenon is possible, because the phase of the incident E_i, reflected E_r, and transmitted E_t change equally in the (vertical) direction of the x axis.

If the perpendicular wave propagates to the interface, it holds [94]

$$1+\rho_\mathrm{r} = 1+\frac{\eta_2-\eta_1}{\eta_2+\eta_1} = \tau_\mathrm{t} = \frac{2\eta_2}{\eta_2+\eta_1}, \tag{16}$$

where η is the wave impedance as $\sqrt{\mu/\varepsilon}$. The content of (16) is to describe that ρ is dependent on the ratio of the refraction indices. In other words, the ratio of the material wave impedances surrounding the interface have the impact on ρ.

For a slanted plane wave propagating to the interface of two materials, the proportion of E_i ($z < 0$) reflects at angle θ_r and the part E_t ($z > 0$) penetrates through the interface at angle θ_t. In the case of a lossy material and perpendicular polarization, the reflection coefficient in (16) is defined by

$$\rho_\mathrm{r} = \frac{\sqrt{\varepsilon_\mathrm{r1}}-\sqrt{\varepsilon_\mathrm{r2}}}{\sqrt{\varepsilon_\mathrm{r1}}+\sqrt{\varepsilon_\mathrm{r2}}}, \tag{17}$$

and the transmission coefficient as

$$\tau_\mathrm{t} = \frac{2\sqrt{\varepsilon_\mathrm{r1}}}{\sqrt{\varepsilon_\mathrm{r1}}+\sqrt{\varepsilon_\mathrm{r2}}}. \tag{18}$$

For the slanted waves, the reflection coefficients can be written as [95]

$$\rho_\mathrm{par} = \frac{\sqrt{\varepsilon_\mathrm{r2}}\cos(\theta_\mathrm{t})-\sqrt{\varepsilon_\mathrm{r1}}\cos(\theta_\mathrm{i})}{\sqrt{\varepsilon_\mathrm{r2}}\cos(\theta_\mathrm{t})+\sqrt{\varepsilon_\mathrm{r1}}\cos(\theta_\mathrm{i})}, \tag{19}$$

$$\rho_\mathrm{per} = \frac{\sqrt{\varepsilon_\mathrm{r2}}/\cos(\theta_\mathrm{t})-\sqrt{\varepsilon_\mathrm{r1}}/\cos(\theta_\mathrm{i})}{\sqrt{\varepsilon_\mathrm{r2}}/\cos(\theta_\mathrm{t})+\sqrt{\varepsilon_\mathrm{r1}}/\cos(\theta_\mathrm{i})}. \tag{20}$$

Respectively, the transmission coefficients are [95]

$$\tau_\mathrm{par} = \frac{\cos(\theta_\mathrm{i})}{\cos(\theta_\mathrm{t})}\frac{2\sqrt{\varepsilon_\mathrm{r2}}\cos(\theta_\mathrm{t})}{\sqrt{\varepsilon_\mathrm{r1}}\cos(\theta_\mathrm{t})+\sqrt{\varepsilon_\mathrm{r1}}\cos(\theta_\mathrm{i})}, \tag{21}$$

$$\tau_\mathrm{per} = \frac{2\sqrt{\varepsilon_\mathrm{r2}}/\cos(\theta_\mathrm{t})}{\sqrt{\varepsilon_\mathrm{r2}}/\cos(\theta_\mathrm{t})+\sqrt{\varepsilon_\mathrm{r1}}/\cos(\theta_\mathrm{i})}. \tag{22}$$

In (19)–(22), the subscripts r1 and r2 denote the propagation media: the former free space and the latter human body tissues. The theory presented in this section is applied by forming a two-path model for the estimation of the radiation pattern shape of an UWB antenna in the proximity of body tissues in Section 5.2.

4.3 Body tissue modelling at microwave frequencies

The dielectric properties of a human body vary with the frequency, which introduces the dispersive modelling of tissues for the evaluation of on-body performance. In narrowband systems, the properties can be easily defined for the single frequency points. In the case of a broad bandwidth, a frequency-dependent fashion must be taken into account. Variation of the tissue properties is considered in Subsection 4.3.1 and modelling in Subsection 4.3.2.

4.3.1 Variation of the dielectric properties of tissues

There are sources and references discussing the variation of tissue properties in the open literature. A widely cited author C. Gabriel has developed a dielectric measurement technique and reported the dielectric properties for over 25 tissue types in the frequency range from 1 MHz to 20 GHz [96]. In addition, Z. N. Chen has demonstrated the variation between ε_r and σ from 1 GHz to 11 GHz for fat, bone, skin, muscle and lungs [21]. Techniques for the estimation of dielectric properties are presented, for instance, in [97] for the estimation of the regional dielectric properties of an inhomogeneous dielectric object. Typical tissue layer thicknesses of different body regions and dielectric properties are presented in [98] and the different measurement techniques of dielectric properties are discussed in [30]. Furthermore, there is a widely used online database in [99], which can be used to define the properties of ε_r, σ and δ_p for the frequencies of 10–100 GHz.

Based on the tissue combinations and thickness variations in [98], the behaviour of the properties of a (dry) skin, fat, muscle, and bone tissues for the UWB range is demonstrated in Fig. 11. The values are collected from the online database in [99]. As demonstrated in Paper [I], the penetration of electromagnetic fields inside tissues is short at UWB frequencies. Propagation will mainly stay around the surface of a body. Since a body is very lossy at UWB frequencies, there is no direct transmission through the body.

4.3.2 Modelling of tissues in simulations

Due to the variation of the tissue properties with the frequency, the definitions for tissue phantom models must be determined for the design of UWB WBAN antenna. From the simulation perspective, tissues can be considered as a lossy dielectric object, which is positioned close to an antenna [80].

The tissue models of various shapes are reported in the open literature. Some authors are using full body models that require powerful computing capacity. Alternatively, many of them are modelling the body with a tissue block, which is shaped depending on the interests. The shape of the tissue block model depends on the objectives, application in addition to the required bandwidth to simulate, and available computer resources. A full body model is the most reliable way for the modelling of on-body performance, but it is not obligatory for a successful design of a wearable antenna. In many cases, it is a reasonable approach to use a significantly reduced tissue phantom at the beginning, and finally verify the results with a larger body model, depending on a target application. A small tissue block close to an antenna is able to give a reliable estimate for the antenna impedance bandwidth. The evaluation of the radiation properties (e.g., efficiency or the shape of radiation pattern) usually requires a larger tissue model. In addition to the size of a tissue model, the frequencies of interest have an impact on the constitution of the tissue model. Within the range of super high and extremely high frequencies (SHF & EHF; ~3 GHz–100 GHz), the combination of the included tissues can be simplified because the penetration depth is relatively small inside the tissues. In the very high and ultra high frequency (VHF & UHF; ~30 MHz–3 GHz) areas, tissue combinations have a stronger impact on the performance results.

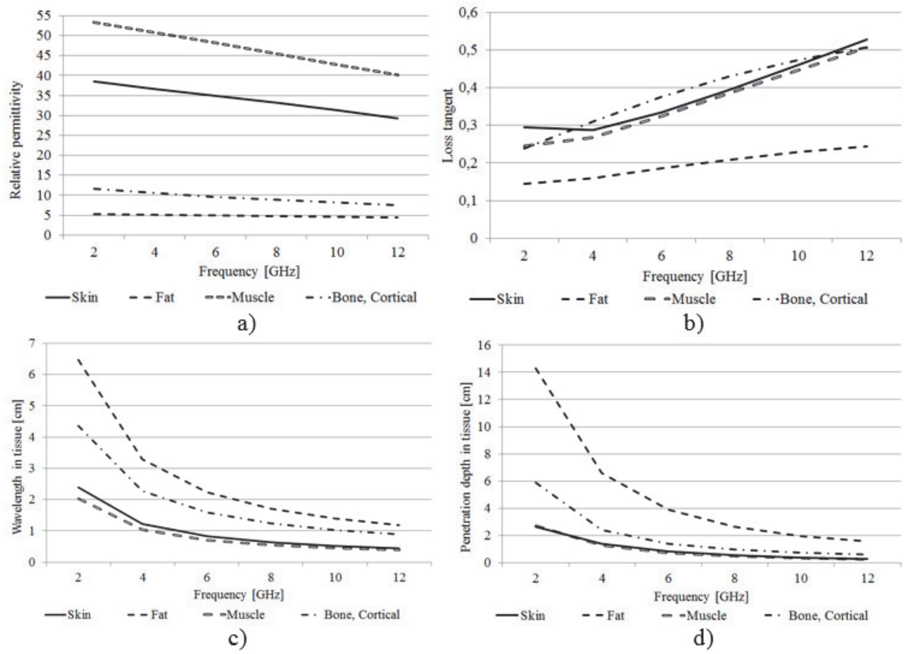

Fig. 11. a) Relative permittivity ε_r, b) loss tangent *tan*δ, c) wavelength λ [cm], and d) penetration depth δ_p [cm] in tissues. (I, published by permission of © The Institution of Engineering and Technology).

Since the upper band edge of UWB is at 10.6 GHz, the required simulation computing capacity is large because of the number of solved mesh cells as the size of cells is small due of a small wavelength. Fig. 12 demonstrates the impact of the frequency range on the required mesh. In free space, some 800,000 mesh cells are required for the frequencies of 0–11 GHz. The same antenna, in the proximity of the square tissue model in Fig. 12a) requires approximately $10 \cdot 10^7$ cells in Fig. 12c). To compare, the same model considered for the frequencies of 0–3 GHz in Fig. 12b) requires approximately $40 \cdot 10^6$ mesh cells. By using a multilevel sub-gridding scheme for 0–11 GHz (which is the feature of CST and ensures that a very dense mesh is only created within critical regions), the amount of solved cells can be reduced to $30 \cdot 10^7$ in Fig. 12d). This indicates a huge additional requirement for the computing capacity in the UWB WBAN systems. In simulations, it is important to define mesh properties so that the grid around the antenna radiator in free space remains equal when a tissue model is involved.

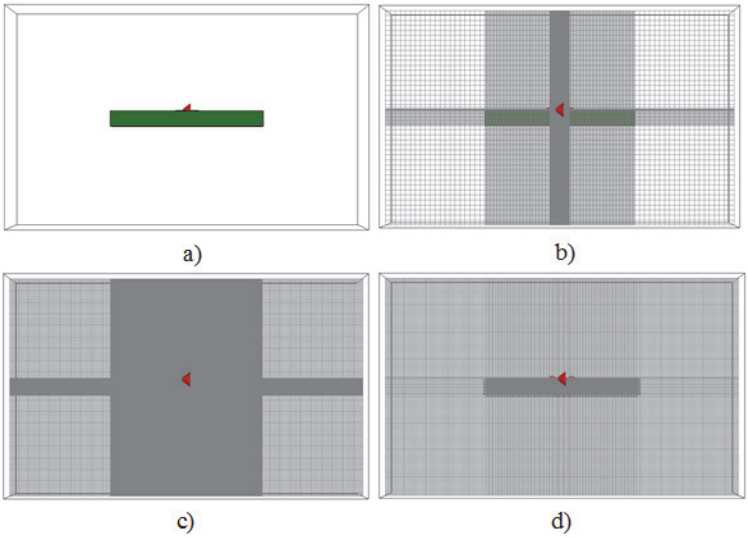

Fig. 12. An example: a) antenna and square tissue model within the bounding box, the defined mesh grid for the model for the frequencies of b) 0–3 GHz and c) 0–11 GHz, and d) mesh grid for the frequencies of 0–11 GHz with sub-gridding. In b)–d), the mesh view cutting plane is in the middle of the symmetric model.

In terms of mobile communications, a standard anthropomorphic model (SAM) head and hand phantoms according to the Cellular Telecommunications & Internet Association (CTIA) have been used for the evaluation of antenna performance in user cases. For WBAN communications, any standardized human body models or use positions have not yet been specified. Hopefully, these will be clarified in the near future to facilitate the comparison of the on-body performance results between the antenna structures.

One of the challenges for the testing of a wearable UWB antenna concerns the lack of phantom models and the difficulty of realizing them with dispersive material definitions, meaning that tissue materials follow the real values over the large frequency band. The relevant question is whether one can manufacture such a phantom or should an engineer test the UWB antenna prototype for different frequency points by changing the tissue liquids for a phantom between each measurement. This problem does not exist with antenna simulations. Constitutive parameters of such liquid-filled phantoms as the SAM are far from the values of real tissues.

Obtaining samples of tissues is reported in Paper [I] as being one of the most difficult problems related to tissue parameters and their definitions. The reason is that live tissue is impossible to measure due to the need to have the measuring device in contact with the tissue [20]. In practice, dead matter is used in all measurements of tissue.

In general, the properties of body tissues can be modelled by using a single frequency point definition, an interpolation method, or a dispersion model. The latter two are valid for broadband systems requiring a broadband fashion for tissues. A single frequency definition can be defined for the UWB, but the same simulations must be repeated for multiple frequency points with various definitions since a single point definition is not valid to follow the variation of tissue properties over the wide bandwidth of UWB. Thus, an UWB antenna designer forces the simulation software to generate the correct broadband behaviour.

Several dispersion models have been generated from the Debye equation. Some examples are the Cole–Cole model, which was proposed in 1941 by Cole and Cole or another variant by Davidson and Cole in 1951 [29]. The Debye model and its many variations have been widely used for more than half a century primarily because they lend themselves to simple curve-fitting procedures [29]. The 3-pole dispersion model is derived for the broad frequency range modelling [100] and the 2-pole Debye dispersion models are developed and applied to the analysis of the interaction between a full human body model and UWB radiation [101].

Based on the overview of the UWB WBAN antennas, some studies were reported using the dispersive method for tissues, which is practically based on the Debye dispersion model. However, as it is clearly visible from the articles, the way or the values to model the dispersive tissues are not always presented by authors. Usually, it is just mentioned that "frequency-dependent tissues have been used" or "tissues were modelled according to" some model.

F. S. Barnes & B. Greenebaum presents in [29] the Debye modelling for tissues at UWB frequencies based on the results of O. P. Gandhi & C. M. Furse in [102–104]. The proposed approach to use 2nd order model is examined in this thesis for the modelling of dispersive tissues. A numerical modelling to calculate a complex permittivity of tissues for a dispersive medium by the Debye equation is equated as [29, 100–101]

$$\varepsilon = \varepsilon_\infty + \frac{(\varepsilon_s - \varepsilon_\infty)}{1 + j\omega\tau_r} = \varepsilon' - j\varepsilon'', \tag{23}$$

where ε_s is static, i.e., the low frequency limit permittivity value, and ε_∞ is infinite, i.e., the high frequency limit (terahertz frequency range) permittivity value. The relaxation time τ_r corresponds to a relaxation frequency f_r as $1/2\pi\tau_r$. As stated in [29], at the relaxation frequency, the permittivity is halfway between its limiting values and the loss factor is at its highest. Extending (23) to be used with two relaxation constants, such as the Debye 2nd order model, is presented in Paper [I].

In Fig. 13, usage of the dispersive tissue values proposed in [29, 102–104] is compared with the interpolation and single-frequency fit procedures against the exact values. The values of σ and $tan\delta$ for the exact ε'' in

$$\varepsilon'' = tan\delta \cdot \varepsilon_r\varepsilon_0 - \sigma / \omega, \tag{24}$$

were acquired from the online database in [99]. The discrepancies with the various methods in comparison with the exact values are the most visible in the lower frequencies. The difference of the dispersive method against other ways can be explained with the definition of static permittivity in (23) that the Debye model includes. The total difference of tissue definitions of the parameters is however relative small, even though those are visible in Fig. 14, where the results of simulations with the square tissue block in Fig. 12(a) for a planar elliptical dipole are shown. In addition, although differences between the methods are visible in the permittivity graphs, their performance does not vary significantly in practice from the antenna’s perspective.

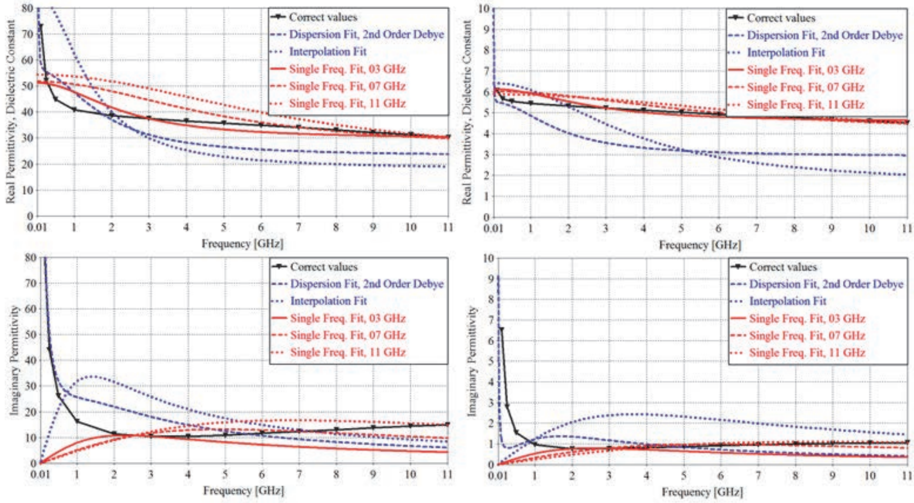

Fig. 13. Ways to model the variations of skin (left) and fat (right) permittivities against the exact values.

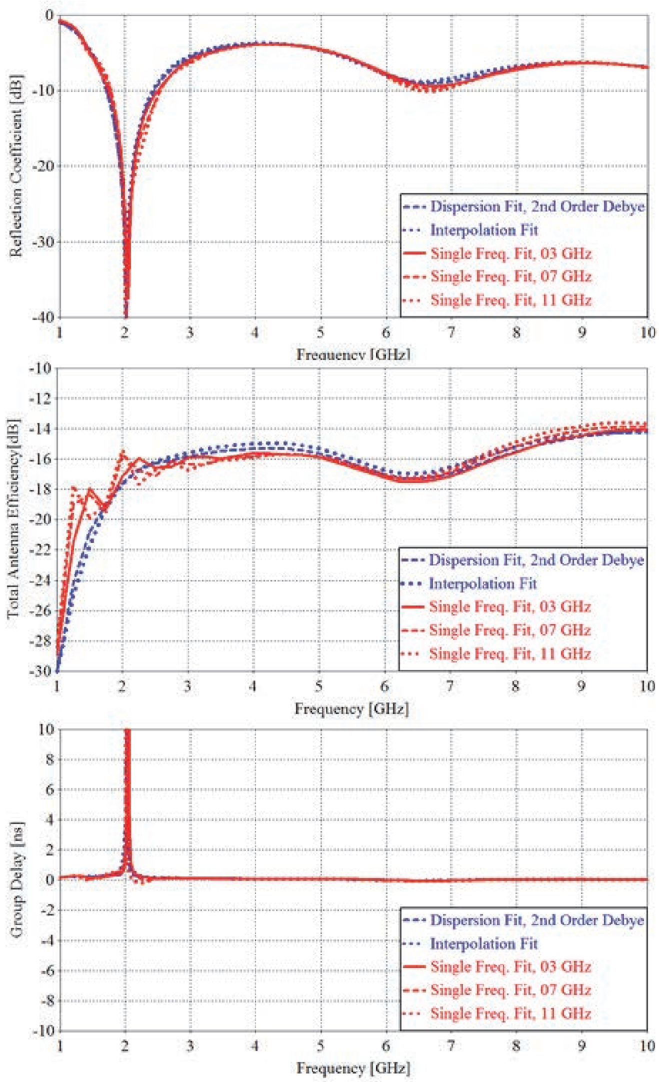

Fig. 14. Impact of various ways to model skin permittivities on antenna performance.

4.4 Exposure of body tissues to electromagnetic fields

In this section, the consideration of heating mechanism in tissues is discussed in Section 4.4.1, followed by the evaluation of the specific absorption rate (SAR) in Section 4.4.2.

Wearable devices might be exposed to electromagnetic radiation. The irradiation is dependent on the amount of the emitted power due to RF components. For a baseline, the emitted RF energy in the existing communication systems can be few watts for some mobile phone terminals. For mobile stations, some hundred watts can be transmitted [30]. In wearable applications, the power fed to the antenna is of natural interest. For the UWB WBAN applications, the FCC regulates the limit of the PSD to follow −41.3 dBm/MHz resulting in the maximum EIRP at the level of 0.5 mW by treating the entire band. The actual exposure in tissues is quantified in terms of *E*- and *H*-fields and incident power density [30], according to standard guidelines by the IEEE [26] and ICNIRP [27].

Since the body is basically formed of water, electrolytes and molecules, the dipolar momentum of those is able to interact with the electric field. This is concluded in [30], according to which the body extracts the energy from the electromagnetic field mainly by its ionic activity.

4.4.1 Generation of heat in tissues

The generation of heat in tissues due to electromagnetic waves is comprehensively discussed in [29, 30]. When *E*-field penetrates straight through the tissues, the electromagnetic energy turns into heat. The dielectric losses of a body are the mechanism generating the heat. When *E*-field travels across a body, the energy of the field decreases resulting in the increase of temperature of the surrounding tissues.

The thermal properties of a WBAN antenna in terms of heating of tissues have not been widely investigated in the literature. In practice, no papers can be found on the topic when searching the IEEE database [92]. One of the reasons might be that the simulators have not been used as topics in academic papers for a long time. On the other hand, in the case of UWB applications, the EIRP level is exceptionally low, which might be the reason one could assume that the heating is not a problem in practice. The tolerable maximum amount of input power of an IR-UWB antenna not to generate heat in tissues is considered in Paper [II]. The examinations are realized for stationary conditions and for transient solutions.

The thermal simulations are based on the Bioheat Equation, which was first suggested in 1948 [105]. The equation as [30]

$$C\rho\frac{\partial T}{\partial t} = \mathrm{K}\cdot\nabla^2 T + h_m + h_b, \tag{25}$$

can be used for estimating the temperature increase in tissues. In (25), C is the specific heat, T the tissue temperature, K the thermal conductivity, ∇^2 is the Laplace operator, h_m the rate of tissue heat production, and h_b the rate of heat transfer from blood tissue.

4.4.2 Specific absorption rate in tissues

The FCC recommends the investigation of SAR values to evaluate the RF exposure level [106]. The SAR parameter is employed to quantify the electromagnetic absorption inside the biological tissue.

The most commonly used SAR limits today are those by the IEEE [26] (1.6 W/kg for any 1 g of tissue) and the ICNIRP [27] (2 W/kg for any 10 g of tissue). The presented guidelines are set in terms of the maximum mass-normalized rates of electromagnetic energy deposition for any 1 g or 10 g of tissue [107]. Hands, wrists, feet and ankles, where SARs up to 4 W/kg for any 10 g of tissue are permitted in both of these standards, have been excluded [107].

The SAR can be based on the conductivity σ of tissue multiplied with the rms value of electric field $\left|\vec{E}\right|$ and divided by the tissue density σ_t [kg/m^3] as [30]

$$\text{SAR} = \frac{\sigma}{\rho}\left|\vec{E}\right|^2 = \frac{\sigma E^2}{2\rho}. \tag{26}$$

The widely accepted IEEE C95.3 averaging method is used in the SAR investigations. It is specified in [26].

In this thesis, the research contribution to SAR is presented in Paper [II], which considers the impact of the input power fed to an UWB antenna for crossing the maximum SAR limits in a WBAN.

5 IR-UWB WBAN antenna close to tissues

The term ‘body effect’ is well known in the field. The impact usually refers to the shift of a resonant frequency of an antenna, known as detuning, and to the absorption of a proportion of the power into human body tissues.

No specific user cases for the comparison of antenna performance have been specified for WBANs by any operator or in any standard. The UWB antenna results for WBANs available in the open literature are relative universal in that regard. The performance results of different articles are challenging to compare, due to the lack of information about several issues. For instance,

- papers do not comprehensively describe the ways to define the tissues of a body tissue phantom,
- the distance to the body tissue phantom is not exactly announced,
- the exact place on a body tissue model is not described,
- studies do not give all the required dimensions for the antenna, feeding or (possible) matching component values.

In addition, the use purpose or an application of a wearable antenna is often somewhat vague, i.e., it is unclear whether the antenna structure should work in some specific use case: in contact with tissue, at some distance to tissue or/and in free space. Because of the lack of the information described and the interest of the author to demonstrate wearable performance in practice, topics such as the distance of an antenna to tissue surface for various parameters are discussed and demonstrated in Section 5.1.

The large bandwidth causes demands for a small-sized antenna to maintain the unchangeable patterns over the FCC UWB bandwidth. Since the methods for the estimation of a pattern shape were not reported earlier, a two-path model is applied to the pattern considerations in Subsection 5.2.1. In addition, as there are always harmful significant minima (or nulls) in antenna patterns for some frequencies within the UWB band, an anisotropic antenna substrate for a WBAN usage is examined for the first time in this thesis. The desired operation by the substrate is to have an impact on the antenna polarization including reflected wave components from a body surface. The proposed method is introduced in detail in Subsection 5.2.2.

The antenna equivalent circuits are not thoroughly investigated for an UWB antenna to present the connection between the radiator dimensions and complex input impedance. In addition, explanation of the operation of an UWB antenna close to tissues with the help of equivalent circuits is an issue with scarce research. Section 5.3 discusses the usage of circuit models for the in-depth analysis of the UWB WBAN antenna.

5.1 The operating distance of an UWB antenna on a body surface

In this section, the focus is on antenna performance over tissue surface. The results regarding the distance to tissue surface in terms of matching, efficiency and gain, as well as the radiation pattern shape are examined in the following subsections. The behaviour is compared with the theoretical calculated near-field boundaries.

5.1.1 Impact on impedance behaviour and matching

The impact of a human body is known to cause a shift of an antenna resonant frequency. J. Holopainen *et al.* have shown in [108] how the shift in the proximity of a user (denoted by the subscript 2) in comparison with the free space situation (subscript 1) can be calculated, by using the generic formula, based on the perturbation theory as [108]

$$\frac{2\pi f_2 - 2\pi f_1}{2\pi f_2} = -\frac{\int_V \left(\left(\varepsilon_{r2} - \varepsilon_{r1}\right)\varepsilon_0 \vec{E}_2 \vec{E}_1^* + \left(\mu_{r2} - \mu_{r1}\right)\mu_0 \vec{H}_2 \vec{H}_1^* \right) dV}{\int_V \left(\varepsilon_{r1}\varepsilon_0 \vec{E}_2 \vec{E}_1^* + \mu_{r1}\mu_0 \vec{H}_2 \vec{H}_1^* \right) dV}, \quad (27)$$

In (27), the subscripts r1 and r2 denote the propagation media: the former free space and the latter human body tissues. Since the human body does not have magnetic properties [30], the term of the magnetic field in the numerator disappears. According to (27), the impact of the tissue on the resonance frequency can be determined through *E*-field and the resonant frequency can only decrease because of the effect of the tissues [108]. The latter is because the tissues' relative permittivity is higher compared to free space (reference). The higher the permittivity of a tissue is, the larger is the change of a resonant frequency downwards.

For a narrowband antenna, the detuning of the resonant frequency is a clearly visible shift. For an UWB antenna, the change in the reflection coefficient is visible, even though the variation is not exactly the same as with single-resonant antennas. Specifically, UWB antennas are explained to be inherently robust against the change of the properties in the surroundings [44], which is the reason why they do not face the equal change of a frequency bandwidth with a narrowband antenna. However, the impedance bandwidth of an UWB antenna expands in the proximity of a body but it cannot be seen as a clear shift of frequency.

The related research contribution is in the demonstration of the impact of distance to body surface on UWB antenna matching for the first time in Paper [V]. The results indicate that the size of a reactive near-field of a planar UWB antenna based on Wheeler's radian sphere is an important factor for the evaluation of the shortest satisfactory distance *D* to body. The studied measurement setup is shown in Fig. 15.

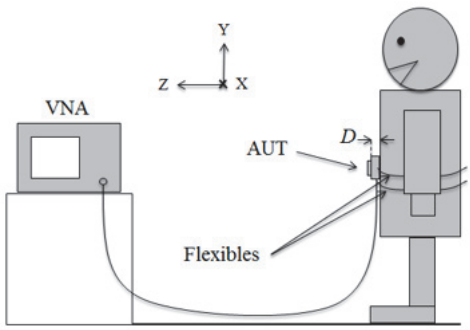

Fig. 15. The measurement setup in a chamber. (V, published by permission of IEEE).

Paper [VI] studies the matching behaviour in the vicinity of body tissue by investigating Babinet's impedance principle (as in Fig. 16). The objective of the paper is to examine whether it is possible to produce a complementary UWB antenna pair of dipole and slot antennas. The interest is in analysing how complementary antennas operate in the proximity of body tissues, and to demonstrate the difference in performance.

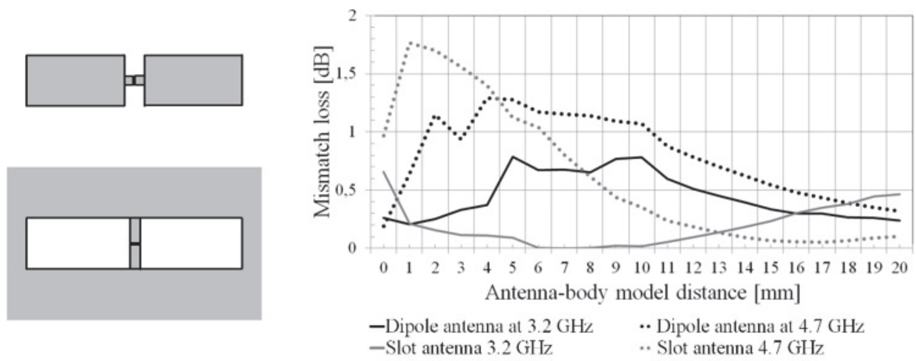

Fig. 16. Theoretical complementary antennas (dipole above, slot below) based on Babinet's principle (left), and the proportion of mismatch loss at 3.2 GHz and 4.7 GHz as a function of antenna–model distance through 0 mm ≤ *D* ≤ 20 mm (right). (VI, reproduced courtesy of the Electromagnetics Academy).

5.1.2 Impact on antenna efficiency and gain

The power loss due to a user in the volume V can be calculated by using a generic formula such as [94]

$$P_1 = \frac{1}{2}\int_V \left(\sigma \vec{E}_2 \vec{E}_1^{\,*}\right) dV + \frac{2\pi f}{2}\int_V \left(\varepsilon_0 \varepsilon_{\mathrm{r}}'' \vec{E}_2 \vec{E}_1^{\,*} + \mu_0 \mu_{\mathrm{r}}'' \vec{H}_2 \vec{H}_1^{\,*}\right) dV. \qquad (28)$$

In (28), the first integral describes a power absorbed by a user, while the second integral determines an average electric and magnetic energy which is accumulated in volume as a function of time. The total loss of an antenna includes both reflection losses due to impedance mismatch, and conduction and dielectric losses due to materials. Fig. 17 shows an example of the separation of the power for a planar elliptical UWB dipole on contact a square skin tissue model in comparison with the operation in free space.

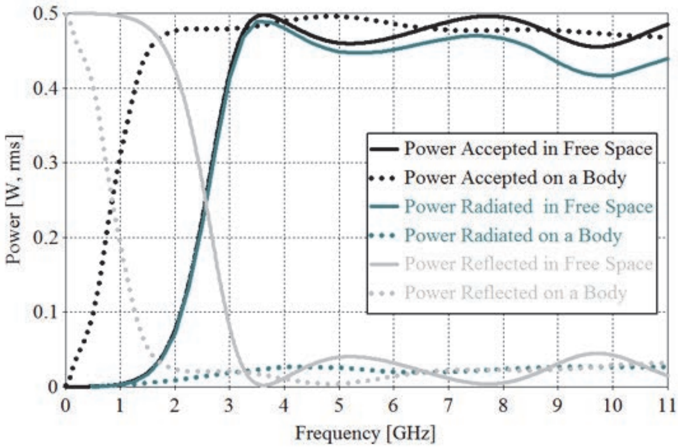

Fig. 17. An example: Consideration of power separation in the antenna structure aligned close to tissues.

Antenna efficiency and gain variations for UWB antennas were not observed to be demonstrated with the clear graphs as a function of a distance to tissue surface in the open literature. The research contribution to the issue is shown in Papers [III] and [IX] by planar UWB antennas. For example, the total antenna efficiency is plotted for various frequencies within the FCC UWB band in Fig. 18, which highlights the difference of performance close to a body in comparison with free space.

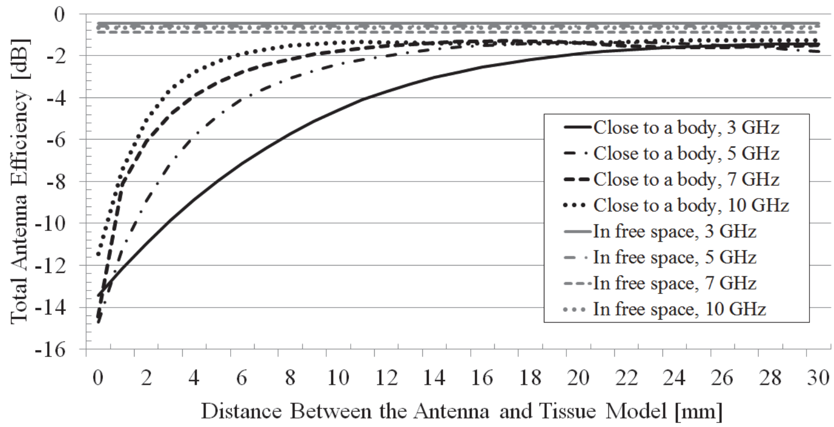

Fig. 18. Simulated total antenna efficiency e_0 for the UWB dipole. ([9], Published by permission of IEEE).

5.1.3 Separation of absorption, mismatch and body losses

The definition of total antenna efficiency does not separate the impact of various dielectric materials such as tissues, which are in the proximity of an antenna. The additional loss parameters are reported being important to consider in order to the accurate evaluation of user influence [54, 109, 110] in terms of mismatch loss

$$L_{\text{mismatch}} = -10\log\left(1-|S_{11}|\right)^2, \tag{29}$$

body loss

$$L_{\text{body}} = e_{0,\text{ fs}} - e_{0,\text{ user}}, \tag{30}$$

and absorption loss

$$L_{\text{abs}} = e_{\text{cd, fs}} - e_{\text{cd, user}}. \tag{31}$$

The loss factors in (29)–(31) can be characterized with and without a user if efficiency and reflection coefficient are known. In (29)–(31), the subscript 'fs' denotes free space and e_{cd} and e_0 are radiation and total antenna efficiencies.

Separation of the loss factors for UWB antennas has not been previously considered in the open literature, which is the reason for the investigation in this thesis. The calculations are presented in Papers [VI] and [VII]. The contribution particularly concerns demonstration of the loss factors with a distance to tissue surface in Paper [VII] and for planar UWB antennas with complementary characteristics in Paper [VI].

5.2 Pattern shape of the planar IR-UWB antenna due to reflections of a tissue surface

In this part, estimation of a pattern shape of a planar IR-UWB antenna is considered by using a two-path model. Based on the findings and challenges to maintain the unchangeable pattern shape with a small-sized broadband antenna, the opportunities to mitigate the harmful pattern nulls and minima are examined by using an artificial anisotropic substrate in Section 5.5.2.

5.2.1 Estimation of pattern shape by two-path model

The human body has a significant impact on the pattern shape in a WBAN. Because of a clearly smaller antenna size compared to a body, a wearable antenna can be considered as a point source [108]. The point source-based modelling is accepted to study electromagnetic wave propagation in the proximity of tissue surfaces [94, 111–112]. In this thesis, a radiation pattern shape is considered with the help of a two-path model [113–114], demonstrated in Fig. 19. The two-path model in this thesis is introduced in Paper [III] and was applied for the context by Dr Erkki Salonen.

The total field for an individual point source (R_1 in Fig. 19) can be written by using (19)–(20) as

$$\boldsymbol{E}_{\mathrm{tot}} = \boldsymbol{E}_1 + \rho \boldsymbol{E}_1 e^{-j2\pi D_{\mathrm{A-T}}(1+\cos 2\theta)/\lambda \cos\theta}, \tag{32}$$

where the subscript 1 denotes the field of source 1, λ is the wavelength and $D_{\mathrm{A\text{-}T}}$ is the radiation source-body surface distance. It is determined that (32) holds the conditions of the parameters in Fig. 19 as

$$\cos\theta = D_{\mathrm{A-T}} / S_1 = (S_1 + S_2) / 2D_{\mathrm{A-T}}. \tag{33}$$

The result of (32) shows the sum field in the far-field region and can be used to visualize patterns for different frequencies and distances as a function of an angle θ. The number of sources can be varied for the model. Since the studied planar elliptical dipole is formed of two symmetrical arms, a perpendicular polarization is formed with two point sources (R_1 and R_2 in Fig. 19) by taking into account their path difference. In this case, the total field is

$$\boldsymbol{E}_{\text{tot}} = \boldsymbol{E}_1 + \rho \boldsymbol{E}_1 e^{\psi_R} + \boldsymbol{E}_2 e^{\psi_{\Delta d}} + \rho \boldsymbol{E}_2 e^{\psi_{\Delta d}} e^{\psi_R}, \tag{34}$$

where e^{ψ_R} is the phase term caused by the reflection and $e^{\psi_{\Delta d}}$ is the phase term due to the path difference d between the sources R_1 and R_2.

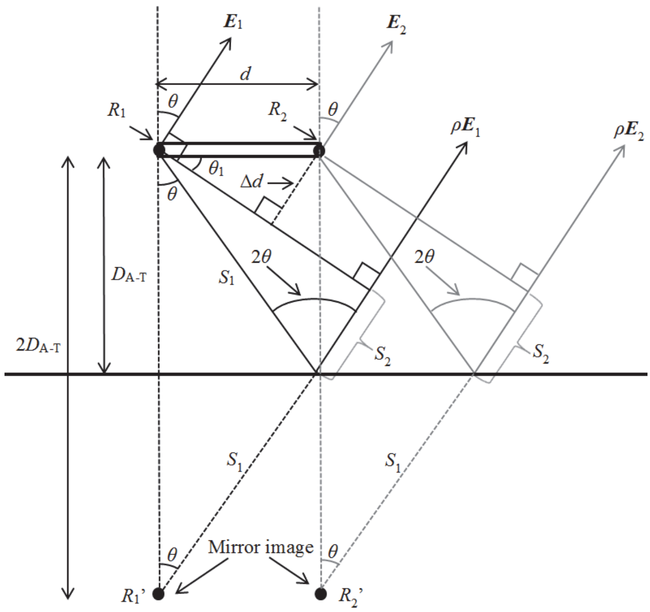

Fig. 19. A two-path model for a dipole antenna with two point sources. The model can be used for the estimation of the positions of pattern minima and nulls at various distances to tissue surface.

A pattern shape in the proximity of an isotropic substrate made of ε_r = 5.0 is compared against the volume of ε_r = 1.0 in Fig. 20. Absorption on contact causes the disappearance of some 20 dB in comparison with the free space patterns. The impact of an increase of the first millimetres is valuable for a notable improved performance in terms of efficiency. If ε_r = 1.0 fulfils the volume between an antenna and a tissue surface, uniform pattern beams are achieved over the bandwidth for the close distances. Nevertheless, a substrate is the factor that most probably fulfils the volume below an antenna. A substrate causes the pattern shape to shrink, mainly for lower frequencies, while notable minima start to appear for higher frequencies because of the reduced λ in the volume.

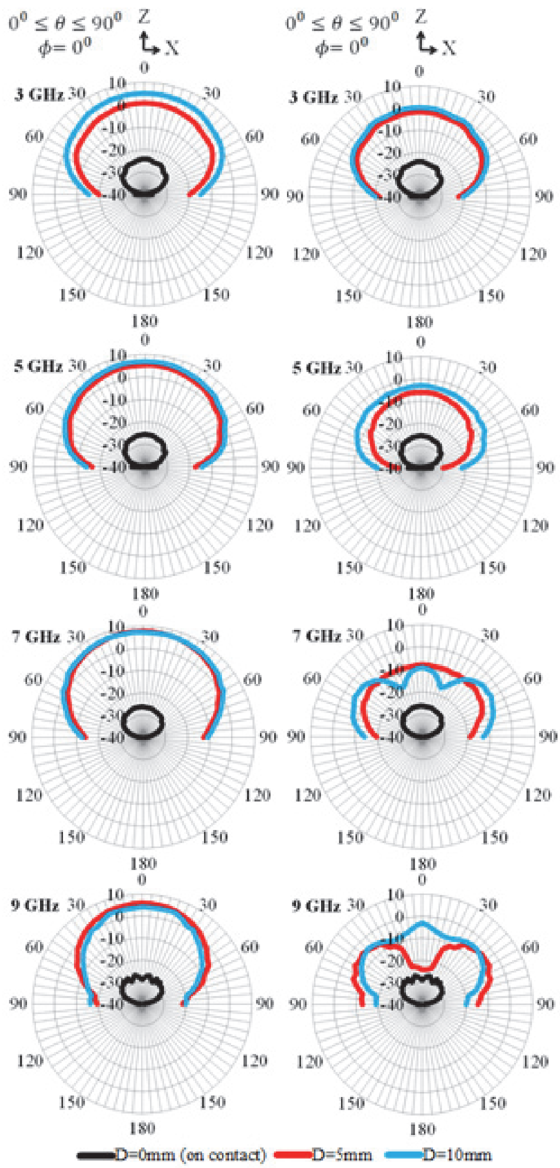

Fig. 20. Demonstration of a pattern shape variation for the *xz*-plane at the frequencies of 3, 5, 7 and 9 GHz for the fixed distances *D* of 0, 5 and 10 mm. In *D* = 0 mm, the antenna is in contact with the tissue, while for *D* = 5 and 10 mm (left) free space or (right) substrate of $\varepsilon_r = 5.0$ fulfils the volume between the antenna and the tissue model.

Several publications have reported the directive pattern properties of a wearable antenna in the close proximity of a body [80, 87–88, 115–117]. Investigations have also verified that in the close vicinity of tissues, pattern shape is conical, relatively directive. Distance to a flat tissue phantom is considered in Fig. 21. The directive pattern shape remains until the distance of $\lambda/2$ to tissue (black line), where the first significant minimum is visible. The pattern shape consisting of the direct and reflected components is directly proportional to D in terms of λ in theory, which means that the same pattern can exist, e.g., at 3, 6 and 9 GHz when the distance on-body in terms of λ is the same. This is the reason why corresponding reflections occur in steps of λ regardless of the frequency with the equivalent λ. Therefore, the following notable additional minima after $\lambda/2$ in addition to 0° direction are also visible in steps of $\lambda/2$ as at λ (0° and 60°, red line) and $3\lambda/2$ (0°, 45° and 70°, blue line).

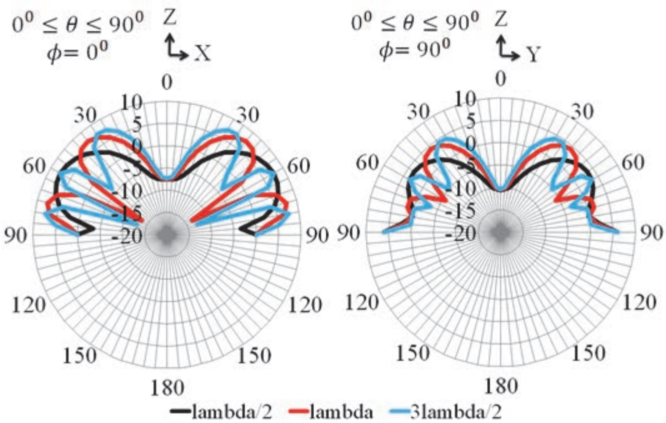

Fig. 21. The first significant minima with distances of $\lambda/2$, λ and $3\lambda/2$.

The considered two-path model is theoretically valid in the far-field of an antenna. The applicability of the model for considerations of reflections in the near-field region is examined in this thesis. Even though the two-path model has some restrictions, as described below, in addition to the theoretical validity only in the far-field, the results are promising. With a two-path model, a point source is assumed, although an antenna radiates from the different points in reality, or as a point-form. It is observed that a plane wave assumption is not valid. In addition, a two-path model has constraints in the very close proximity to body due to the geometrical restrictions. Further, the model assumes the direct and reflected components to be parallel. A ground level is supposed to be of infinite size. In reality, the antenna slightly shadows the reflections in the z direction.

The pattern results from using a two-path model for both polarizations are shown in Fig. 22 in comparison with the simulation results of a planar elliptical dipole on the *xz*- and *zy*-planes at 5 GHz on a tissue phantom. For the two-path model calculations, the values of $\varepsilon_{r1} = 1$ and $\varepsilon_{r2} = \{31, 26, 25, 24\}$ for {3, 5, 7, 9 GHz}, in a respective order. The results show that in the close proximity, the two-path model encounters minor problems with angles θ close to zero, as the antenna is positioned in front of the reflected waves, thus affecting them in reality. This is due to the fact that the two-path model assumes the reflected component to propagate freely. As can be seen, the pattern shape can be estimated rather accurately for the perpendicular polarization. For the parallel polarization, the results are not necessarily comparable when angles become large. This is due to the different fashion of an antenna to radiate in comparison with the two-point sources as well as the model supposed, as it has an infinite reflecting surface. The size of a tissue model is limited to 100 × 100 cm on the *xy*-plane.

In conclusion, the absolute value of gain for the angles close to the direction of the normal of a body surface could be given based on the patterns estimated by the two-path model. The model has constraints close to angles of $\theta = 90°$. Therefore, it is proposed that a simple two-path model can be used as an initial assumption for far-field patterns, as it can predict a good preliminary shape, i.e., the directions of minima and maxima in patterns.

5.2.2 Changing antenna polarization in the proximity of a body with anisotropic substrate

An antenna substrate can be used as a polarizer in a way that it has the impact on the pattern minima. The idea to realize such a substrate and the research contribution to the issue is presented in Paper [IV] by introducing a design for an anisotropic substrate for the first time in WBAN usage. Constitutive parameters of the anisotropic material are a function of the direction of the applied field, which is the reason why the properties vary in a different manner depending on the directions of consideration. By designing an artificial anisotropic material with the thin sheets made of materials having different relative permittivities, a polarizing substrate can be designed. The considered anisotropic substrate concept is shown in Fig. 23. The principal coordinates of the anisotropic material are denoted here by *x*’, *y*’ and *z*’.

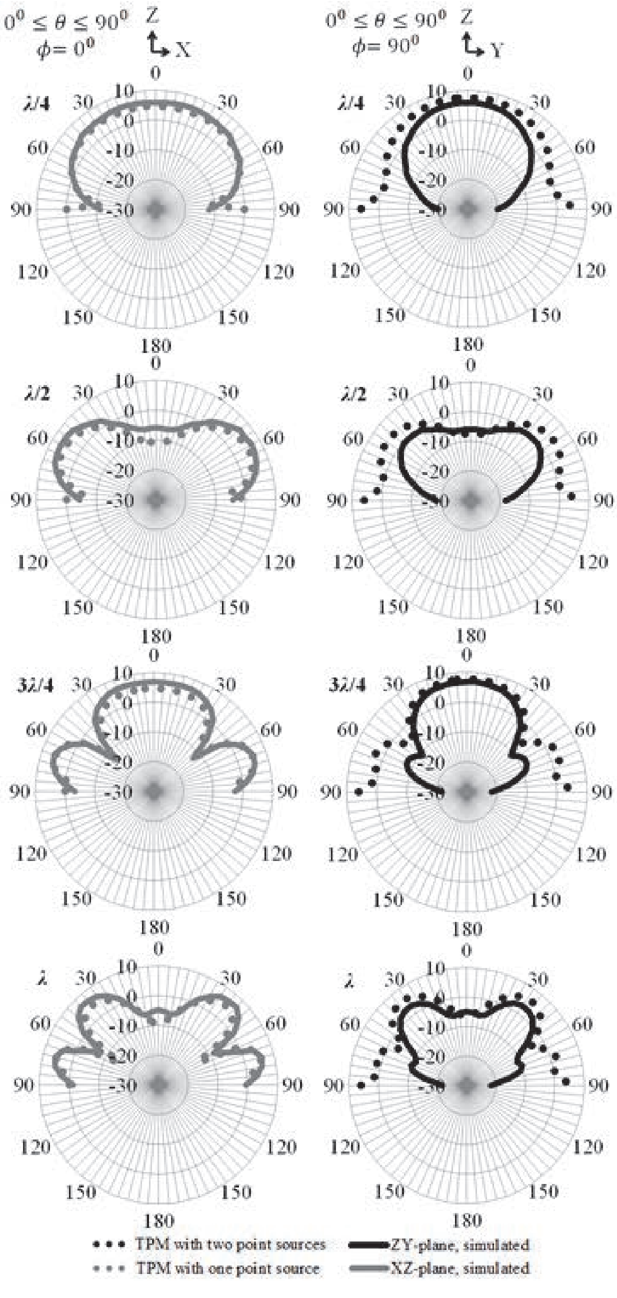

Fig. 22. Comparison of the two-path model with the simulated patterns.

The substrate in Fig. 23 must be aligned to the angle 45° with respect to the polarization direction y of the antenna to acquire the desired operation. The operation of the concept is explained in detail in Paper [IV].

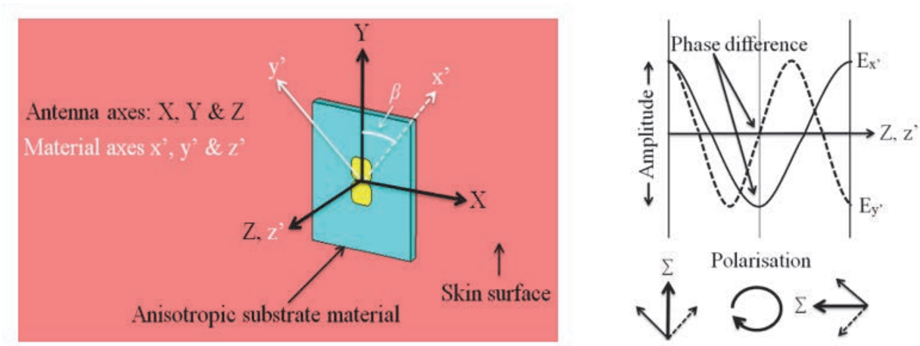

Fig. 23. Setup for the considered anisotropic material (left): principal coordinates of material (*x*', *y*') are required to rotate *β* = 45° from the polarization direction *y* of the antenna. In the right, polarization of reflected wave is shown to rotate 90° if phase shift of components to directions *x*', *y*' is set equal to 180°. (IV, published by permission of IEEE).

The Maxwell–Garnett formula is used to calculate the effective permittivity ε_{eff} ε_{eff} of dielectric mixtures. For instance, the effective permittivity in the x'-direction can be presented with the depolarization factor N_x as [118]

$$\varepsilon_{\text{eff},x'} = \varepsilon_{\text{e}} + p\varepsilon_{\text{e}} \frac{\varepsilon_{\text{i}} - \varepsilon_{\text{e}}}{\varepsilon_{\text{e}} + (1-p) N_{\text{x}} (\varepsilon_{\text{i}} - \varepsilon_{\text{e}})}, \tag{35}$$

where ε_{e} and ε_{i} are the permittivity values of the environment and inclusion materials, p is the volume factor, i.e., the volume portion of the inclusion material. The depolarization factors can be calculated analytically for ellipsoidal particles and as a special case, for thin discs on the yz-plane, depolarization factors are $N_{x'} = 1$, $N_{y'} = N_{z'} = 0$. Using these factors, the permittivity in the perpendicular direction $\varepsilon_{\text{eff},x'}$ and the parallel directions $\varepsilon_{\text{eff},y'} = \varepsilon_{\text{eff},z'}$ of stacked thin dielectric discs or sheets, can be presented by using in simplified formulas in Paper [IV]. It should be noted that the sheets must be significantly thinner with wavelength λ. The procedure to design the anisotropic material is explained in detail and the performance is shown in Paper [IV].

5.3 Analysing planar UWB antennas by using equivalent circuits

Antenna equivalent circuits consisting of lumped elements have been customary for characterizing properties for the antenna input impedance Z_{in}. There are many ways to apply equivalents, for instance, to model an antenna and to understand antenna operation. The impedance properties of a circuit model must correlate with the modelled antenna, which might cause a challenge particularly for the UWB antennas since the parameters are frequency-dependent [119]. Since antenna equivalent circuits are not comprehensively explained for UWB antennas, the connection between the radiator dimensions and complex input impedance and the operation of an UWB antenna close to tissues are examined in this thesis.

Firstly, in Paper [VIII], the analysis of the connection of wideband dipole antenna dimensions and input impedance is demonstrated for the first time, as seen in Fig. 24. The physical dipole dimensions in terms of length and width are examined and the impact on antenna impedance parameters is shown. Some findings include, for instance, that the resistance of a parallel-resonant stage behaves as the maximum value of real part of dipole impedance with an influence on bandwidth together with the ratio of parallel capacitance *C* and inductance *L*. The increase of the antenna physical width has an effect on bandwidth, because the wider the antenna, the higher the capacitance in the antenna feed.

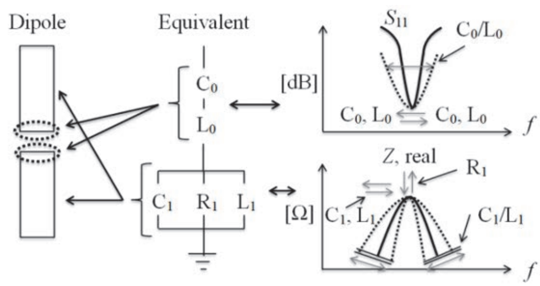

Fig. 24. The impedance dependency of UWB dipole and equivalent circuit. (VIII, reproduced courtesy of the Electromagnetics Academy).

The second contribution concerns the analysis of the impact of tissue within the reactive near-field of the UWB antenna and is introduced for the first time in Paper [IX]. The parasitic components for the equivalent models are proposed for taking the impact of tissue on the antenna design into account, as visible in Fig. 25. The antenna impedance behaviour is presented in terms of capacitance, inductance and resistance as a function of the radiator distance on the tissue surface for the studied antennas. Some findings are that the capacitance increases with the distance to tissue surface by achieving the maximum value close to the reactive near-field boundary and the inductance has the maximum on contact with the tissue, decreasing strongly within the first millimetres and remaining constant at longer distances.

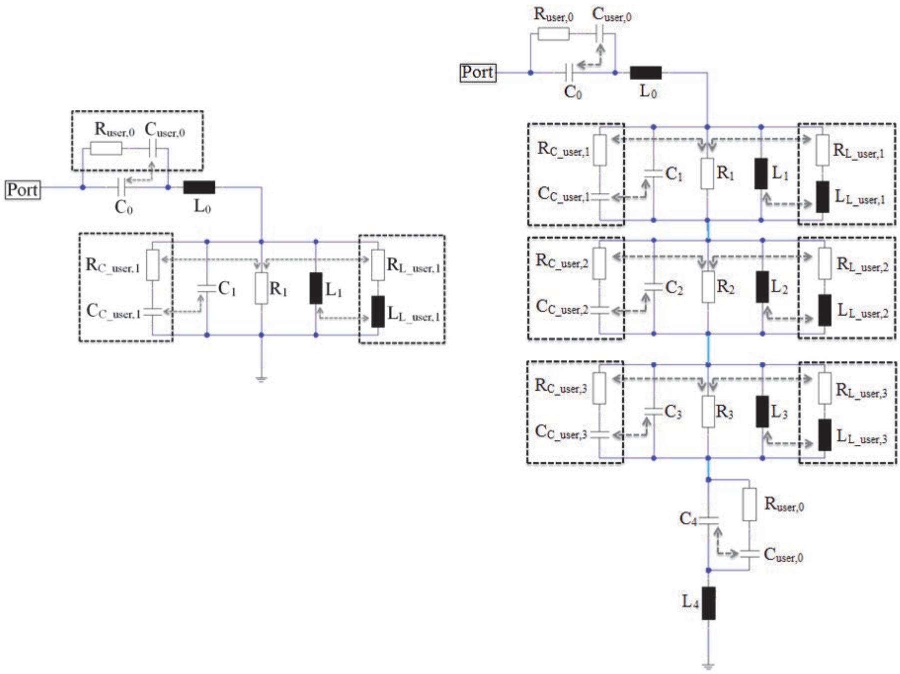

Fig. 25. Final equivalent circuit for a single-resonant dipole (left), and a multi-resonant dipole (right) indicating the proportion of tissue by parasitic components inside the black dashed rectangular boxes and the connection between the free space components with additional parasitic to form the final physical behaviour by grey dashed arrows. (IX, reproduced courtesy of the Electromagnetics Academy).

6 Summary of original publications

In this section, the research work of the reviewed original papers of the thesis is summarized. For each paper, the numbers of the research questions to which the paper responds are presented.

[I] Ultra Wideband Loop Antenna on Contact with Human Body Tissues

Paper [I] provides answers to Questions 1–2 of this thesis. In this paper, the impact of the thickness of human body tissue layer on the performance of a planar loop antenna in UWB WBAN applications was characterized for the first time.

A wideband loop structure, printed on an FR4 substrate, was designed for the examinations. Good agreement between the simulations and measurements in free space was acquired. The performance was examined in terms of matching, gain, efficiency, patterns and SAR in proximity of a layered tissue phantom by using a simulator. Matching results were also obtained by measurements with a real human being. Tissues were confirmed to load the antenna such that the wider matching bandwidth is achieved in relation to free space meanwhile the radiation characteristics are significantly deteriorated. The largest proportion of radiated gain was observed in the direction away from the body. The variation of the thickness of skin was noticed to have the most significant influence on the performance results. Tissue characteristics in the FCC UWB frequency range were considered. Based on the observations, tissues having the highest water content were noticed to have the highest relative permittivity (e.g., skin and muscle) decreasing with the frequency, while the losses in tissue were noticed to increase. The absolute value of λ inside tissue varies mostly for fatty tissue (from 4.7 cm to 1.5 cm) between the lower (3.1 GHz) and higher (10.6 GHz) UWB band edges. Tissues with the lowest water content were also with the highest depth of penetration inside tissues, especially at 3 GHz (δ_p = 11.5 cm for fat versus e.g. δ_p = 2 cm for skin).

[II] On the Evaluation of Biological Effects of Wearable Antennas on Contact with Dispersive Medium in Terms of SAR and Bio-Heat by Using FIT Technique

Paper [II] provides answers to Questions 2–3 of this thesis. This paper considers biological effects in terms of a SAR and temperature rise in tissues by using planar antennas, namely a loop and dipole, for UWB WBAN applications.

Temperature and power losses were acquired for the first time for planar UWB antennas with a simulator in vicinity of a tissue phantom. The impact of antenna input power on temperature and maximum SAR results was compared against the IEEE and ICNIRP limits by using 1 g and 10 g averaging masses. The idea was to identify how much power it is possible to feed to the UWB antenna in order to cross the maximum SAR limits in WBANs or until an antenna starts to heat the tissues in the stationary situation or as the transient condition. Provided that the FCC's UWB regulations are followed, the user is safe from harmful biological effects caused by antennas based on the results of this study. It was observed that tissues having high permittivity and loss tangent, hence having a notably high water content, e.g., skin and muscles, might cause more concern from a SAR and temperature point of view than fatty tissue. These findings provided useful information for the most suitable position of an implantable WBAN device.

[III] Radiation Properties of the Planar UWB Dipole in the Proximity of Dispersive Body Models

Paper [III] provides answers to Questions 1 and 4–6 of this thesis. The paper investigated the radiation properties for a planar dipole antenna in UWB WBAN applications.

In the examinations, two different tissue phantom models (a layered and a full body) with the frequency-dependent fashion were considered. The aim of the paper was to investigate phenomena in the proximity of a body in terms of electromagnetic wave reflections, which is the reason why the examined distances to body surface were relative high. The antenna performance was considered in terms of the realized maximum gain and total antenna efficiency, 3D radiation patterns at some specific distances, and reflections and absorption of *E*-field distributions at various distances to body. The reflections were compared with the preliminary assumption of a two-path model with a single point source, the analysis of which was extended further in the manuscript of the thesis.

[IV] Antenna Close to Tissue: Avoiding Radiation Pattern Minima with Anisotropic Substrate

Paper [IV] provides answers to Questions 5 and 7 of this thesis. In this paper, the impact of an artificial anisotropic substrate was studied in order to mitigate the radiation pattern nulls of an antenna for UWB WBAN applications.

Because of the large bandwidth, there are always harmful significant minima (i.e., nulls) in antenna patterns for some frequencies. The antenna–body distance was shown to have a notable influence on the pattern shape. The impacts of permittivity of a substrate on possible reflections were demonstrated. To address this challenge, the purpose of the paper was to show the design approach of an artificial anisotropic substrate for the wearable UWB antenna. This was the first time that the anisotropic concept was applied to a WBAN context. The proposed substrate improved gain performance in addition to the pattern shape of a broadband antenna by avoiding the appearance of harmful pattern minima. The anisotropic substrate was formed by assembling sheets with relative permittivities $\varepsilon_e \approx 1$ and $\varepsilon_i \approx 9$ (subscripts: for the environment and inclusion materials) as a stack in order to enable effectively different permittivities $\varepsilon_{x'} \approx 5.0$ and $\varepsilon_{y'} \approx 1.8$ for wave components propagating in between an antenna and a body. The substrate was concluded to modify the sum polarization of an antenna such that smoother patterns over the bandwidth were achieved.

[V] Effect of the Antenna-Human Body Distance on the Antenna Matching in UWB WBAN Applications

Paper [V] provides answers to Questions 4–5 of this thesis. This paper examines the interaction between planar antennas, namely a loop and a dipole, and body tissues for the variation of matching in UWB WBAN applications.

The studied range over body surface was 0–30 mm, which can be a practical use distance for the on-body antenna in reality. The matching results were compared with the reactive near-field boundaries in proximity of a square tissue model and a whole body. UWB antenna matching results were not earlier shown as a function of a distance to body surface. Antennas were also measured in a chamber and the matching results were obtained with a real human being.

Significant differences between antennas were not observed and they were concluded to perform well in the case that the distance is long enough. The size of the reactive near-field was observed to be an important factor for the evaluation of the shortest satisfactory antenna–body distance.

[VI] The Comparative Analysis of UWB Antennas with Complementary Characteristics: A Functionality in FS and Applicability for the Usage Close to Tissues

Paper [VI] provides answers to Questions 4–5 of this thesis. In this paper, planar complementary antennas, namely a dipole and a slot, were considered for UWB WBAN applications.

The complementarity of planar UWB antennas was studied because no reports were found about the topic in the literature. The antennas were first formed to appear as complementary structures based on Babinet's principle without a substrate material. The influence of a substrate on the complementary was evaluated and it was observed to affect the radiators to diminish the capability to appear as ideal complements based on the principle. The considered antenna types were re-designed to have similar S_{11} to cover the lower UWB band (3.24–4.74 GHz) due to the challenges to maintain unchangeable operation for the entire FCC band. The antennas were concluded to appear complementary based on the pattern duality, although the principle was not ideally satisfied. In addition, the performance close to tissues was analysed and discrepancies shown in terms of mismatch and body loss behaviour. Although free space performance was observed to appear almost equal (excluding a pattern duality), the performance was found to differ close to tissues. For instance, based on matching, strong variations for the slot were noticed in the studied range in comparison with the dipole. However, total body losses of both antennas were observed to appear close to each other.

[VII] Conductive Layer under a Wearable UWB Antenna: Trade-off between Absorption and Mismatch Losses

Paper [VII] provides answers to Questions 4–5 of this thesis. The paper studied the reduction of antenna absorption loss in proximity of tissues for UWB WBAN applications. The same antennas were used in this study as in Papers [VIII–IX].

The reason to study the issue arises from the common problem with wearable antennas, which is the influence of body tissues: they decrease the performance of an antenna due to detuning and electromagnetic absorption. A ground plane is proposed to mitigate the absorption, which might be very efficient for an antenna with narrowband operation and available matching components. However, for UWB, the difficult aspects of a ground plane are admitted in the field. The impedance behaviour of UWB antennas is conceded to be sensitive to the shape of an antenna, which is the reason why taking a ground plane into account in a design might involve challenges for proper matching in practice. Due to the lack of results regarding the issue, Paper [VII] discussed the impact of a conductive layer in-between skin tissue and broadband dipoles. The effect of a conductive layer on antenna operation is considered by separating the proportion of body, absorption and mismatch losses. Different planar UWB dipole antennas were considered in this study: a multi-resonant to cover the FCC UWB band and three single-resonants at 3 GHz, 6 GHz and 9 GHz in order to compare the antenna behaviour. The performance was first examined in the closeness of the tissue model by following the characterization of the impact of a conductive layer. The conductive layer was observed to decrease absorption loss up to 10 dB in the lowest UWB frequencies. Nevertheless, the trade-off was realized with mismatch losses in the case to achieve the better body loss. The aim of this study was to generate reference results for future studies, which should be realized in terms of the co-design of the layer and an antenna, for instance.

[VIII] Impedance Dependency on Planar Broadband Dipole Dimensions: An Examination with Antenna Equivalent Circuits

Paper [VIII] provides answers to Question 8 of this thesis. In this paper, the connection between complex input impedance and the physical dimensions for planar UWB antennas was considered. This study used the same antennas as Papers [VII, IX].

This was the first time the effect of both an actual radiator width and length on impedance behaviour was presented for broadband dipoles. The antenna operation was compared with lumped-element equivalent circuits consisting of series-resonant and parallel-resonant stages. The main findings were that the series-resonant circuit of equivalent was observed to be analogous to the antenna feeding area. In addition, the physical dipole dimensions in terms of length and width were connected to parallel-resonant part, which mainly determined the antenna input impedance. In particular, the resistance of a parallel-resonant stage was observed to behave as the maximum value of the real part of dipole impedance with an influence on bandwidth together with the ratio of parallel capacitance *C* and inductance *L*. The increase of the physical width of the antenna had an effect on bandwidth, because the wider the antenna, the higher the capacitance in the antenna feed. Also the traditional broadband dipoles were considered, as they can be used to explain the operation of other antennas, e.g., widely used monopole and patch antennas as for future works.

[IX] Analysis of the Impedance Behaviour for Broadband Dipoles in Proximity of a Body Tissue: Approach by Using Antenna Equivalent Circuits

Paper [IX] provides answers to Questions 4–5 and 9 of this thesis. The paper considered antenna operation close to tissues for UWB WBAN applications by using lumped-element equivalent circuits. This study used the same antennas as Papers [VII–VIII].

The antenna performance was characterized for the range of reactive near-field in terms of efficiency, impedance and matching to 50 Ω. The impedance behaviour of the antennas was presented in terms of capacitance, inductance and resistance as a function of a radiator distance to tissue surface for UWB antennas for the first time. In addition, the parasitic components for the series-resonant and parallel-resonant stages of the equivalent models were proposed in order to take into account the impact of tissue on the antenna design. The main findings of the study are that the capacitance was observed to increase with the distance to tissue surface by achieving the maximum value close to the reactive near-field boundary. The inductance has the maximum value on contact the tissue, decreasing strongly with the first millimetres and remaining constant with the higher distances. In addition, the maximum value of input resistance was seen to clearly increase with the distance, having the maximum value in the first third of the studied range, descending close to the value in free space at the boundary at the end. The results can be extended in many ways because the traditional broadband dipoles were used. One interesting subject to study in the future is the characteristics of bendable wearable antennas by using equivalent models to understand the physical effect of bending the radiator on impedance behaviour.

7 Discussion

In this chapter, discussions about the results of the thesis are presented. In Section 7.1, the results are compared with the material in the literature. The significance of the research work is discussed in Section 7.2, and the limitations of the research along with recommendations for future studies are discussed in Section 7.3.

7.1 Theoretical implications

During the research work for this thesis, several issues were observed to be crucial to gather to gain a sufficient understanding about the topic. The approach of the dissertation concerned the ideology that one needs to first understand the operation of an UWB antenna in free space and the antenna operation in the proximity of tissue in order to be able to compensate the harmful effects and to design the antenna properly. The research challenge concerned multiple sub-issues at the theoretical and practical level, which needed to be understood in order to consider the topic.

The theoretical foundations and research background of the thesis were separated into two larger entities. The first part in Chapter 3 presented the fundamental findings of UWB antennas, whereas the second part in Chapter 4 concentrated on understanding the electromagnetic field in the proximity of human body tissues. The theoretical information in Chapter 3 was mainly gathered based on books [20, 21, 24, 35, 40, 44] and two renowned journals [45–46]. The available materials enabled the research work and strongly supported the examinations of this thesis. Throughout the literature review in Sections 3.4 and 3.5, and by combining the content of the theory in Chapter 4, the apertures in the general research in open literature were illustrated for the author.

The aim of this thesis is to demonstrate how the information available can be utilized for antenna design, and particularly, for understanding the operation of UWB WBAN antennas. The author considers that the UWB antenna is the component, the fundamental theory for which is provided in Chapter 3, that connects the information presented in Chapter 4 to the title of this thesis. From the perspective of theoretical implications, the thesis includes a theory which was crucial to comprehend in order to realize most of the investigations presented in the thesis.

7.2 Practical implications

The thesis concerns the IR-UWB WBAN antennas that can be utilized, for instance, in future wireless medical and sports applications. As the focus is in general on the WBAN antennas, excluding in-body communications, there are several additional applications to which the content of this thesis can be applied. The considered physical layer technology is UWB – although, the information can be adapted to other PHY solutions on-body – introduced in the international WBAN standard IEEE802.15.6 [22]. The results of the thesis have direct implications for commercial companies, e.g., for the design of wearable devices.

The thesis presented several new findings that are useful to understand in the research field concerned or in general. The findings and observations increase the practical understanding about the analysis and design of WBAN antennas. Some examples are:

- the impact of the variation of the outermost tissue layer thickness on antenna performance in terms of various antenna parameters;
  - The information increases general understanding about the possible variations of a WBAN antenna operation for the number of possible device end users.
- the effect of the use distance on the performance above a body tissue phantom surface in steps of millimetres in order to clearly indicate the advantage of higher (or required) use position/distance to body;
  - The information shows that the size of the reactive near-field is a relevant indicator of a satisfactory antenna performance for a planar antenna without a ground plane. The findings of P. S. Hall & Y. Hao [20] support these results.
- the simple method of estimating a preliminary UWB radiation pattern shape due to the fact that simulations with a body phantom are known to be time-consuming;
  - The model can be exploited by an antenna designer, and is indeed fast in comparison with the simulations as the model can be run in real time.
- an artificially anisotropic substrate having an influence on the antenna sum polarization in order to mitigate the harmful pattern nulls;

  - The information created a new approach to WBAN antennas. The considered substrate material opens opportunities for several applications also for mobile devices in addition to wearable electronics.
- the connections between antenna input impedance and antenna dimensions with the help of equivalent circuit models; and
  - The equivalent circuits are known to be a successful tool for understanding the operation of an antenna for a long time, but have a clear benefit for understanding the operation of an antenna.
- the impact of human body tissue on equivalent circuit topology in terms of additional lumped-element components.
  - The information increases the general understanding about the operation of an antenna in the vicinity of tissues and indicates the most harmful influences from the antenna perspective.

7.3 Research limitations and recommendations for further studies

There are several issues which were not possible to study in detail during the work for this thesis due to the limited available computing capacity for 3D EM antenna simulations in the laboratory and practical defects regarding the measurement setup that caused some limitations for the research. At the end, the research work for the thesis was carried out within the time frame of three years, during which the author also completed the post-graduate studies in terms of courses, had teaching commitments and was learning the ropes of working in the academic world. During the research period, several ideas emerged that were left for detailed examination in the future. The thoughts and ideas in terms of limitations and recommendations are discussed in this part to share the topics related to the research focus of this thesis that are important to examine and check.

This dissertation considers the operation of IR-UWB WBAN antennas in the closeness of human tissues. Due to the large number of sub-issues that could be included under the title, universal research is inevitably involved for this thesis.

The antennas used for the studies are planar structures, which are useful to examine in the context of phenomena related to the operation of an antenna in the vicinity of lossy propagation media. The approach was chosen in order to increase the understanding about the factors and occurrences related to the performance of

WBAN antennas. However, from the device point of view, there are several challenging issues to be examined in the operation of UWB antennas in terms of the impact of mechanical near-by components and available spaces in practice, not to mention the size of the device on the whole.

It has been understood that the primary focus of academic research concerns comprehension of phenomena related to the topic of this thesis and sharing information for the wider audience. After the propagation mechanisms and phenomena are realized and explained by academic research, it is time for industry to apply the information. However, the author wishes that academic research is carried out in close collaboration with the industrial partners from the very beginning and throughout the future research projects by having discussions about the issues that are important and need to be investigated in general. This also helps to establish clear guidelines regarding what are the research targets and realistic to research.

It has been understood that a planar dipole, which was used several times in the investigations of this thesis, is not the solution, e.g., for a wrist watch or a body worn device of a small size – and neither is any other planar antenna without a ground plane. Other authors such as H. Schantz [42, 44, 47–48, 57] and Z. N. Chen [59, 63, 79] have also studied similar kinds of dipole structures, which is sufficient to gain general understanding about the operation in an environment due to polarization purity it has, in addition to the fact that a dipole can be fundamentally used to explain the operation of any other antenna type. However, it is recommended that the next step of the related antenna research, by using planar antennas, is to increase cooperation with the research partners in order to define how to include the mechanical restrictions in the work and consider practical antenna solutions for a device. Performance could be compared with 3D antenna radiator structures in order to demonstrate the trade-off between various antenna parameters on a body, the size of an antenna and on-body channel performance at the end. Currently, the author's research work needs information about a body-worn device concept to be able to start to apply the knowledge of the antenna behaviour to new radiator structures and surroundings.

As the propagation environment of the thesis objective addresses wearable devices close or on contact a human body, one of the challenges in relation to the implementation of a WBAN is to overcome the path loss on the channel. Based on the reviews of the open literature, comprehensive studies have not been carried out to give the answer to the question about the most dedicated WBAN antenna type to maintain the dominant normal polarization for different antenna orientations on a body, for instance, aligned parallel, perpendicular or crosswise each other. This is one of the items which was preliminary considered during the research of this thesis in [14, 17–19], but the topic was left for future research. The propagation mechanism is crucial to understand in order to further minimize the path loss and device power consumption and because the total field is known to be a combination of incident creeping and surface waves from the antennas' perspective at the on-body link. In the open literature, the effect of polarization with respect to a body surface of the incident wave is examined and the normal polarization is concluded to outperform the tangential one for the paths along the surface [111, 112, 120]. In order to achieve the best performance for transceivers in addition to the satisfactory system reliability, a WBAN channel needs to be fundamentally understood [121], and the effective antenna shows an important branch of the performance for the body worn communicating device. The phenomenon related to the issue is crucial to understand and strongly recommended for future studies. The research question involves the theory of creeping waves in addition to the unified theory of diffraction [122–125].

One approach, recommended for investigations of the antenna polarization, is to set the channel performance against the first analytical WBAN path loss model by

$$G = \frac{P_{\mathrm{RX}}}{P_{\mathrm{TX}}} = \frac{c^{10/6}\pi^{4/3}}{4\pi^2\left|1-0188e^{-j\pi/3}\right|^2} G_{\mathrm{TX}} G_{\mathrm{RX}} \frac{1}{d}\frac{1}{f^{10/6}}\frac{1}{a^{2/3}}$$

$$\mathrm{x}\left|\left[e^{-\alpha d}e^{-jkd} + e^{-\alpha(p-d)}e^{-jk(p-d)}\right]^2\right|, \tag{36}$$

where α is the attenuation factor as

$$\alpha_{Np/m} = \frac{\pi^{1/3}\left|1-0188e^{-j\pi/3}\right|\cos\pi/6}{\lambda^{1/3}a^{2/3}}, \tag{37}$$

which was derived in 2011 [124]. The factors in (36)–(37) are explained in detail in [124]. The analytical model is beneficial, since solving the huge problem of a BAN channel numerically requires great computing power [126], resulting in resolving Maxwell's equations in (7)–(10) for each point of a body. It is highly recommended to compare the on-body antenna performance with the path loss model in (36)–(37).

In addition to optimize the antenna polarization with respect to a body surface, it is of interest to consider whether the information about polarization can be used for determining the position of a user's body, for instance, in terms of standing, sleeping or sitting. An alternative aspect could be to define a body position by combining the information about several on-body nodes, which are aligned on legs, abdomen and hands.

It has been understood during the research work that the impedance behaviour of a WBAN on-body antenna can be estimated with a relatively small block of tissue phantom. Nevertheless, an excessively small phantom model might slightly distort the radiation pattern shape. Therefore, it is recommended to invest in the simulation capacity to be able to run full body model simulations. Also the channel studies involve full body models and heavy simulations. However, lossy cylinders are reported as being the reliable assumption to model a whole body in the field [111–112, 121, 124], but the information does not remove the fact of the required huge simulation capacity.

Furthermore, the anisotropic antenna substrate in Paper [IV] is an interesting topic for future research. Based on the findings of the research work, the substrate works efficiently with great possibilities to have an impact on the antenna characteristic. For instance, the following items, recommended for examinations, are to study the manufacturing opportunities and the miniaturization of the size of the substrate. Apart from the opportunities in a WBAN, the proposed concept has several applications to apply in mobile device concepts.

The development of equivalent circuit models in Papers [VIII, IX] is an important and challenging issue for further research. A straightforward approach is to apply the information about a dipole equivalent to other antenna types to derive corresponding circuit studies, for instance, those used with a ground plane. Another interesting topic is to develop equivalent circuits for bendable or textile antennas to understand the physical operation of bending the radiator on impedance behaviour in detail. An alternative approach could be to evaluate the circuits including tissue models given in Paper [IX] in a way that they can be directly used to indicate the required changes for the antenna radiator dimensions to create an antenna to be more tolerant with respect to body effects.

In addition, it is recommended to organize measurement campaigns for larger groups of people to investigate the effect of body size (thin, fat, tall, and short) and gender (female and male) on the antenna performance. It is of interest to understand the variation in the antenna operation between various users, use positions, genders, and so forth. The modelling of the properties of tissues and the antenna distance to phantom were clearly expressed, which further simplifies the work of researchers to repeat the studies.

8 Conclusions

WBAN antennas have been under intense research in recent years. In this dissertation, the wideband technology of three possible physical layer solutions in the international IEEE802.15.6 WBAN standard was examined. During the determination of the research questions, the work was focused on the IR-UWB technology based on the FCC regulations, which was the reason why in-body applications were excluded from the content. Even though several investigations of WBAN antennas have been reported in the open literature, there is plenty of room for the sympathetic antenna research related to the interaction mechanism and phenomena in the vicinity of a body, particularly with respect to the UWB frequencies. In addition to examining the opportunities of wideband radiators close to body in the thesis, the impact of use distance to body was demonstrated. Furthermore, different ways to analyse the connection of dimensions with respect to impedance behaviour were considered. All the studies in the original papers [I]–[IX], criticized by anonymous reviewers, contemplated UWB WBAN applications, proposed new insight for WBAN antenna research and contained results that have not been presented in the open literature earlier.

The characteristics of human body tissues at the microwave frequency band were examined and demonstrated for four outermost tissue layers of the body. The impact of the tissue layer thickness on the planar antenna performance was demonstrated in terms of the reflection coefficient, efficiency, pattern behaviour and SAR values. The influence of the thickness of only the skin tissue had a major impact on the achieved performance. In recent years, the impact of electromagnetic radiation due to the existence of both mobile device and base station antennas on a human body has aroused discussion also in the daily newspapers and national magazines. Temperature rise and power losses in body tissues were shown for the planar UWB antennas. Provided that the FCC regulations on the US band are followed, the international SAR limits by the IEEE and ICNIRP cannot be exceeded.

The issues affecting the shape of radiation pattern of the wearable UWB antenna were considered. The method for estimating a preliminary pattern shape was investigated by using a simple two-path model. Even though the theoretical model is only valid in the far-field of an antenna, it was able to show the preliminary pattern shape also in the near-field. Due to the generation of pattern minima/nulls for some frequencies of the UWB antenna close to body, the ways to mitigate the harmful impacts were studied. An artificially anisotropic antenna substrate material was introduced for a WBAN for the first time. In addition to the improved gain performance, the derived substrate enabled avoiding the appearance of pattern minima. The anisotropic material modified the sum polarization such that smoother patterns over the bandwidth were achieved.

The impedance behaviour was demonstrated for the range of antenna reactive near-field (0–30 mm) on a body surface. The findings with measurements for two types of antennas (slot-loop and dipole) were verified by simulations close to tissues. The differences of the impedance variations against the boundary fields were only marginal between antenna types, and both of the antennas were observed to perform in a similar fashion with the distance. For the shortest possible satisfactory antenna–body distance, the size of the reactive near-field was concluded to be an important factor.

For the evaluation of WBAN devices, the existence of a ground plane might involve critical challenges for the realization of matching the UWB antennas in practice. The effect of the conductive layer on antenna characteristics was examined by separating the proportion of body, absorption and mismatch losses for various broadband dipoles with different bandwidths. Even though the layer was observed to decrease absorption loss up to 10 dB in the lowest frequencies, the trade-off was realized with mismatch losses in the case to achieve the better body loss. The natural progression of the observed results is to study the co-design of the layer and an antenna, since the reference results of this thesis are now available for the separation of loss factors.

By using the same dipole configurations, the impact of body tissues on antenna impedance behaviour was considered to separate the impact of tissue on antenna impedance. The effect of actual radiator width and length on impedance behaviour was demonstrated. The main findings were that the series-resonant circuit is analogous to the antenna feeding area and that the physical dipole dimensions in terms of length and width have a connection with the parallel-resonant part. Based on the observations related to the antenna performance close to tissues, the impedance behaviour of antennas was presented in terms of capacitance, inductance and resistance as a function of the radiator distance on the tissue surface for UWB antennas. It was of interest to separate the proportion of the impedance in terms of the parasitic components for the series-resonant and parallel-resonant stages of the equivalent models for taking the impact of tissue into account in the antenna design. The main findings were that the capacitance increases with the distance to tissue surface by achieving the maximum value close to the reactive near-field boundary, the inductance has the maximum value on contact the tissue, decreasing strongly with the first millimetres and remaining constant with the longer distance, and the maximum value of input resistance was seen to clearly increase with distance, having the maximum value in the first third of the studied range, descending close to the value in free space at the boundary at the end.

References

1. Tuovinen T, Yekeh Yazdandoost K & Iinatti J (2011) Monopole Ultra Wideband Antenna for On-Body Communication in Wireless Body Area Network. In Proc of Loughborough Antennas & Propagation Conference (LAPC): 1–5.
2. Berg M, Sonkki M, Myllymäki S, Tuovinen T & Salonen E (2012) Effect of the Mobile Terminal Antenna Efficiency on the Cellular Network Issues. In Proc of European Conference on Antennas and Propagation (EuCAP): 1–5.
3. Tuovinen T, Yekeh Yazdandoost K & Iinatti J (2012) Comparison of the Performance of the Two Different UWB Antennas for the Use in WBAN On-Body Communication. In Proc of European Conference on Antennas and Propagation (EuCAP): 1–5.
4. Tuovinen T, Yekeh Yazdandoost K & Iinatti J (2012) Ultra Wideband Loop Antenna for On-Body Communication in Wireless Body Area Network. In Proc of European Conference on Antennas and Propagation (EuCAP): 1–5.
5. Särestöniemi M, Tuovinen T, Hämäläinen M, Yekeh Yazdandoost K, Kaivanto E & Iinatti J (2012) Applicability of Finite Integration Technique for the Modelling of UWB Channel Characteristics. In Proc of International Symposium on Medical Information and Communication Technology (ISMICT), 1–5.
6. Tuovinen T, Berg M, Yekeh Yazdandoost K, Salonen E & Iinatti J (2012) Human Body Effect on the Polarization Properties of the New UWB Dipole Antenna in WBAN UWB Applications. In Proc of International Conference on Body Area Networks (Bodynets), UWBAN Workshop: 1–7.
7. Särestöniemi M, Tuovinen T, Hämäläinen M, Yekeh Yazdandoost K & Iinatti J (2012) Channel Modeling for UWB WBAN On-Ext Communication Link with Finite Integration Technique. In Proc of International Conference on Body Area Networks (Bodynets), UWBAN Workshop: 1–7.
8. Tuovinen T, Berg M, Yekeh Yazdandoost K, Salonen E & Iinatti J (2012) Impedance Behaviour of Planar UWB Antennas in the Vicinity of a Dispersive Tissue Model. In Proc of Loughborough Antennas & Propagation Conference (LAPC): 1–5.
9. Tuovinen T, Berg M, Yekeh Yazdandoost K, Salonen E & Iinatti J (2012) Near-Field Region Radiation of Planar UWB Antennas Close to a Dispersive Tissue Model. In Proc of Loughborough Antennas & Propagation Conference (LAPC): 1–5.
10. Särestöniemi M, Tuovinen T, Hämäläinen M, & Iinatti J (2013) Finite Integration Technique for the Modelling of WBAN Communication Links in Complex Environments. In Proc of International Symposium on Medical Information and Communication Technology (ISMICT), Special Organized Session "Antennas and Propagation for Body Area Network": 1–5.
11. Kumpuniemi T, Tuovinen T, Hämäläinen M, Yekeh Yazdandoost K, Vuohtoniemi R, & Iinatti J (2013) Measurement-Based On-Body Path Loss Modelling for UWB WBAN Communications. In Proc of International Symposium on Medical Information and Communication Technology (ISMICT): 1–5.

12. Tuovinen T, Kumpuniemi T, Hämäläinen M, Yekeh Yazdandoost K, & Iinatti J (2013) Effect of the Antenna-Human Body Distance on the On-Ext and On-On Channel Link Path Gain in UWB WBAN Applications. In Proc of International Conference on the IEEE Engineering in Medicine and Biology Society (EMBC): 1–5.
13. Kumpuniemi T, Hämäläinen M, Tuovinen T, Yekeh Yazdandoost K, & Iinatti J (2013) Generic Small Scale Channel Model for On-Body UWB WBAN Communications. In Proc of International Conference on Body Area Networks (Bodynets), UWBAN Workshop: 1–7.
14. Tuovinen T, Berg M and Salonen E (2014) The Effect of Antenna Pattern and Polarization for Launching Creeping Waves on a Skin Surface. In Proc of European Conference on Antennas & Propagation (EuCAP): 1–4.
15. Niemelä V, Paso T, Tuovinen T, Haapola J, Hämäläinen M, & Iinatti J (2014) Propagation Effects and Antenna Properties and Their Impact on ED Receivers' Performance in Body Sensor Network. In Proc of International Symposium on Medical Information and Communication Technology (ISMICT): 1–5.
16. Kumpuniemi T, Hämäläinen M, Tuovinen T, Yekeh Yazdandoost K, & Iinatti J (2014) Radio Channel Modelling for Pseudo-Dynamic WBAN On-Body UWB Links (2014) In Proc of International Symposium on Medical Information and Communication Technology (ISMICT): 1–5.
17. Berg M, Tuovinen T & Salonen E (2014) Low Profile Antenna with Optimum Polarization for 2.4 GHz On-Body Sensor Node. Accepted: Loughborough Antennas & Propagation Conference (LAPC). Loughborough, United Kingdom: 1–5.
18. Tuovinen T, Berg M, Whittow W and Salonen E (2014) Performance of WBAN On-Ground Antenna Type with Relation to Analytical Path Loss Model. Accepted: Loughborough Antennas & Propagation Conference (LAPC). Loughborough, United Kingdom: 1–5.
19. Berg M and Tuovinen T (2014) Propagation Along a Human Body Surface in WBAN: Remarks of Desirable Antenna Characteristics. Invited Talk: To be Presented in Mobile Health Conference 2014: 1–4.
20. Hall PS & Hao Y (2006) Antennas and Propagation for Body-Centric Wireless Communications. Artech house.
21. Chen ZN (2007) Antennas for Portable Devices. John Wiley & Sons.
22. IEEE (2012) Standard 802.15.6 for Local and Metropolitan Area Networks, 802.15.6: Wireless Body Area networks.
23. Federal Communications Commission (2002) First Report and Order in the matter of revision of Part 15 of the Commission's rules regarding ultrawideband transmission systems, ET-Docket 98-153, FCC 02-48.
24. Opperman I, Hämäläinen M & Iinatti J (2004) UWB Theory and Application. John Wiley & Sons.
25. Toftgård J, Hornsleth SN & Andersen JB (1993) Effects on Portable Antennas of the Presence of a Person. IEEE Transactions on Antennas and Propagation 41(6): 739–746.

26. IEEE (2008) Std C95.3 Recommended Practice for Measurements and Computations of Radio Frequency Electromagnetic Fields With Respect to Human Exposure to Such Fields, 100 kHz – 300 GHz.
27. ICNIRP (1998) Guidelines for limiting exposure to time-varying electric, magnetic, and electromagnetic fields (up to 300 GHz). Health Physics 74: 494–522.
28. IEEE (2011) WPAN Task Group 6 Body Area Networks.
29. Barnes FS & Greenebaum B (2007) Bioengineering and Biophysical Aspects of Electromagnetic Fields, 3rd ed. CRC Press, Taylor & Francis Group.
30. Sânchez-Hernândez DA (2009) High Frequency Electromagnetic Dosimetry. Artech House.
31. Pozar DM (1998) Microwave Engineering, 2nd ed. John Wiley & Sons.
32. Balanis CA (2005) Antenna Theory, 3rd ed. John Wiley & Sons.
33. Saunders SR (2003) Antennas and Propagation for Wireless Communication Systems. John Wiley & Sons.
34. Stutzmann WL & Thiele GA (1998) Antenna Theory and design, 2nd ed. John Wiley & Sons.
35. Allen B, Dohler M, Okon E, Malik W, Brown A & Edwards D (2006) Ultra Wideband Antennas and Propagation for Communications, Radar and Imaging. John Wiley & Sons.
36. Computer Simulation Technology (CST). (2012) [Online]. Available: http://www.cst.com.
37. Satimo. (2014) [Online]. Available: http://www.satimo.com/content/products/starlab.
38. Schantz, HG (2003) A Brief History of UWB Antennas. IEEE Aerospace and Electronic Systems Magazine 19(4): 22–26.
39. EUWB consortium (2011) Ultra-Wideband: Past, Present and Future: 1–79.
40. Begaud X (2011) Ultra Wide Band Antennas. ISTE and John Wiley & Sons.
41. IEEE (2011) Standard 802.15.4 for Local and Metropolitan Area Networks, 802.15.4: Low-Rate Wireless Personal Area Networks.
42. Schantz HG (2003) Introduction to Ultra-Wideband Antennas. In Proc of IEEE Conference on Ultra Wideband Systems and Technologies. Brownsboro, USA: 1–9.
43. Fernandes JR & Wentzloff (2010) Recent Advances in IR-UWB Transceivers: An Overview. In Proc IEEE ISCAS International Symposium. Lisbon, Portugal: 3284–3287.
44. Schantz HS (2005) The Art and Science of Ultrawideband Antennas. Artech house.
45. Adamiuk G, Zwick T, & Wiesbeck W (2012) UWB Antennas for Communication Systems. Proceedings of the IEEE 100(7): 2308–2321.
46. Wiesbeck W, Adamiuk G & Sturm C (2009) Basic Properties and Design Principles of UWB Antennas. Proceedings of the IEEE 97(2): 372–385.
47. Schantz HS (2003) Bottom Fed Planar Elliptical UWB Antennas. In Proc IEEE Conference on Ultra Wideband Systems and Technologies: 219–223.
48. Schantz H (2002) Planar Elliptical Element Ultra-Wideband Dipole Antennas. In Proc IEEE AP-S International Symposium. Yokosuka, Japan: 1–4.

49. Chen ZN, Wu XH, Yang LN & Chia MYW (2004) Considerations for Source Pulses and Antennas in UWB Radio Systems. IEEE Transactions on Antennas and Propagation 52(7): 1739–1748.
50. Sipal V, Allen B & Edwards D (2010) Analysis and Mitigation of Antenna Effects on Wideband Wireless Channel. IET Electronic Letters 46(16): 1159–1160.
51. Schantz H (2004) Dispersion and UWB Antennas. In Proc of International Workshop on Ultra Wideband Systems: 161–165.
52. Hertel T & Smith G (2003) On the Dispersive Properties of the Conical Spiral Antenna and Its Used for Pulse Radiation. IEEE Transactions on Antennas and Propagation 51(7): 1426–1433.
53. Morton MA, Comeau JP, Cressler JD, Michell M & Papapolymerou J (2006) Source of Phase Error and Design Considerations for Silicon-Based Monolithic High-Pass/Low-Pass Microwave Phase Shifters. IEEE Transaction on Microwave Theory and Technology 54(12): 4032–4040.
54. Berg M, Sonkki M & Salonen E (2011) Absorption Loss Reduction in a Mobile Terminal with Switchable Monopole Antennas. IEEE Transactions on Antennas and Propagation 59(11): 4379–4383.
55. Qing X & Chen ZN (2004) Transfer Functions Measurement for UWB Antenna. Proc IEEE AP-S International Symposium. Sendai, Japan: 2532–2535.
56. Kwon DH (2006) Effect of Antenna Gain and Group Delay Variations on Pulse-Preserving Capabilities of Ultrawideband Antennas. IEEE Transactions on Antennas and Propagation 54(8): 2208–2215.
57. Schantz HS & Fullerton L (2001) The Diamond Dipole: A Gaussian Impulse Antenna. In Proc IEEE AP-S International Symposium. Boston, USA: 100–103.
58. Kwon DH & Kim Y (2006) Suppression of Cable Leakage Current for Edge-Fed Printed Dipole UWB Antennas Using Leakage-Blocking Slots. IEEE Antennas and Wireless Propagation Letters 5: 183–186.
59. Low XN, Chen ZN & See TSP (2009) A UWB Dipole Antenna with Enhanced Impedance and Gain Performance. IEEE Transactions on Antennas and Propagation 57(10): 2959–2966.
60. Nazli H, Emrullah B, Turetken B, & Sezgin M (2010) An Improved Design for Planar Elliptical Dipole Antenna for UWB Applications. IEEE Antennas and Wireless Propagation Letters 9: 264–267.
61. Gao F, Zhang F, Lu L, Ni T, & Jiao Y (2013) Low-Profile Dipole Antenna with Enhanced Impedance and Gain Performance for Wideband Wireless Applications. IEEE Antennas and Wireless Propagation Letters 12: 372–375.
62. Shambavi K, & Alex ZC (2010) Printed Dipole Antenna with Band Rejection Characteristics for UWB Applications. IEEE Antennas and Wireless Propagation Letters 9: 1029–1032.
63. Wu XH, & Chen ZN (2005) Comparison of Planar Dipoles in UWB Applications. IEEE Transactions on Antennas and Propagation 53(6): 1973–1983.

64. Agrawall NP & Ray KP (1998) Wide-Band Planar Monopole Antennas. IEEE Transactions on Antennas and Propagation 46(2): 294–295.
65. Evans JA & Ammann MJ (1999) Planar Trapezoidal and Pentagonal Monopoles with Impedance Bandwidths in Excess of 10:1. In Proc of IEEE AP-S International Symposium: 1558–1561.
66. Liang J, Chiau CC, Chen X & Parini CG (2005) Study of a Printed Circular Disc Monopole Antenna for UWB Systems. IEEE Transactions on Antennas and Propagation 53(11): 3500–3504.
67. Chen ZN, See TSP & Qing X (2007) Small Printed Ultrawideband Antenna with Reduced Ground Plane Effect. IEEE Transactions on Antennas and Propagation 55(2): 383–388.
68. Tanyer-Tigrek FM, Tran DP, Lager IE & Lighart LP (2009) CPW-Fed Quasi-Magnetic Printed Antenna for Ultra-Wideband Applications. IEEE Antennas and Propagation Magazine 51(2): 61–70.
69. Chair R, Kishk AA & Lee KF (2004) Ultrawide-band Coplanar Waveguide-Fed Rectangular Slot Antenna. IEEE Antennas and Wireless Propagation Letters 3: 227–229.
70. Schantz HS & Barnes M (2001) The COTAB UWB Magnetic Slot Antenna. In Proc IEEE AP-S International Symposium. Boston, USA: 104–107.
71. Schantz H (2003) UWB Magnetic Antennas. In Proc IEEE AP-S International Symposium. Tennille, USA: 604–607.
72. Kwon DH & Kim YK (2007) Small Low-Profile Loop Wideband Antennas with Unidirectional Radiation Characteristics. IEEE Transactions on Antennas and Propagation 55(1): 72–77.
73. Nakano H, Fukasawa M & Yamauchi J (2002) Discrete Multiloop, Modified Multiloop, and Plate-Loop Antennas – Multifrequency and Wide-Band VSWR Characteristics. IEEE Transactions on Antennas and Propagation 50(3): 371–378.
74. Mandal MK & Chen ZN (2011) Compact Dual-Band and Ultrawideband Loop Antennas. IEEE Transactions on Antennas and Propagation 59(8): 2774–2779.
75. Rogers Corporation. [Online]. Available: http://www.rogerscorp.com/acm/index.aspx.
76. Welch TB, Musselman RL, Emessience BA, Gift PD, Choudbury DK, Cassadine DN & Yano SM (2002) The Effects of the Human Body on UWB Signal Propagation in an Indoor Environment. IEEE Journal on Selected Areas in Communications 20(9): 1778–1782.
77. Alomainy A, Hao Y, Parini CG, & Hall PS (2005) Comparison between Two Different Antennas for UWB On-Body Propagation Measurements. IEEE Antennas and Wireless Propagation Letters 4: 31–34.
78. Klemm M, Kovcs IZ, Pedersen GF, & Troester G (2005) Novel Small-Size Directional Antenna for UWB WBAN/WPAN Applications. IEEE Transactions on Antennas and Propagation 53(12): 3884–3896.
79. Chen ZN, Ammann MJ, Qing X, Wu XH, See TSP, & Cai A (2006) Planar Antennas. IEEE Microwave Magazine, December: 63–73.

80. Chen ZN, Cai A, See TSP, Qing X & Chia MYW (2006) Small Planar UWB Antennas in Proximity of the Human Head. IEEE Transactions on Microwave Theory and Techniques 54(4): 1846–1857.
81. Zhao Y, Hao Y, Alomainy A, & Parini CG (2006) UWB On-Body Radio Channel Modeling Using Ray Theory and Subband FDTD Method. IEEE Transactions on Microwave Theory and Techniques 54(4): 1827–1835.
82. Klemm M & Troester G (2006) EM Energy Absorption in the Human Body Tissues Due to UWB Antennas. Progress in Electromagnetic Research PIER62: 261–280.
83. Khaleghi A, & Balasingham I (2008) Non-Line-Of-Sight On-Body Ultra Wideband (1-6 GHZ) Channel Characterisation using Different Antenna Polarisations. IET Proceedings – Microwaves, Antennas & Propagation 3(7): 1019–1027.
84. See TSP & Chen ZN (2009) Experimental Characterization of UWB Antennas for On-Body Communications. IEEE Transactions on Antennas and Propagation 57(4): 866–874.
85. Alomainy A, Sani A, Rahman A, Santas JG, & Hao Y (2009) Transient Characteristics of Wearable Antennas and Radio Propagation Channels for Ultrawideband Body-Centric Wireless Communications. IEEE Transactions on Antennas and Propagation 57(4): 875–884.
86. Thompson W, Cepeda R, Hilton G, Beach MA, & Armour S (2011) An Improved Antenna Mounting for Ultra-Wideband On-Body Communications and Channel Characterization. IEEE Transactions on Microwave Theory and Techniques 59(4): 1102–1108.
87. Chahat N, Zhadobov M, Sauleau R & Ito K (2011) A Compact UWB Antenna for On-Body Applications. IEEE Transactions on Antennas and Propagation 59(4): 1123–1131.
88. See TSP, Chiam TM, Ho MCK, & Yuce MR (2012) Experimental Study on the Dependence of Antenna Type and Polarization on the Link Reliability in On-Body UWB Systems. IEEE Transactions on Antennas and Propagation 60(11): 5373–5380.
89. Vorobyov A & Yarovoy A (2012) Human Body Impact on UWB Antenna Radiation. Progress in Electromagnetic Research PIER M 22: 259–269.
90. Koohestani M, Pires N, Skrivervik AK, & Moreira AA (2013) Bandwidth Enhancement of a Wearable UWB Antenna Near a Human Arm. Microwave and Optical Technology Letter 55(12): 2965–2967.
91. Abbasi QH, Rehman MU, Yang X, Alomainy A, Qaraqe K, & Serpedin E (2013) Ultrawideband Band-Notched Flexible Antenna for Wearable Applications. IEEE Antennas & Wireless Propagation Letters 12: 1606–1609.
92. IEEE Xplore Digital Library. [Online]. Available: http://ieeexplore.ieee.org/Xplore/home.jsp.
93. Maxwell JC (1865) A Dynamical Theory of the Electromagnetic Field. Philosophical Transactions on Royal Society Publishing 155: 459–512.
94. Räisänen AV & Lehto A (2003) Radio Engineering for Wireless Communication and Sensor Applications. Artech House.

95. Sihvola A & Lindell I (2000) Sähkömagneettinen kenttäteoria: 2. Dynaamiset kentät (in English: Electromagnetic theory: 2. Dynamic fields), 2nd ed. Otatieto.
96. Gabriel C (1996) Compilation of the Dielectric Properties of Body Tissues at RF and Microwave Frequencies. Brooks Air For Technical Report, AL/OE-TR-1996.0037.
97. Kurrant DJ & Fear EC (2011) Regional Estimation of the Dielectric Properties of the Breast: Skin, Adipose, and Fibroglandular Tissues. Proc 5th European Conference on Antennas and Propagation. Rome, Italy: 3073–3077.
98. Christ A, Klingenböck A, Samaras T, Goiceanu C & Kuster, N (2006) The Dependence of Electromagnetic Far-Field Absorption on Body Tissue Composition in the Frequency Range From 300 MHz to 6 GHz. IEEE Transactions on Microwave Theory and Technique 54(5): 2188–2195.
99. Italian National Research Council: Calculation of the Dielectric Properties of Body Tissues in the frequency range 10 Hz – 100 GHz, http://niremf.ifac.cnr.it/tissprop/htmlclie/htmlclie.htm.
100. Fujii M (2012) Maximum Frequency Range Limit of Multi-Pole Debye Models of Human Body Tissues. IEEE Microwave and Wireless Components Letters 22(2): p. 73– 75.
101. Fujii M, Fujii R, Yotsuki R, Wuren T, Takai T & Sakagami I (2010) Exploration of Whole Human Body and UWB Radiation Interaction by Efficient and Accurate Two-Debye-Pole Tissue Models. IEEE Transactions on Antennas and Propagation 58(2): 515–524.
102. Gandhi OP, Gao B-Q & Chen J-Y (1993) A Frequency-Dependent Finite-Difference Time Domain Formulation for General Dispersive Media. IEEE Transactions on Microwave Theory and Techniques 41(4): 658–665.
103. Furse CM, Chen J-Y & Gandhi OP (1994) The Use of the Frequency-Dependent Finite-Difference Time-Domain Method for Induced Current and SAR Calculations for a Heterogeneous Model of the Human Body. IEEE Transactions on Electromagnetic Compatibility 26(2): 128–133.
104. Gandhi OP & Furse CM (1997) Currents Induced in the Human Body for Exposure to Ultrawideband Electromagnetic Pulses. IEEE Transactions on Electromagnetic Compatibility 39(2): 174–180.
105. Pennes HH (1948) Analysis of tissue and arterial blood temperature in the resting human forearm. Journal of Applied Physiology 1(2): 93–122.
106. Chan K, Cleveland RF & Means DL (1997) Evaluating compliance with FCC guidelines for human exposure to radio frequency electromagnetic fields. FCC OET bulletin 65 (ed. 97-101) Supplement C.
107. Kang G & Gandhi OP (2004) Effect of Dielectric Properties on the Peak 1- and 10-g SAR for 802.11 a/b/g Frequencies 2.45 and 5.15 to 5.85 GHz. IEEE Transactions on Electromagnetic Compatibility 46: 268–274.
108. Holopainen J, Valkonen R, Kivekäs O, Ilvonen J, Martìnez L, Vainikainen P, Kelly JR & Hall PS (2010) Equivalent Circuit Model-Based Approach on the User Body Effect of a Mobile Terminal Antenna. In Proc of Loughborough Antennas & Propagation Conference (LAPC): 217–220.

109. Berg M (2011) Methods for Antenna Frequency Control and User Effect Compensation in Mobile Terminals. D.Sc thesis. Univ. Oulu, Dept. Communications Engineering.
110. Balzano Q, Irwin J & Steel R (1975) Investigation of the Impedance Variation and Radiation Loss in Portable Radios. In Proc of International Antennas and Propagation Society Symposium: 89–92.
111. Fort A, Keshmiri F, Crusats GR, Craeye C & Oestges C (2010) A Body Area Propagation Model Derived from Fundamental Principles: Analytical Analysis and Comparison With Measurements. IEEE Transactions on Antennas and Propagation 58(2): 503–514.
112. Keshmiri F, Fort A & Craeye C (2009) Analysis of Wave Propagation for BAN Applications. In Proc of 3rd European Conference on Antennas & Propagation: 709–712.
113. Mackowiak M & Correia LM (2010) A Statistical Approach to Model Antenna Radiation Pattern in Off-Body Radio Channel. In Proc of 21st International Personal Indoor and Mobile Radio Communications: 1091–1095.
114. Vaughan R & Anderson JB (2003) Channels, Propagation and Antennas for Mobile Communications. London: IEE Electromagnetic Wave Series 50.
115. See TSP, Chen ZN & Qing XM (2009) Proximity Effect of UWB Antenna on Human Body. In Proc of Asia Pacific Microwave Conference: 2192–2195.
116. Chen WT & Chuang HR (1998) Numerical Computation of Human Interaction with Arbitrarily Oriented Superquadric Loop Antenna in Personal Communications. IEEE Transactions on Antennas and Propagation 46(6): 821–828.
117. Alomainy A, Hao Y & Davenport DM (2010) Parametric Study of Wearable Antennas with Varying Distance from the Body and Different On-Body Positions. In Proc of IET Seminar on Antennas & Propagation for Body-Centric Wireless Communications: 84–89.
118. Sihvola A (2008) Electromagnetic Mixing Formulas and Applications. IET Electromagnetic Wave Series.
119. Wang Y, Li JZ & Ran LX (2008) An Equivalent Circuit Modelling Method for Ultra-Wideband Antennas. Progress in Electromagnetics Research 82: 433–445.
120. Hall PS, Hao Y, Nechayev YI, Alomainy A, Constantinou CC, Parini C, Kamarudin MR, Salim TZ, Hee DTM, Dubrovka R, Owadally AS, Song W, Serra A, Nepa P, Gallo M & Bozzetti M (2007) Antennas and Propagation for On-Body Communication Systems. IEEE Antennas & Propagation Magazine 49(3): 41–58.
121. Ma D & Zhang WX (2009) Analytic Propagation Model for Body Area Network Channel Based on Impedance Boundary Condition. In Proc of 3rd European Conference on Antennas & Propagation: 974–978.
122. Paknys R & Wang N (1986) Creeping Wave Propagation Constants and Modal Impedance for a Dielectric Coated Cylinder. IEEE Transactions on Antennas and Propagation 34(5): 674–680.

123. Pathak PH, Wang N, Burnside WD & Kouyomjian RG (1981) A Uniform GTD Solution for the Radiation from Sources on a Convex Surface. IEEE Transactions on Antennas and Propagation 29(4): 609–622.
124. Alves T, Poussot B & Laheurte JM (2011) Analytical Propagation Modeling of BAN Channels Based on the Creeping-Wave Theory. IEEE Transactions on Antennas and Propagation 59(4): 1269–1274.
125. Conway GA & Scanlon WG (2009) Antennas for Over-Body-Surface Communication at 2.45 GHz. IEEE Transactions on Antennas and Propagation 57(4): 844–855.
126. Gupta A & Abhayapala TD (2008) Body Area Networks: Radio Channel Modelling and Propagation Characteristics. In Proc of Communications Theory Workshop: 58–63.

Original articles

I Tuovinen T, Berg M, Yekeh Yazdandoost K & Iinatti J (2013) Ultra Wideband Loop Antenna on Contact with Human Body Tissues. In: IET Microwaves, Antennas & Propagation 7(7): 588–596.

II Tuovinen T, Berg M, Yekeh Yazdandoost K, Hämäläinen M & Iinatti J (2013) On the Evaluation of Biological Effects of Wearable Antennas on Contact with Dispersive Medium in Terms of SAR and Bio-Heat by Using FIT Technique. In: IEEE 7th International Symposium on Medical Information and Communication Technology (ISMICT), Special Organized Session: Antennas and Propagation for Body Area Network. Tokyo, Japan: 149–153.

III Tuovinen T, Berg M, Yekeh Yazdandoost K, Salonen E & Iinatti J (2012) Radiation Properties of the Planar UWB Dipole in the Proximity of Dispersive Body Models. In: EAI 7th International Conference on Body Area Networks (BodyNets). Oslo, Norway: 1–7.

IV Tuovinen T, Berg M & Salonen E (2014) Antenna Close to Tissue: Avoiding Radiation Pattern Minima with Anisotropic Substrate. In: IEEE Antennas and Wireless Propagation Letters. (In press)

V Tuovinen T, Kumpuniemi T, Yekeh Yazdandoost K, Hämäläinen M & Iinatti J (2013) Effect of the Antenna-Human Body Distance on the Antenna Matching in UWB WBAN Applications. In: IEEE 7th International Symposium on Medical Information and Communication Technology (ISMICT). Tokyo, Japan: 193–197.

VI Tuovinen T, Berg M & Salonen E (2013) The Comparative Analysis of UWB Antennas with Complementary Characteristics: A Functionality in FS and Applicability for the Usage Close to Tissues. In: 34th Progress in Electromagnetics Research Symposium (PIERS). Stockholm, Sweden: 134–138.

VII Tuovinen T, Berg M, Salonen E, Hämäläinen M & Iinatti J (2014) Conductive Layer under a Wearable UWB Antenna: Trade-off between Absorption and Mismatch Losses. In: IEEE 8th International Symposium on Medical Information and Communication Technology (ISMICT). Florence, Italy: 1–5.

VIII Tuovinen T & Berg M (2014) Impedance Dependency on Planar Broadband Dipole Dimensions: An Examination with Antenna Equivalent Circuits. In: Progress in Electromagnetics Research (PIER) 144: 249–260.

IX Tuovinen T, Berg M & Iinatti J (2014) Analysis of the Impedance Behaviour for Broadband Dipoles in Proximity of a Body Tissue: Approach by Using Antenna Equivalent Circuits. In: Progress in Electromagnetics Research (PIER) B 59: 135–150.

Original publications are not included in the electronic version of the dissertation.

488. Celentano, Ulrico (2014) Dependable cognitive wireless networking : modelling and design
489. Peräntie, Jani (2014) Electric-field-induced dielectric and caloric effects in relaxor ferroelectrics
490. Aapaoja, Aki (2014) Enhancing value creation of construction projects through early stakeholder involvement and integration
491. Rossi, Pekka M. (2014) Integrated management of groundwater and dependent ecosystems in a Finnish esker
492. Sliz, Rafal (2014) Analysis of wetting and optical properties of materials developed for novel printed solar cells
493. Juntunen, Jouni (2014) Enhancing organizational ambidexterity of the Finnish Defence Forces' supply chain management
494. Hänninen, Kai (2014) Rapid productisation process : managing an unexpected product increment
495. Mehtonen, Saara (2014) The behavior of stabilized high-chromium ferritic stainless steels in hot deformation
496. Majava, Jukka (2014) Product development : drivers, stakeholders, and customer representation during early development
497. Myllylä, Teemu (2014) Multimodal biomedical measurement methods to study brain functions simultaneously with functional magnetic resonance imaging
498. Tamminen, Satu (2014) Modelling the rejection probability of a quality test consisting of multiple measurements
499. Tuovinen, Lauri (2014) From machine learning to learning with machines : remodeling the knowledge discovery process
500. Hosio, Simo (2014) Leveraging Social Networking Services on Multipurpose Public Displays
501. Ohenoja, Katja (2014) Particle size distribution and suspension stability in aqueous submicron grinding of $CaCO_3$ and TiO_2
502. Puustinen, Jarkko (2014) Phase structure and surface morphology effects on the optical properties of nanocrystalline PZT thin films
503. Tuhkala, Marko (2014) Dielectric characterization of powdery substances using an indirectly coupled open-ended coaxial cavity resonator

Book orders:
Granum: Virtual book store
http://granum.uta.fi/granum/

UNIVERSITY OF OULU P.O. Box 8000 FI-90014 UNIVERSITY OF OULU FINLAND

A C T A U N I V E R S I T A T I S O U L U E N S I S

ISBN 978-952-62-0591-5 (Paperback)
ISBN 978-952-62-0592-2 (PDF)
ISSN 0355-3213 (Print)
ISSN 1796-2226 (Online)

UNIVERSITY of OULU
OULUN YLIOPISTO